2008

Structure of the Central Skagit Gneiss Complex, North Cascades, Washington

Zachary David Michels
San Jose State University

INFORMATION TO USERS

This manuscript has been reproduced from the microfilm master. UMI films the text directly from the original or copy submitted. Thus, some thesis and dissertation copies are in typewriter face, while others may be from any type of computer printer.

The quality of this reproduction is dependent upon the quality of the copy submitted. Broken or indistinct print, colored or poor quality illustrations and photographs, print bleedthrough, substandard margins, and improper alignment can adversely affect reproduction.

In the unlikely event that the author did not send UMI a complete manuscript and there are missing pages, these will be noted. Also, if unauthorized copyright material had to be removed, a note will indicate the deletion.

Oversize materials (e.g., maps, drawings, charts) are reproduced by sectioning the original, beginning at the upper left-hand corner and continuing from left to right in equal sections with small overlaps.

ProQuest Information and Learning
300 North Zeeb Road, Ann Arbor, MI 48106-1346 USA
800-521-0600

STRUCTURE OF THE CENTRAL SKAGIT GNEISS COMPLEX, NORTH CASCADES, WASHINGTON

A Thesis

Presented to

The Faculty of the Department of Geology

San Jose State University

In Partial Fulfillment

of the Requirements for the Degree

Master of Science

by

Zachary David Michels

December 2008

SAN JOSE STATE UNIVERSITY

The Undersigned Thesis Committee Approves the Thesis Titled

STRUCTURE OF THE CENTRAL SKAGIT GNEISS COMPLEX,

NORTH CASCADES, WASHINGTON

by

Zachary David Michels

APPROVED FOR THE DEPARTMENT OF GEOLOGY

Robert S Miller 11/12/08

Dr. Robert Miller, Department of Geology Date

Jonathan D. Miller 11/12/08

Dr. Jonathan Miller, Department of Geology Date

11/12/08

Dr. Richard Sedlock, Department of Geology Date

APPROVED FOR THE UNIVERSITY

David K Pond 11/17/08

Associate Dean, Office of Graduate Studies and Research Date

ABSTRACT

STRUCTURE OF THE CENTRAL SKAGIT GNEISS COMPLEX,
NORTH CASCADES, WASHINGTON

by Zachary D. Michels

The tonalitic orthogneiss-dominated Central Skagit Gneiss Complex of the Cretaceous to Eocene North Cascades crystalline core consists of four units, differentiated on field and petrographic observations. New U/Pb zircon analyses yield crystallization ages for the orthogneisses between ~66 and 48 Ma. Microstructures indicate medium- to high-temperature (400–650 °C) deformation. Much deformation in the adjacent dextral Gabriel Peak tectonic belt, a segment of the 500-km-long Ross Lake fault system, predates crystallization of ca. 49.3 Ma orthogneisses. Lineations in the Eocene gneisses dominantly record subhorizontal NNE stretching discordant to the NW regional trend of the Cascades core and the tectonic belt. This discordance may reflect a change in the Eocene strain field, which is best recorded in rocks that were hot and ductile at the time. Thus, structures in the Central Skagit Gneiss Complex probably record some of the latest ductile deformation in the core.

ACKNOWLEDGMENTS

I would like to thank my committee members for their hard work and extensive support to see this project to completion. Field assistance was provided by Robert Miller, Kristin Hageseth, Scott Morford, Koni Morford, Erin Shea, Noah McLean, Jessica Stanley, and Pamela Clay, who all worked very hard to help map, discuss observations, and carry samples. I would also like to thank everyone at the M.I.T. Department of Earth, Atmospheric and Planetary Sciences, especially Dr. Sam Bowring, who made it possible for me to utilize high precision geochronologic lab instruments for this study. I wish to extend thanks to the employees and rangers associated with the North Cascades National Park and the Lake Chelan National Recreation Area, all of whom assisted and accommodated me in countless ways during field research. Finally, I acknowledge the National Science Foundation (Grant EAR-0511062), which partially supported this research.

TABLE OF CONTENTS

Page

LIST OF FIGURES

LIST OF TABLES

Page

INTRODUCTION

Exhumed mid- to deep-crustal crystalline complexes provide insights into ductile processes driving material transport in continental orogens. Most models of orogenic crustal flow are based on studies in collisional settings (e.g., Anatolian, Grenvillian, and Himalayan orogenic belts), but much less is known about flow beneath contractional continental magmatic arcs. It is also unclear to what extent deformation in the upper crust of arcs is coupled with flow in the deeper, more-ductile parts of the crust.

The Cretaceous to Paleogene North Cascades crystalline core (Cascades core; Fig. 1) of Washington and southwest British Columbia is a thick contractional continental magmatic arc that straddles the boundary between the outboard Insular superterrane and Intermontane superterrane of the northwestern North American Cordillera (e.g., Monger et al., 1982; McGroder, 1991; Miller et al., 1993a). Ductile deformation at mid- to deep-crustal levels of the northern part of the Cascades core persisted into the Eocene (e.g., Haugerud et al., 1991). Some of the youngest cooling ages (e.g., Engels et al., 1976; Richards and McTaggart, 1976; Miller et al., 1989; Haugerud et al., 1991) and ductile deformation are in the antiformal Skagit Gneiss Complex (Fig. 2).

The Skagit Gneiss Complex is composed of variably deformed and metamorphosed plutons, including lineated and foliated biotite-hornblende

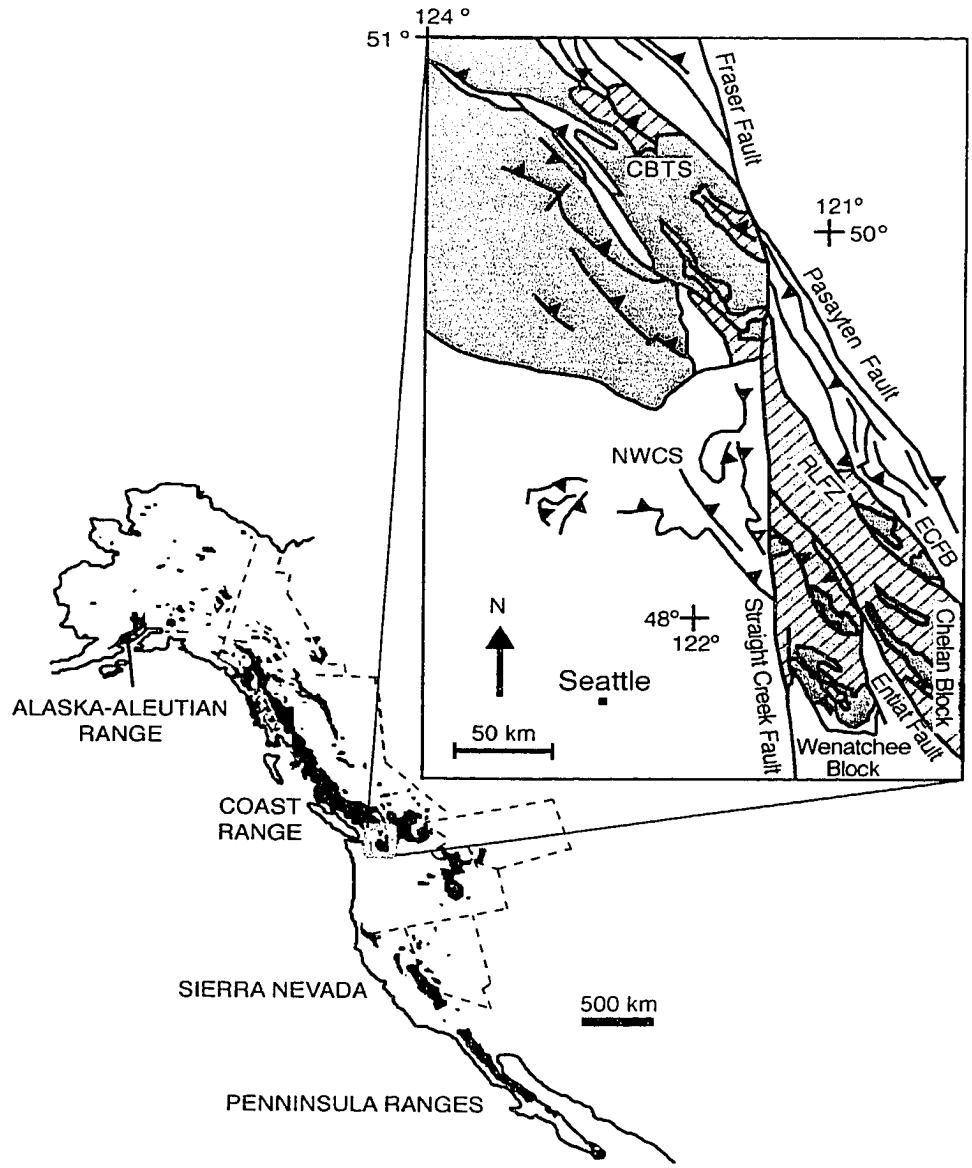

Figure 1. Sketch map of Mesozoic and Paleogene arc plutons in the western North American Cordillera (modified after Miller and Paterson, 2001a). Inset emphasizes distribution of metamorphic rocks (lined blue-grey pattern) and plutons (orange pattern). The dextral Fraser–Straight Creek fault offsets the Cascades core from the main part of the Coast belt. The Entiat fault is a Tertiary high-angle fault that divides the Cascades core into the western Wenatchee and eastern Chelan blocks. CBTS, Coast Belt thrust system; ECFB, Eastern Cascades fold belt; NWCS, Northwest Cascades thrust system; RLFZ, Ross Lake fault zone.

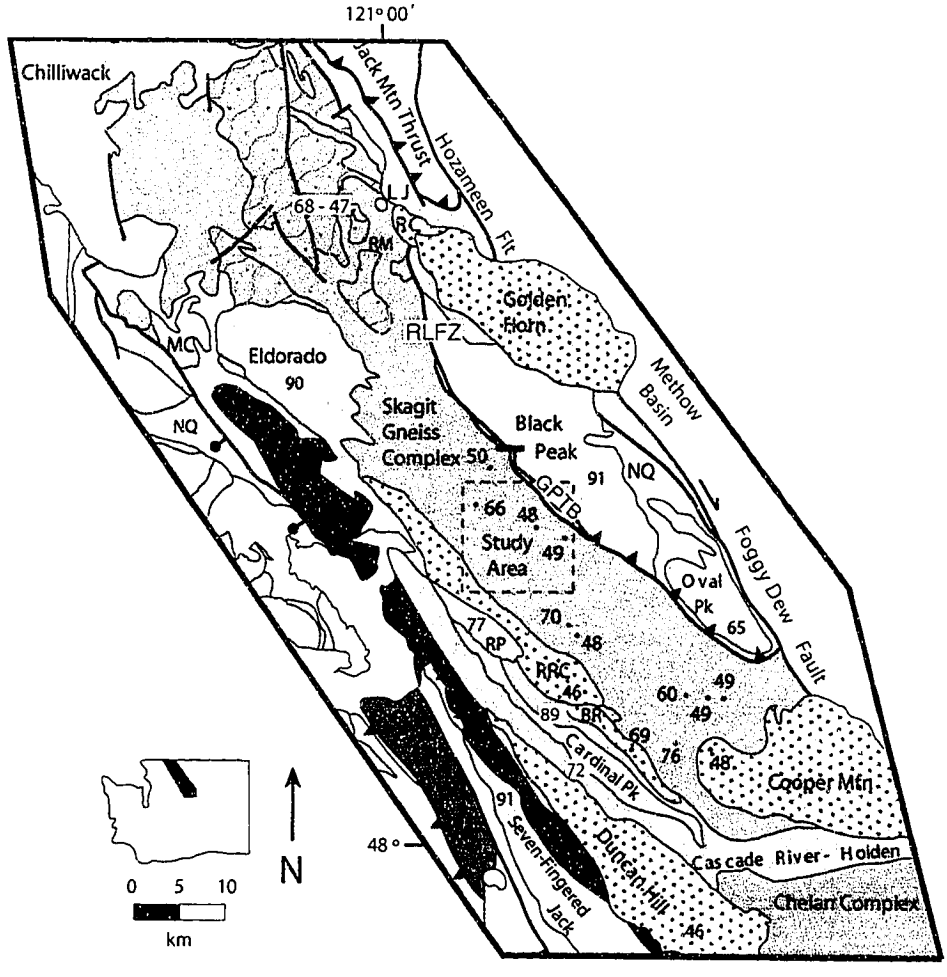

Figure 2. Sketch map of the Skagit Gneiss Complex and a portion of the Cascades core. Dashed box outlines research area. Plutonic rocks shaded orange; stippled pattern indicates Eocene crystallization ages. Yellow shading indicates undifferentiated Cenozoic rocks. Patterned portions in the Skagit Gneiss Complex are rich in paragneiss. BPB, Black Peak batholith; BR, Bearcat Ridge orthogneiss; GPTB, Gabriel Peak tectonic belt; LJ, Little Jack unit; MC, Marble Creek pluton; NQ, Napeequa unit; RC, Ruby Creek plutonic complex; RLFZ, Ross Lake fault zone; RM, Ruby Mountain; RP, Riddle Peaks pluton; RRC, Railroad Creek pluton. Ages shown in Ma for dated plutons and crystallization ages of orthogneiss within the Skagit Gneiss Complex.

orthogneisses, trondhjemitic pegmatites, and subordinate bodies of meta-supracrustal rocks (Misch, 1966, 1968; Yardley, 1978; Haugerud et al., 1991; Whitney, 1992). Parts of the complex, and particularly the metasedimentary rocks, are migmatitic. Pluton emplacement in the complex is coeval with ductile deformation and amphibolite-facies metamorphism (Haugerud et al., 1991).

Transpression dominated the Cascades core from ~72 to 55 Ma (Miller and Bowring, 1990; Hurlow and Nelson, 1991). North of the study area, migmatites in a paragneiss-rich portion of the Skagit Gneiss Complex near Ruby Mountain (Fig. 2) record peak metamorphic conditions of 8–10 kbar and 700–800 °C (Whitney, 1992; Gordon et al., 2008). Leucosomes in the eastern margin of the Skagit Gneiss yield zircon crystallization ages ranging from ca. 68 to 47 Ma (Gordon et al., 2007), indicating that parts of the complex were affected by metamorphism, partial melting, and magmatism until the late stages of orogeny. In contrast, the temperatures and timing of metamorphism and ductile deformation in the central part of the complex are so far poorly constrained. This investigation focuses on characterizing rock units and patterns of medium- to high-temperature deformation in an ~160 km^2, orthogneiss-dominated portion of the Central Skagit Gneiss Complex (Fig. 2).

Geologic Setting

The metamorphic and plutonic core of the North Cascades forms the southernmost segment of the >1500 km-long Cretaceous to Paleogene Coast Plutonic Complex, and has been translated southward from the complex along the dextral Straight Creek–Fraser Fault (Fig. 1). The main part of the Cascades core largely comprises Paleozoic to Mesozoic island arc and oceanic terranes that underwent amphibolite-facies metamorphism beginning in the mid-Cretaceous (Misch, 1966; Tabor et al., 1987, 1989), synchronous with NE–SW contraction (e.g., Misch, 1966; Miller et al., 2006).

The Cascades core is bounded by a Cretaceous thrust to the southeast (Miller, 1985) and by major high-angle Tertiary faults to the west and northeast (e.g., Misch, 1966; Miller et al., 1994). The major internal brittle structure is the Tertiary Entiat fault (Tabor et al., 1984), which divides the core into the Wenatchee block and the Chelan block (Figs. 1 and 2; Haugerud et al., 1991). The Chelan block is subdivided into the Swakane and Chelan Mountains terranes.

Major supracrustal units in the Chelan Mountains terrane are the Cascade River–Holden assemblage and the Napeequa complex (Fig. 2; Tabor et al., 1987). The Cascade River–Holden assemblage forms part of a Triassic arc sequence that is intruded by the strongly-deformed, tonalitic Triassic Dumbell plutons (Tabor et al., 1989). These plutons comprise the

roots of the Triassic arc. The Holden assemblage consists of amphibolites, hornblende gneisses, hornblende-biotite schists, and less abundant calc-silicate rocks, marbles, and leucocratic gneisses (Cater, 1982; Miller et al., 1994). The Napeequa complex has an oceanic protolith (Tabor et al., 1987), and is composed of quartzites, amphibolites, siliceous schists, and marbles (Cater, 1982; Tabor et al., 1987). The Twisp Valley schist (Adams, 1964) and Rainbow Lake schist are correlated with the Napeequa complex (Miller et al., 1993b).

The Swakane terrane is not intruded by pre-Miocene arc plutons, and is composed entirely of the Swakane Gneiss. The Swakane Gneiss is dominantly biotite ± garnet and muscovite gneiss with subordinate garnet amphibolite (e.g., Mattinson, 1972; Tabor et al., 1987; Paterson et al., 2004). Protoliths of the Swakane gneiss were deposited in the Cretaceous and rapidly buried (Matzel et al., 2004). Both the Swakane Gneiss and the Napeequa unit record clockwise P-T-t paths with peak metamorphic conditions of 9–12 kbar and 640–740 °C (Valley et al., 2003).

In the Chelan block, the Swakane Gneiss forms the footwall of the Dinkelman decollement (Alsleben, 2000; Paterson et al., 2004), and is structurally overlain by the Napeequa complex. It has been proposed that the contact between these units was originally a SW-directed thrust (Tabor et al., 1987; Hurlow and Nelson, 1991; Paterson et al., 2004), reactivated by top-to-N–NNE motion during exhumation (Paterson et al., 2004) However, little

evidence of top-to-WSW-directed motion is preserved in the Swakane Gneiss (Alsleben, 2000), and burial may have been accomplished along a structure that is no longer exposed (Matzel et al., 2004). Subhorizontal stretching in the gneiss is thought to be post-55 Ma (Paterson et al., 2004) and may overlap with Eocene deformation in the Skagit Gneiss Complex.

Magmatism in the Cascades core was sporadic, with widespread and voluminous mid-Cretaceous plutonism between ~96 Ma and 88 Ma (e.g., Mattinson, 1972; Walker and Brown, 1993; Matzel et al., 2006). Later intrusions migrate eastward in the central (ca. 78–72 Ma) and northeastern (ca. 68–45 Ma) parts of the core (Miller et al., 1989). Highly elongate, heterogeneous Late Cretaceous plutons form part of a narrow, NW-striking belt of elongate and variably deformed intrusive complexes (Miller and Paterson, 2001b). Deformed Eocene crystalline rocks indicate that magmatism ca. 50–45 Ma was in part coeval with ongoing ductile deformation (e.g., Haugerud et al., 1991).

K–Ar and $^{40}Ar/^{39}Ar$ biotite cooling ages from the southern part of the Wenatchee block range from 90 to 81 Ma (e.g., Engels et al., 1976; Tabor et al., 1987; Evans and Davidson, 1999) and indicate that the southern end of the Cascades core cooled moderately fast to rapidly during the Cretaceous. In contrast, concordant hornblende and biotite dates of ~46 Ma in the northern part of the Skagit Gneiss Complex indicate rapid cooling at a much younger time (Haugerud et al., 1991; Wernicke and Getty, 1997). The

complex thus remained hot into the Eocene, recording the younger part of the thermal and structural history of the Cascades core.

Thermobarometric data from supracrustal rocks in migmatitic parts of the Skagit Gneiss Complex indicate peak metamorphic conditions of 650–725 °C at 8–10 kbar, representing burial to depths of 25–35 km (Whitney, 1992). Models for the development of the Cascades core attribute burial and crustal thickening to either mid-Cretaceous intra-arc shortening (e.g., Brandon et al., 1988; McGroder, 1991; Paterson and Miller, 1998), or to magma loading by plutons (Brown and Walker, 1993). After shortening, the crustal thickness of the Cascades core was probably ≥ 55 km (Miller and Paterson, 2001b).

The Ross Lake fault zone (Fig. 1) forms the northeastern boundary of the Cascades core and juxtaposes amphibolite-facies rocks of the Skagit Gneiss Complex against lower-greenschist-facies strata (e.g., Misch, 1966; Miller and Bowring, 1990; Miller et al., 1994). It is an ~10-km-wide system of dominantly dextral strike-slip faults, with components of Paleocene reverse slip and Eocene normal slip, that was active from at least 65 to 45 Ma (e.g., Misch, 1966; Haugerud, 1985; Miller and Bowring, 1990; Miller et al., 1994). Within the study area, the Gabriel Peak tectonic belt (Figs. 2 and 3) is the southeastern extension of the Ross Lake fault and separates the Skagit Gneiss Complex from the Rainbow Lake schist and the ~90 Ma Black Peak batholith to the east (Fig. 3). Foliation in this zone is subparallel to

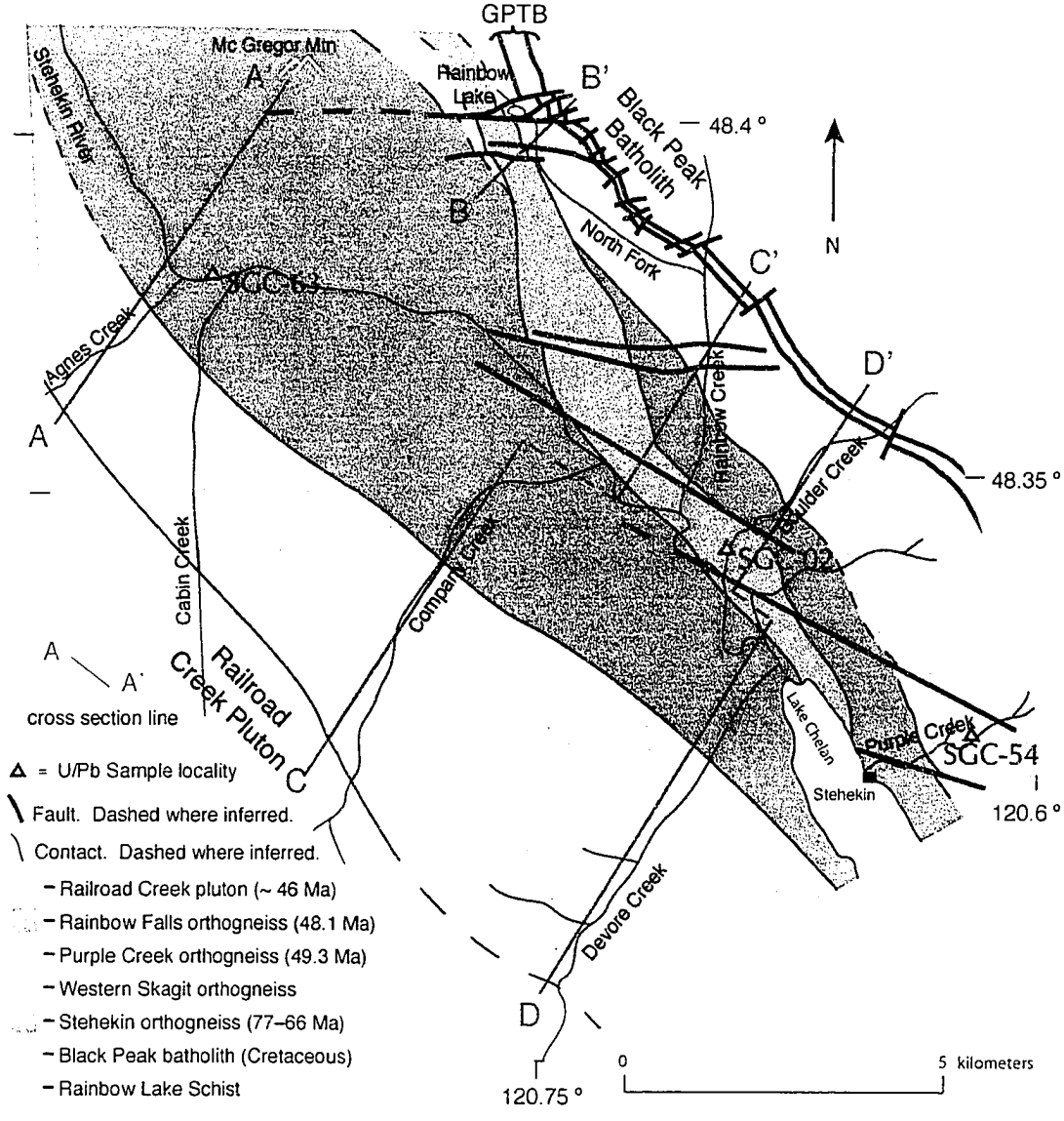

Figure 3A. Map of study area emphasizing rock units, sample sites, and localities mentioned in text. GPTB = Gabriel Peak tectonic belt. Cross-sections shown in Figure 3B.

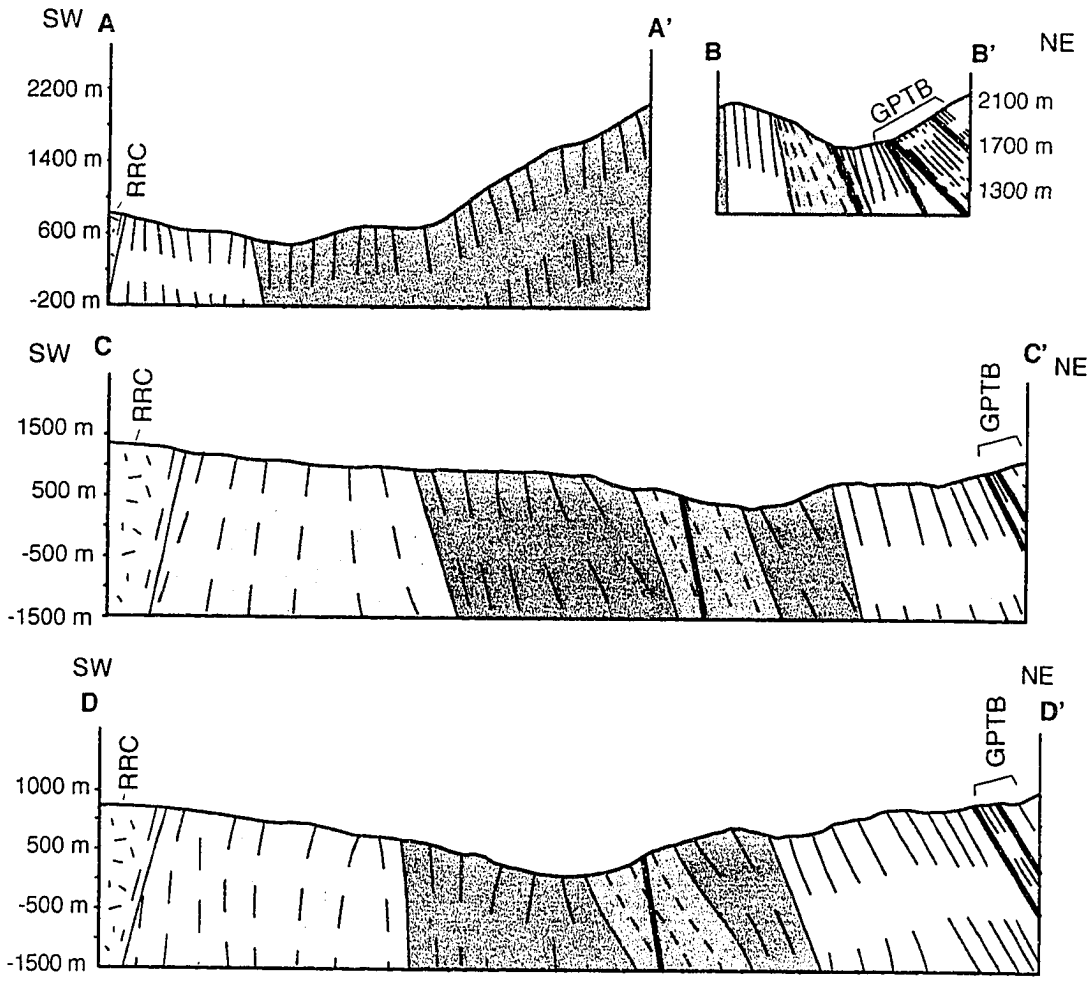

Figure 3B. Cross-sections (no vertical exaggeration) through the central Skagit Gneiss Complex. Explanation for rock units given in Figure 3A. Dashes and lines are parallel to foliation (inferred from measurements). Locations of cross-section lines are shown in Figure 3A. GPTB, Gabriel Peak tectonic belt; RRC, Railroad Creek pluton.

NW-trending contacts and generally dips 65–70° NE (Miller and Bowring, 1990; Miller et al., 1994).

On the SW side of the Gabriel Peak tectonic belt, N- to NE-trending lineations have been mapped in the study region (e.g., Adams, 1961; Libby, 1964; Dragovich and Norman, 1995; Miller, 1987) and are a major focus of this study. These lineations deviate by more than 40° from the dominant NW regional grain and the Gabriel Peak tectonic belt. In the deeply exhumed Swakane biotite gneiss, subhorizontal stretching lineations are inferred to be subparallel to Eocene top-to-N to -NNE displacement during exhumation (Paterson et al., 2004; Miller et al., 2006), and may overlap with deformation in the Skagit Gneiss Complex. Structures in orthogneisses in the Central Skagit Gneiss Complex may help constrain the extent of Eocene ductile deformation, and contribute to a better understanding of crustal flow in the orogen. This study focuses on the timing, patterns, and temperature conditions of mid- to deep-crustal deformation in an orthogneiss-dominated portion of the complex.

Methods

In order to better understand the history and tectonic significance of the Skagit Gneiss Complex, a three-part investigation was conducted: (1) field study; (2) petrographic study; and (3) isotopic (U/Pb) geochronologic study.

The research area covers ~160 km^2 between the north end of Lake Chelan and McGregor Mountain (Figs. 2 and 3). This area has received little modern structural and petrological study, and previous reconnaissance-scale mapping was completed before topographic maps were available (Adams, 1961; Libby, 1964). A major objective of this field study is to describe structural patterns in the Central Skagit Gneiss Complex and interpret the contact relationships between adjacent units (i.e., intrusive vs. tectonic).

During the Summer of 2006, field observations were made within three NE–SW-trending corridors through the Skagit Gneiss Complex. The study corridors are roughly equally spaced (~5 km apart) and are elongate approximately perpendicular to the strike of regional structures. The corridors range from 8 km to 12 km in length. Structural mapping was conducted using the Stehekin, Sun Mountain, Mt. Lyall, McAllester Mountain, and McGregor Mountain U.S. Geological Society 7 1/2' quadrangle topographic base maps (1:24,000 scale). Plate 1 displays all structures mapped during this study.

During the Fall of 2006, fifty-eight oriented samples were cut into thin-sections along a surface parallel to lineation and perpendicular to foliation. Subsequent microscopic investigation focused on identifying metamorphic mineral assemblages, ductile microstructures and deformation mechanisms, and kinematic indicators for sense-of-shear.

Isotopic (U/Pb) geochronologic analyses were conducted on single-grain zircon fractions from three gneiss samples with igneous protoliths. The

resultant age data are synthesized with structural observations from this study to constrain the timing of magmatism and latest ductile deformation in the Central Skagit Gneiss Complex.

ROCK UNITS

Tonalitic orthogneiss of the Skagit Gneiss Complex comprises >90% of the rocks in the study area. Granodioritic to granitic orthogneisses make up <5% of the area. Metamorphosed supracrustal rocks are sparse in the study area, and the Rainbow Lake schist (Figs. 2 and 3) is the only mappable metasedimentary unit. Orthogneisses enclose lenses of amphibolite and biotite-schist and are cut by abundant veins and sheets of pegmatitic trondhjemite.

Rainbow Lake Schist

The Rainbow Lake schist (Figs. 2 and 3) forms a NW-striking, NE-dipping belt that is <300 m thick within the the Gabriel Peak tectonic belt. The unit is composed predominantly of biotite ± garnet ± muscovite ± staurolite ± sillimanite schist, quartzose schist, and amphibolite. These rocks were previously mapped as Twisp Valley schist by Adams (1964) and are currently correlated with rocks of the oceanic Napeequa unit (Miller et al., 1993b; Miller

et al., 1994).

The brown weathering and compositional layering of the Rainbow Lake schist make it useful as a structural marker in the field. Leucocratic, garnet-bearing granitic sills form thin layers (<25 cm thick) within most of the unit and thicker layers (1 m to 3 m thick) near the structural base. Biotite schist layers are ubiquitous and range from 15 cm to ~2 m in thickness. Amphibolites are 10 cm to ~2.5 m thick. Quartzite layers are typically less than 1 m thick.

Mineral assemblages and modes indicate oceanic sedimentary protoliths metamorphosed at amphibolite-facies conditions (>500 °C). Quartz + biotite ± garnet ± staurolite ± sillimanite assemblages are inferred to have pelitic protoliths. Garnet and staurolite form the most common porphyroblasts. Some rocks contain retrograde chlorite, which replaces biotite. Amphibolites in the unit contain hornblende + plagioclase ± biotite ± quartz. Rare marbles composed of calcite ± quartz ± garnet ± plagioclase are metamorphosed impure limestones. Quartzites are interpreted as metacherts. The inferred protoliths support correlation with rocks of the oceanic Napeequa unit, the age of which is only constrained to predate emplacement of the oldest (96 Ma) Cretaceous plutons in the Cascades core. Thermobarometric analyses of garnet-biotite-sillimanite schists from the Rainbow Lake schist near Boulder Creek (Fig. 3) indicate metamorphic pressures of 5–7 kbar at 600 °C (S.M. Gordon, written communication, 2008), compatible with conditions at depths of ~15–25 km. These results are in

broad agreement with previously obtained metamorphic pressures and temperatures from the Rainbow Lake Schist (Miller et al., 1993b).

The Rainbow Lake schist extends NW and SE from the study area as discontinuous lenses for a total length of ~45 km (Adams, 1961; Tabor et al., 1989; Miller et al., 1993b). The NE contact is a 10- to 20-m-wide mylonitic zone that contains discrete lenses (<30 m long) of Rainbow Lake schist amidst marginal gneissic rocks of the Cretaceous Black Peak batholith (e.g., Adams, 1961; Miller, et al., 1994). The SW contact of the Rainbow Lake schist with orthogneisses of the Central Skagit Gneiss Complex (Fig. 3A) is a 5- to 10-m-wide zone that contains xenoliths of the schist enclosed by strongly deformed sheets of tonalitic Skagit orthogneiss (Fig. 4).

Rocks of the Skagit Gneiss Complex

The first descriptions by Misch (1952) of rocks now assigned to the Skagit Gneiss Complex included various gneissic rocks in one heterogeneous unit called the Skagit Gneiss. Adams (1961) expanded the southern extent of Misch's (1952, 1966, 1968) Skagit Gneiss, and separated the unit into the War Creek gneiss, Rainbow Lake schist, and central, eastern, and western McGregor gneisses. The differentiation of the gneiss units was chiefly based on the presence or absence of hornblende (Adams, 1961).

This study reinterprets rocks mapped as Skagit Gneiss Complex and

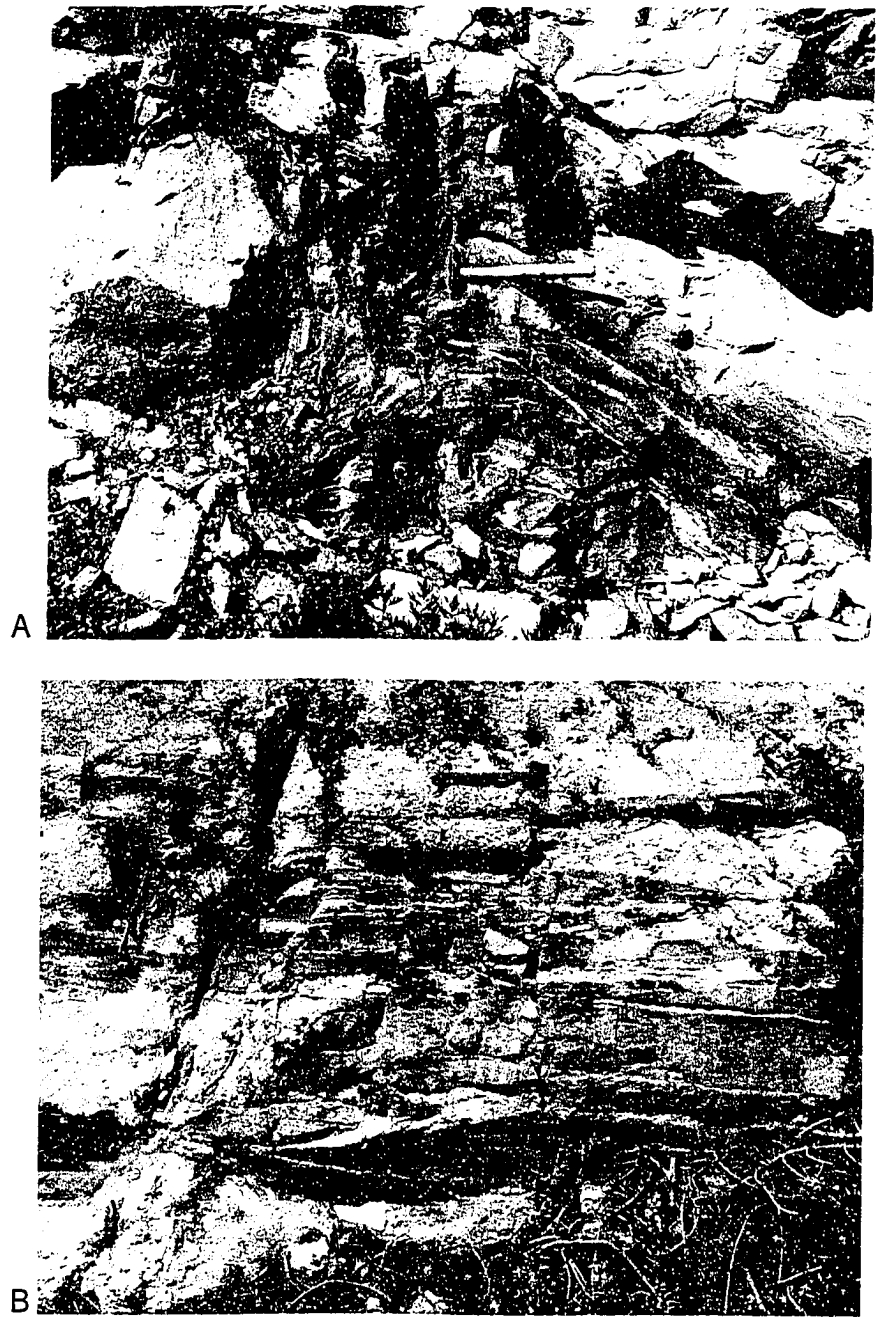

Figure 4. Supracrustal lenses in orthogneiss at the contact of the Rainbow Lake schist with the Skagit Gneiss Complex. (A) Biotite-schist xenolith enveloped by orthogneiss in the Gabriel Peak tectonic belt. View is looking northeast, with hammer for scale. (B) Asymmetric lens of biotite schist in Skagit orthogneiss in the Gabriel Peak tectonic belt. View is looking east; pencil (~15 cm) for scale.

further differentiates gneiss units based on field, petrographic, and geochronologic data. Color index, relative abundance of major minerals, and cross-cutting relationships form the main criteria for unit differentiation. Major orthogneiss mineral constituents include plagioclase, quartz, biotite, ± hornblende, ± K-feldspar, ± muscovite. Common accessory minerals include sphene, apatite, and zircon.

In the study area, the Central Skagit Gneiss Complex forms a northwest-southeast elongate belt that is ~11 km wide. Along the southwest contact, <3-m-thick sheets of the ca. 46 Ma Railroad Creek pluton (see below) concordantly intrude the gneiss complex (Fig. 3). This undeformed pluton is elongate parallel to the regional structural trend of the Cascades core and to foliation in the adjacent Skagit rocks. It constrains the SW extent of ductile deformation in the study area.

The Skagit Gneiss Complex is texturally and modally heterogeneous. It is composed primarily of tonalitic to trondhjemitic orthogneisses that are cut by abundant pegmatitic and aplitic trondhjemites, and by syn-kinematic to post-kinematic granitic to tonalitic dikes and sills. Orthogneisses range in age from at least ~66 Ma to ~48 Ma (see geochronology section). The following rock descriptions are organized by the inferred ages of units, beginning with the oldest. Petrographic characteristics of units are reported as needed to differentiate rock types. Microstructural and mesoscopic structural analysis is addressed in subsequent chapters.

Stehekin Orthogneiss

Cross-cutting relationships indicate that the Stehekin orthogneiss is the oldest unit in the Central Skagit Gneiss Complex. It forms an ~5-km-wide body in map view and has an apparent structural thickness of at least 3 km. The most abundant rock type is a leucocratic (color index ~8), medium- to coarse-grained biotite tonalite orthogneiss. The unit is differentiated from other Skagit orthogneisses by the typical lack of hornblende and by the presence of migmatite-rich zones.

The migmatites are well exposed at elevations below 730 m in road cuts and cliffs on either side of the Stehekin River valley and on the NE side of Lake Chelan (Plate 1). Migmatitic gneiss in the unit is largely orthogneiss with concordant lenses (<5 m thick) of biotite schist, garnet-biotite schist, and amphibolite cross-cut by leucocratic pegmatite sheets ranging from 1 cm to 10 m in thickness. The schists and amphibolites in the lenses are broadly similar to metasedimentary rocks in northern and southern parts of the Skagit Gneiss Complex that are inferred to be correlative with rocks of the Holden assemblage (Miller et al., 1994). Agmatitic and stromatic migmatites are most common in the study area and locally contain ptygmatic leucosomes.

Orthogneiss makes up at least 90% of the unit and is intruded by strongly deformed dikes and sills of fine- to medium-grained biotite tonalite orthogneiss. Aligned biotite best defines foliation. Lineation is defined by elongated quartz and plagioclase aggregates. In the northern part of the

area, lineation is locally stronger than foliation (L > S). Elsewhere, foliation and lineation are equally well-developed.

The Stehekin orthogneiss is elongate subparallel to the NW regional strike of the Skagit Gneiss Complex. The southwest contact with undifferentiated orthogneiss is delineated by a drastic decrease in abundance of leucocratic pegmatite, a decrease in abundance of metasedimentary lenses, and by the disappearance of hornblende. The eastern contact is intruded concordantly by <10-m-thick gneissic sheets of Eocene units described below.

Major constituents of the Stehekin orthogneiss are plagioclase, quartz, biotite, and locally, hornblende. Accessory minerals include muscovite, sphene, rutile, garnet, fibrolite, apatite, zircon, and magnetite. Altogether, the accessory phases rarely comprise more than 1% of the rock by volume. The average modal abundances (volume percentages) of minerals in the orthogneisses are: plagioclase, 55%; quartz, 35%; K-feldspar, 4%; biotite, 3%; chlorite, 2%; hornblende, >0.5%; sphene, <0.5%. Garnets are locally present as inclusions in poikilitic plagioclase crystals. Plagioclase is locally slightly sericitized, and biotite is rarely altered to chlorite. Metamorphic fibrous sillimanite (discussed below) was observed in one sample of the Stehekin orthogneiss collected near the base of McGregor Mountain (Plate 1).

Plagioclase typically makes up 50% to 55% of the orthogneiss.

Trondhjemitic pegmatites in the southern half of the unit contain up to 70% plagioclase. Plagioclase is mostly 0.5 mm to 2 mm in length, but in pegmatites falls in the 1 to 2 cm range. Oscillatory zoning and local synneusis are relict magmatic features. Poikilitic plagioclase phenocrysts are up to 3 mm in diameter, and contain orthogonal (Fig. 5) and randomly oriented biotite inclusions, and locally contain garnet.

Quartz is a major constituent in all of the rocks of the unit. On average, it makes up 30–35% of the orthogneiss; it is more abundant in leucocratic segregations. Many crystals have developed subgrains. In the most deformed rocks, quartz aggregates form elongate ribbons that are typically <5 cm long.

The average grain size of biotite ranges between 0.1 and 0.5 mm, although in the coarse-grained rocks, it ranges up to 2 mm in length. Tiny inclusions of apatite and acicular zircon grains occur inside many biotite crystals. Biotite is typically bent around plagioclase crystals and is recrystallized in shear bands.

K-feldspar is unevenly distributed in the Stehekin orthogneiss and makes up <5% of most rocks in the northern half of the unit. Crystals are usually smaller than 0.5 mm in diameter. In the pegmatites in the southern part of the unit, K-feldspar also forms up to 2-mm-long poikilitic phenocrysts (Fig. 6). The phenocrysts contain scattered inclusions of small (<0.1 mm) biotite and quartz crystals. Myremekite lobes are typical at the contact

Figure 5. Poikilitic plagioclase from Stehekin orthogneiss with orthogonal biotite inclusions and isotropic garnet (~0.55 mm diameter, center) inclusion (base of picture is 4 mm).

Figure 6. Poikilitic K-feldspar phenocryst in Stehekin orthogneiss containing randomly oriented biotite crystals. Base of picture is 4 mm.

between K-feldspar phenocrysts and plagioclase.

One sample of Stehekin orthogneiss (Fig. 7) contains ~8% K-feldspar associated with ~1% fibrous sillimanite, and 1% muscovite. The fibrolite is surrounded by muscovite, quartz, and K-feldspar, and is interpreted to have formed during the breakdown of muscovite and quartz to form sillimanite + K-feldspar at temperatures exceeding 650 °C (i.e., Winter, 2001).

Hornblende is most common near the eastern contact, where it locally constitutes up to 3% of the rocks by volume. Hornblende is subhedral and forms as inclusions in some K-feldspar phenocrysts.

Sphene is widespread and locally forms euhedral crystals in less-deformed rocks. Typically, sphene is brittlely deformed, appearing as fragmented crystals, <0.25 mm in diameter, in the groundmass of the orthogneiss. It is absent in leucocratic pegmatites and aplites. Sphene is slightly more abundant, although still <1% in hornblende-bearing rocks.

Western Skagit Orthogneiss

The Western Skagit orthogneiss (Fig. 3) is heterogeneous and incorporates all of the gneisses west of the Stehekin orthogneiss. Medium- to coarse-grained tonalitic orthogneisses form the majority of rocks and contain rare (<2% of the unit), concordant lenses of biotite schist that are 10 cm to 5 m long and 1 cm to 50 cm wide. The most abundant rocks are foliated biotite orthogneisses with local hornblende. Biotite chiefly defines the foliation.

Figure 7. Photomicrograph (crossed-polars) of Stehekin orthogneiss. In the center of the photo, fibrolite is surrounded by muscovite, quartz and K-feldspar. Field of view is 1.5 mm.

Concordant lenses, 5 cm to ~20 m thick, of medium- to fine-grained, lineated biotite gneiss with local hornblende are widespread and make up approximately 15% of the unit. This rock type also occurs as <2-m-wide lenses in the Stehekin orthogneiss. The Western Skagit orthogneiss is intruded by 2- to 40-cm-thick concordant and discordant sheets of trondhjemitic pegmatite.

The average volume percentage of major minerals in the unit are: plagioclase, 50%; quartz, 32%; K-feldspar, 9%, biotite, 6–7%; and hornblende, 1–2%. Accessory minerals include sphene, apatite, magnetite, and zircon. Trondhjemitic pegmatites in the unit contain higher percentages of plagioclase and quartz, which locally make up more than 90% of the rocks by volume.

The Western Skagit orthogneiss intrudes migmatitic gneiss of the Stehekin unit to the east. The contact is drawn based on the abundance of pegmatite, as the Western Skagit orthogneiss contains <5% pegmatitic trondhjemite on average. To the west, the unit is intruded by the Eocene Railroad Creek pluton.

Purple Creek Orthogneiss

The heterogeneous Purple Creek orthogneiss is composed of sheets of medium-grained, lineated (L > S) biotite-hornblende tonalite gneiss that grades eastward into medium-grained, well-foliated (S = L) biotite tonalite

leucogneiss. Foliation is defined by the preferred orientation of biotite and elongate quartz. Lineation is chiefly defined by elongated quartz and plagioclase aggregates, and by aligned hornblende. The unit is distinguished by an increase in the abundance of hornblende compared to the Stehekin orthogneiss to the west. Swarms of contact-parallel, ellipsoidal dioritic enclaves (Fig. 8) are present up to 20 m into the Purple Creek orthogneiss. Enclaves with higher average aspect ratios (10:1) are also found locally within the main body of the Purple Creek orthogneiss and near the contact with the Rainbow Falls orthogneiss (see below). These enclaves are commonly associated with wispy biotite- and hornblende-rich schlieren.

Two distinct rock types comprise enclaves in the Purple Creek orthogneiss (Fig. 8). The most common is medium-grained, porphyritic diorite that contains hornblende phenocrysts ranging up to 2 cm in length (Fig. 9). This rock type typically forms large enclaves that measure up to 2 m long and 0.75 m wide in the northern half of the study area. The other enclaves are only present locally near the western contact and are dark-colored, fine-grained, porphyritic tonalite that contains plagioclase phenocrysts ranging from 2 mm to 12 mm in length. These enclaves are smaller (<30 cm long and 15 cm wide) than the dioritic enclaves.

Enclaves in the Purple Creek orthogneiss typically have hornblende-enriched rims that are <1 cm thick and most pronounced at the edges of the tonalite enclaves. Hornblende in the rim is typically finer-grained than the rest

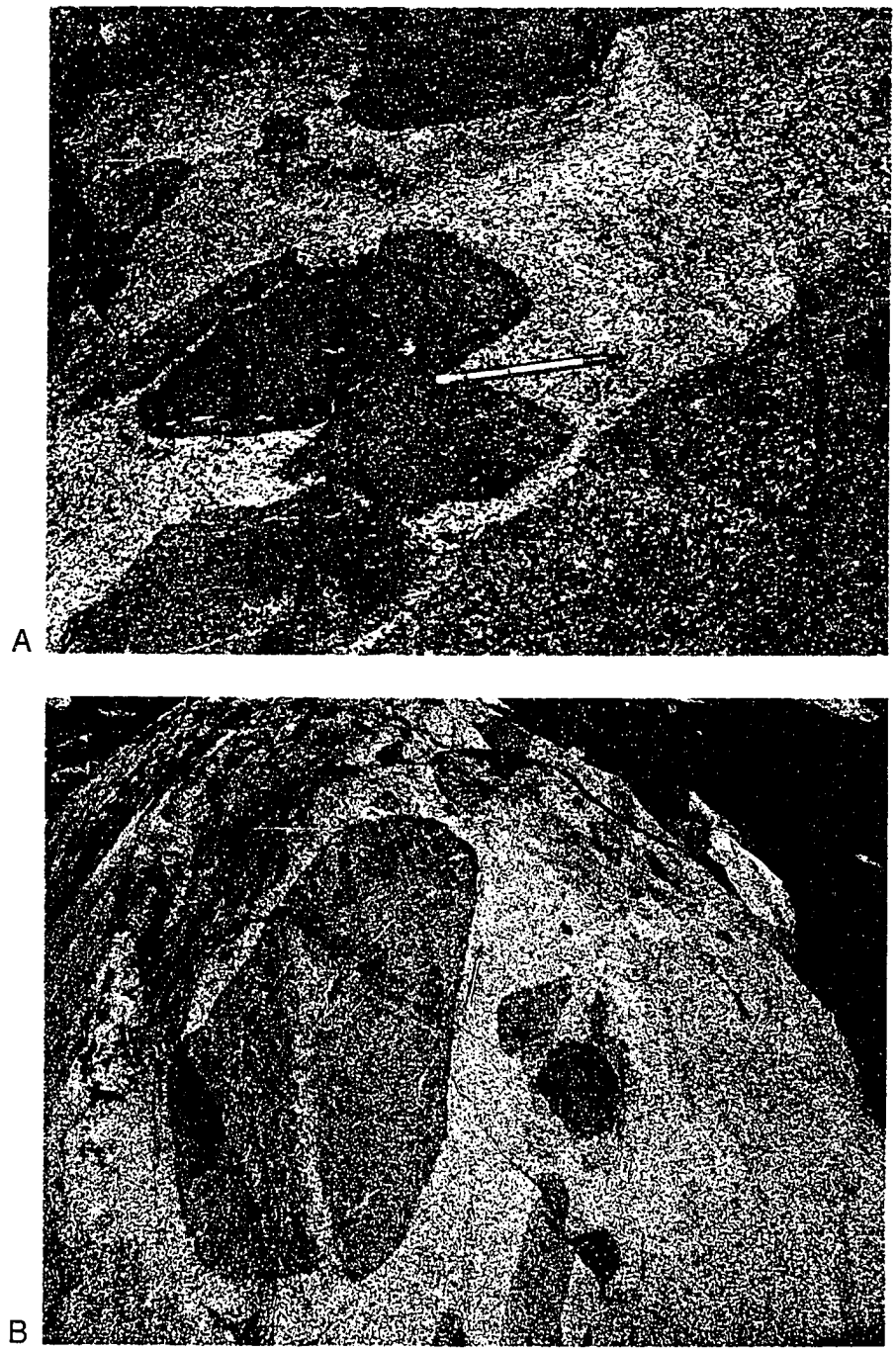

Figure 8. Swarms of ellipsoidal diorite and tonalite enclaves in Purple Creek orthogneiss ~10 m from the contact between the Purple Creek and Stehekin orthogneisses. Pencil for scale is ~15 cm long. Tip of pencil points north in both photographs. (A) Diorite and tonalite enclaves (see text for descriptions) with quenched hornblende-rich reaction rims. (B) Diorite enclaves, which dominate at the contact in the northern half of the study area.

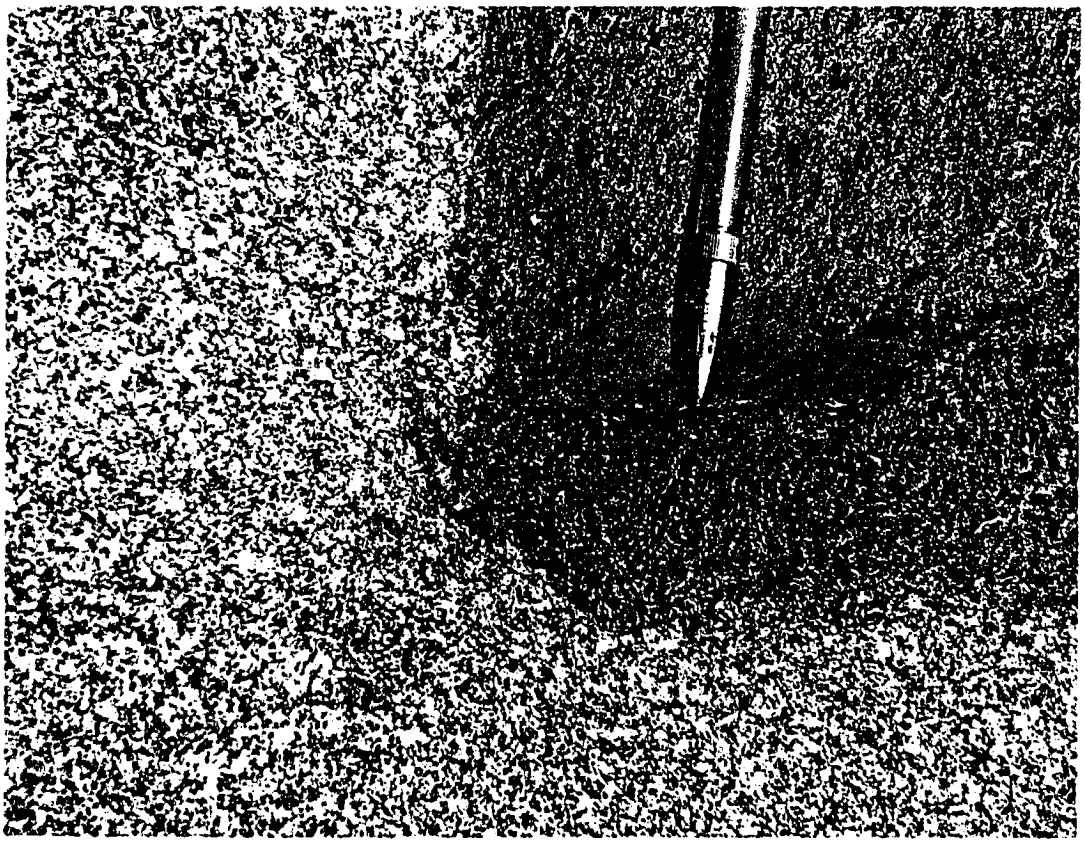

Figure 9. Hornblende-phyric diorite enclave with narrow (1–2 mm) hornblende reaction rim in weakly-foliated Purple Creek orthogneiss. Strong hornblende-defined foliation in the enclave is subparallel to the mean foliation orientation in the unit (pencil for scale).

of the enclave. The tonalitic enclaves locally contain small (<3 mm) phenocrysts of sphene that give the rock an appearance and modal mineralogy similar to those of the Rainbow Falls orthogneiss (see below). The hornblende-rimmed enclaves are interpreted to indicate magma quenching during mingling along the western contact.

The eastern contact of the Purple Creek orthogneiss with the Rainbow Lake schist marks the limit of the Skagit Gneiss complex in the study area. Here, the Purple Creek orthogneiss is slightly more leucocratic (color index ~4), and foliation and lineation are equally developed. The tectonic boundary separating these units is characterized by a <10-m-wide zone of intense sheeting, and the orthogneiss encloses tabular and asymmetric lenses of biotite schist and amphibolite. The asymmetry of these features suggests dextral shear across the the tectonic contact as described in more detail in the kinematics chapter.

The western contact is marked by <10-m-thick concordant sheets of Purple Creek orthogneiss that intrude the Stehekin orthogneiss. This contact is delineated where sheets of hornblende-bearing Purple Creek orthogneiss make up <50% of the outcrop. The Stehekin–Purple Creek contact is cut out in the northern half of the field area by the discordant intrusion of the Rainbow Falls orthogneiss.

Major constituents of the Purple Creek orthogneiss are plagioclase, quartz, biotite, hornblende, and locally sphene. Quartz on average makes up

35% to 40% of the unit. Plagioclase makes up at least 45% of the rocks, and up to 60% in coarse-grained leucocratic rocks. Hornblende varies from 2% to 8%. Accessory minerals include apatite, magnetite, rutile, and zircon.

Rainbow Falls Orthogneiss

The Rainbow Falls orthogneiss consists dominantly of grey (color index ~35), medium-grained, hornblende-biotite tonalitic orthogneiss with subordinate sheets (<20 m thick) of fine-grained hornblende-biotite tonalite. Foliation is moderate to weak in strength, and locally absent in some of the tonalite sheets. It is defined by alignment of biotite and elongate quartz aggregates. Lineation is consistently much better-developed than foliation, and is defined by a subhorizontal preferred orientation of hornblende crystals and spindle-shaped clusters of quartz and plagioclase.

The Rainbow Falls rocks consist mainly of plagioclase, quartz, biotite, hornblende, and minor sphene. Compared to other units in the study area, the orthogneiss contains the least volume of quartz on average (~28%), and the greatest average volume of biotite (~9%) and hornblende (~7%). Accessory minerals include apatite, rutile, and zircon. Local trondhjemitic pegmatites contain up to 40% quartz and up to 60% plagioclase. The abundance of sphene is distinctive of the Rainbow Falls rocks. Sphene makes up greater than 1% of the unit on average, and commonly occupies the center of plagioclase clusters (Fig. 10). Sphenes inside clusters are up to

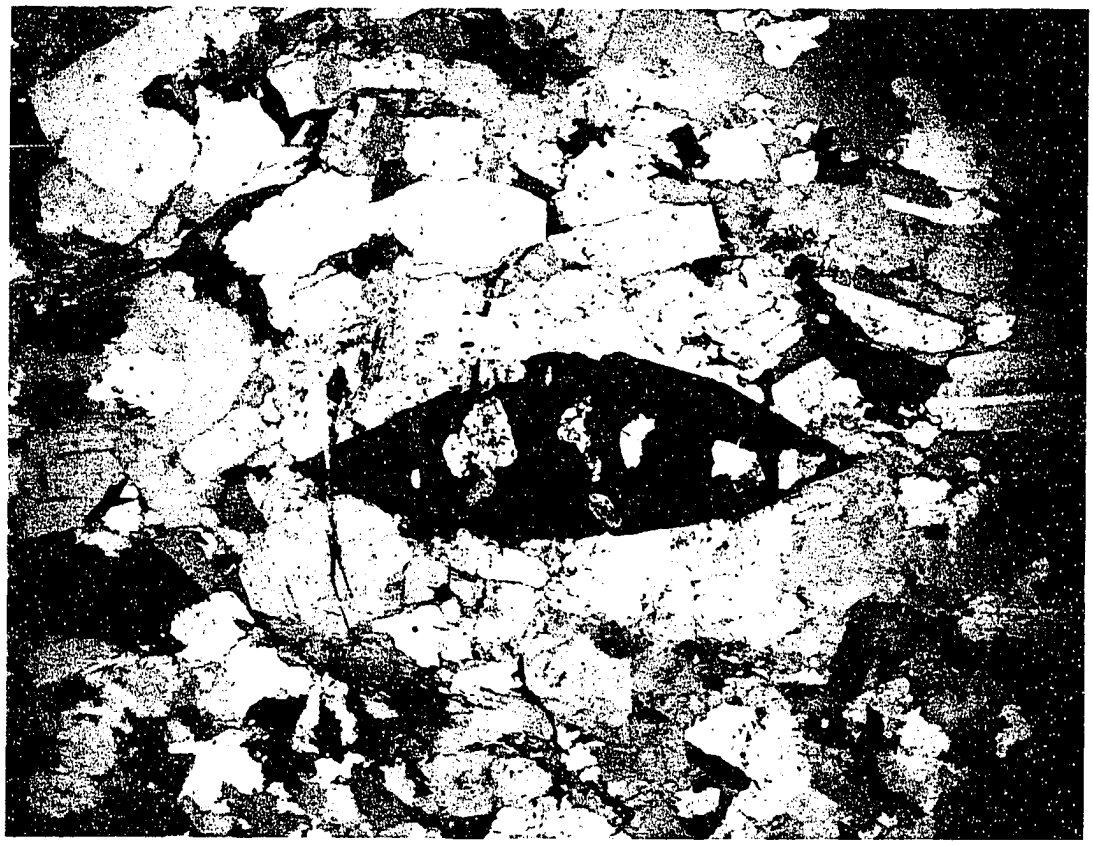

Figure 10. Photomicrograph of characteristic sphene-cored, ellipsoidal plagioclase cluster in Rainbow Falls orthogneiss (crossed-polars). Base of photo is 8 mm.

1 cm in length and are euhedral. The origin of these unusual clusters is unknown.

The western half of the orthogneiss is finer-grained and contains characteristic, variably-deformed quartz-plagioclase clusters up to 1 cm in diameter, which locally comprise up to 10% of the rock. To the northeast, clusters disappear and orthogneiss grades into medium-to coarse-grained, more-gneissose rocks richer in quartz and plagioclase. The eastern half of the unit is characterized by well-foliated hornblende-biotite tonalite orthogneiss with a color index of ~30.

The Rainbow Falls orthogneiss is the youngest unit (ca. 48 Ma, see below) in the study area and discordantly intrudes the Purple Creek and Stehekin orthogneisses. It forms a NNW-trending, ~1.5-km-wide outcrop belt (Plate 1). The western intrusive boundary with the Stehekin orthogneiss and Purple Creek orthogneiss dips >65° to the east. It is drawn where <2-m-thick sheets of the intruding Rainbow Falls rocks comprise <50% of the outcrop.

Dikes and Other Late Intrusions in the Skagit Gneiss Complex

Pre- to syn-kinematic and post-kinematic dikes are present in the study area. The dikes are typically fine-grained and range from 1 cm to ~5 m in thickness. Post-kinematic dikes cut all ductile fabrics and unit contacts. The dikes in the study area have not been directly dated, but post-kinematic dikes

cut orthogneisses dated at 48–49 Ma (see below), indicating a maximum age of ~48 Ma.

Andesitic and rhyodacitic dikes were studied in thin section (Fig. 11). Trachytic texture is well-developed in one andesite with phenocrysts of plagioclase, K-feldspar, hornblende, clinopyroxene, and biotite. The rhyodacite dikes contain phenocrysts of quartz, plagioclase, K-feldspar, biotite, and hornblende. Grain boundaries of quartz phenocrysts in the rhyodacite dikes are locally lobate, indicating resorption.

Railroad Creek Pluton

Major mineral constituents of the undeformed Railroad Creek pluton, as observed from three hand samples and thin sections from the study area, are: quartz (~35%), plagioclase (~40%), K-feldspar (~18%), biotite (~4%), hornblende (~2%), and chlorite (<1%). These granodiorites are medium-grained, have hypidiomorphic granular texture, and contain oscillatory-zoned, unambiguously igneous plagioclase crystals (Fig. 12). Quartz is slightly undulose to strain-free. Micro-faulting and cracking are observed in only a few plagioclase crystals. One hand-sample contains slightly elongated quartz grains with aspect ratios of ~1.5:1.

Figure 11. (A) Andesitic dike with trachytic texture under plane polarized light. Base of photo is 4 mm. (B) Rhyodacitic dike under cross-polarized light. Quartz in center of photo has highly lobate grain boundaries, indicating partial resorption. Base of photo is 8 mm.

A

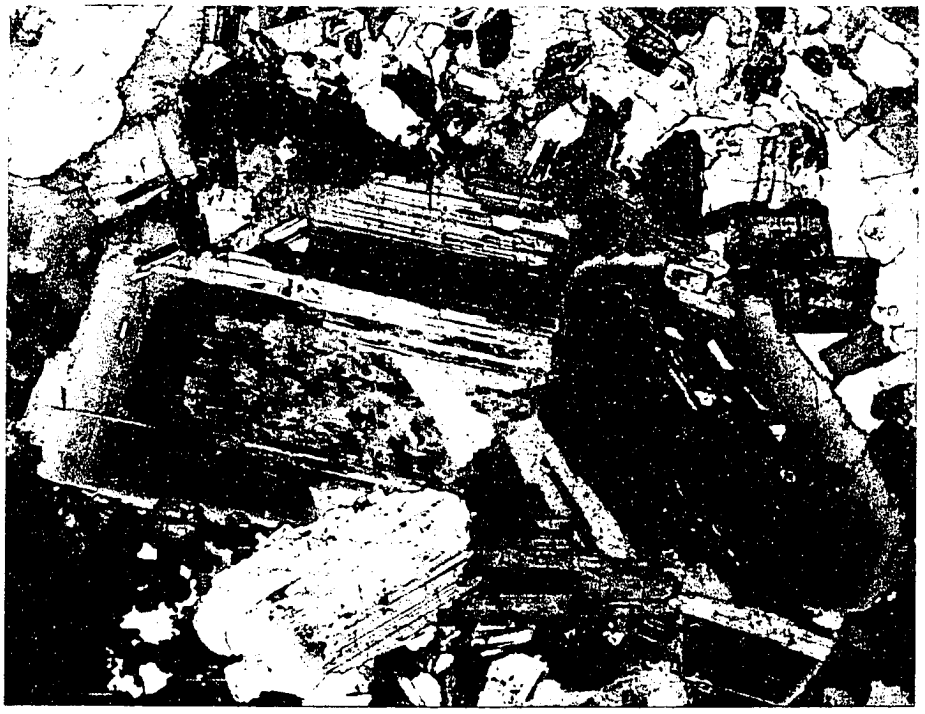

B

Figure 12. Photomicrographs (crossed-polars) of igneous textures in Railroad Creek pluton. (A) Cluster of zoned plagioclase phenocrysts (base of photo = 8 mm). (B) Poikilitic K-feldspar containing inclusions of zoned plagioclase, biotite, and hornblende (base of photo = 8 mm).

The Railroad Creek pluton is an elongate body that intrudes the central Skagit Gneiss Complex, marking the southwest limit of orthogneiss (Libby, 1964; Cater and Wright, 1967) and ductile deformation in the research area. Crystallization of the pluton occurred at ca. 46 Ma (McLean et al., 2006), indicating that it is one of the youngest plutons in the Cascades core. The northern part of the contact with Central Skagit Gneiss rocks is drawn along a sharp boundary between homogeneous granodiorite and deformed heterogeneous tonalite orthogneiss. In the southern half of the study area, weakly to non-deformed sheets (0.5 m to 20 m in thickness) of granodiorite intrude the Western Skagit unit in a 150-m-wide, contact-parallel zone. The sheets are broadly concordant with foliation in the orthogneiss, but are locally discordant by up to 15°.

U-PB GEOCHRONOLOGY

New U-Pb analyses of three orthogneiss samples (Fig. 13) from the Skagit Gneiss Complex are presented in Table 1 and illustrated in Figures 14, 15, and 16. The samples were chosen from different volumetrically significant orthogneiss units within the study area. Sample localities are shown in Figure 3A and Plate 1.

Isotopic ages were determined by single-grain zircon U/Pb ID-TIMS. Zircons were analyzed at the Department of Earth, Atmospheric and

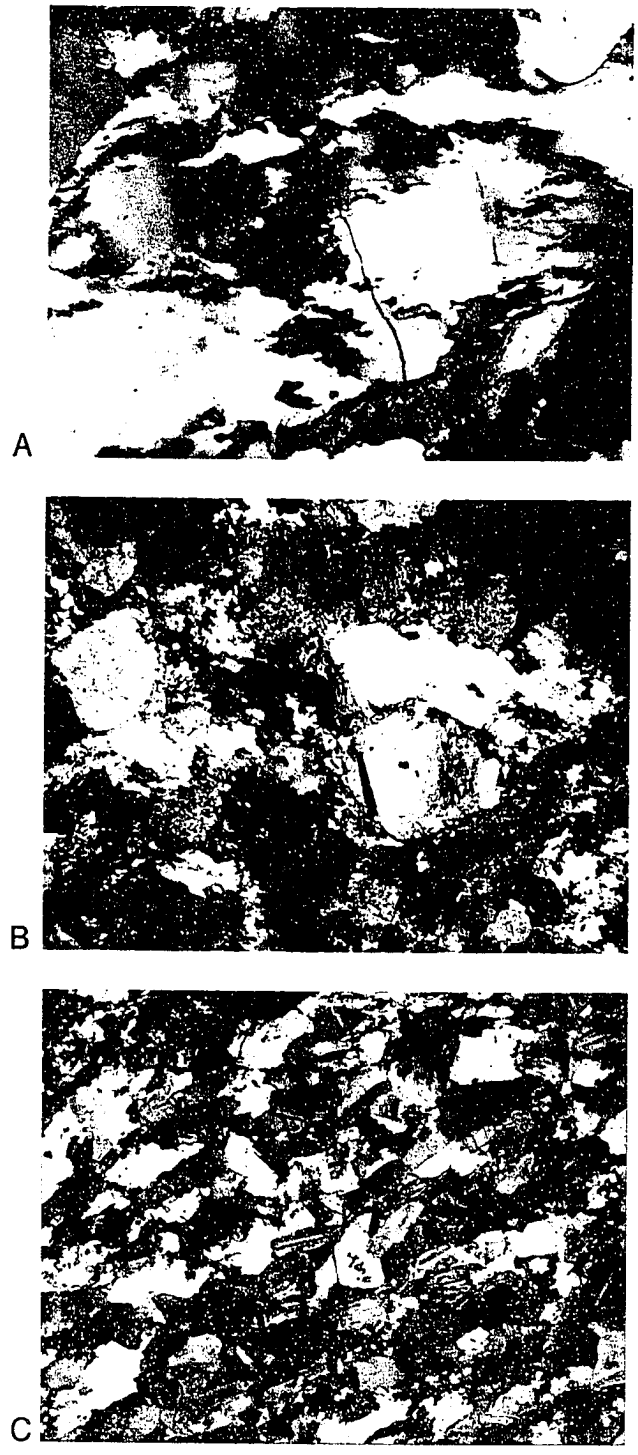

Figure 13. Photomicrographs of samples dated by U-Pb method. (A) Sample #SGC-63 from Stehekin orthogneiss (base of photo = 2 mm). (B) Sample #SGC-54 from Purple Creek orthogneiss (base of photo = 10 mm). (C) Sample #SGC-02 from Rainbow Falls orthogneiss (base of photo = 5 mm).

Table 1. U and Pb analyses and ages of rocks from the Central Skagit Gneiss Complex.

Sample	Fraction	Sample weight (µg)	U (ppm)	Total Pb (ppm)	206 Pb* / 204 Pb	208 Pb / 206 Pb	206 Pb / 238 U	% err	207 Pb / 235 U	% err	207 Pb / 206 Pb	% err	Age (Ma) 206 Pb / 238 U	Age (Ma) 207 Pb / 235 U	Age (Ma) 207 Pb / 206 Pb	corr. coef.‡	Pb (pg)	Blank (pg)	DISCORD	Alpha (%/amu)	TH / U	Locality UTM's (Zone 10)
SGC-63	s21	9.47	92.3	0.90	679.4	0.0546	0.0103	(.08)	0.0683	(.47)	0.0480	(.45)	66.1	67.1	101.4	0.41	0.91	0.90	35.01	0.25	0.17	
	M-13	22.38	129.7	1.26	905.8	0.0509	0.0103	(.06)	0.0673	(.32)	0.0475	(.30)	65.9	66.2	75.9	0.37	0.95	0.94	13.26	0.25	0.16	0660163
	s-17	15.46	180.6	1.88	1891.8	0.0465	0.0111	(.05)	0.0724	(.24)	0.0475	(.23)	70.9	71.0	73.3	0.31	0.67	0.66	3.19	0.25	0.15	5360586
	s22	9.72	127.7	1.35	1166.8	0.0642	0.0110	(.06)	0.0723	(.35)	0.0476	(.34)	70.6	70.9	78.2	0.34	0.77	0.77	9.69	0.25	0.20	
	s30	7.67	79.6	0.93	636.5	0.0733	0.0120	(.07)	0.0794	(.55)	0.0478	(.53)	77.2	77.5	88.4	0.45	0.98	0.97	12.73	0.25	0.23	
	s18	12.22	229.3	2.42	2076.2	0.0709	0.0110	(.05)	0.0718	(.18)	0.0475	(.17)	70.3	70.4	74.6	0.37	0.77	0.76	5.81	0.25	0.22	
	s25	9.47	166.7	1.75	2097.3	0.0509	0.0111	(.07)	0.0728	(.32)	0.0476	(.30)	71.2	71.4	78.9	0.35	0.56	0.55	9.80	0.25	0.16	
	z8	14.77	117.8	1.25	1531.2	0.0702	0.0110	(.05)	0.0727	(.22)	0.0477	(.21)	70.8	71.3	86.0	0.36	0.54	0.53	17.69	0.25	0.22	
SGC-54	z1	9.12	2.1	0.02	684.6	0.0527	0.0075	(.08)	0.0487	(.75)	0.0470	(.71)	48.3	48.3	49.8	0.49	1.50	1.00	3.15	0.25	0.16	
	s5	5.15	1.2	0.01	683.9	0.1680	0.0077	(.07)	0.0505	(.46)	0.0477	(.43)	49.3	50.0	83.5	0.38	0.89	0.88	41.10	0.25	0.52	0676948
	s10	5.73	1.1	0.01	817.5	0.1108	0.0077	(.06)	0.0500	(.48)	0.0472	(.46)	49.4	49.6	59.9	0.37	0.66	0.65	17.65	0.25	0.34	5353709
	s21	10.73	1.1	0.01	830.2	0.1144	0.0077	(.06)	0.0501	(.49)	0.0473	(.47)	49.3	49.6	66.1	0.35	0.63	0.62	25.49	0.25	0.35	
	L1b	9.12	0.3	0.00	218.6	0.1016	0.0080	(.11)	0.0520	(1.30)	0.0469	(1.24)	51.6	51.5	42.9	0.55	0.70	0.69	-20.43	0.25	0.32	
	zS1	13.01	0.9	0.01	848.8	0.0636	0.0083	(.07)	0.0542	(.39)	0.0471	(.37)	53.6	53.6	56.0	0.37	0.59	0.58	4.32	0.25	0.20	
	zS3	11.99	1.2	0.01	1241.0	0.0793	0.0098	(.06)	0.0648	(.31)	0.0480	(.29)	62.9	63.8	97.4	0.37	0.60	0.59	35.62	0.25	0.24	
	zS12	8.11	0.6	0.00	476.1	0.0572	0.0077	(.07)	0.0498	(.66)	0.0470	(.63)	49.3	49.4	51.7	0.51	0.67	0.66	4.54	0.25	0.18	
SGC-02	s3z	6.57	1.7	0.01	1044.5	0.0551	0.0075	(.06)	0.0485	(.30)	0.0470	(.28)	48.1	48.1	50.1	0.38	0.79	0.78	3.99	0.25	0.17	
	s23z	6.87	0.8	0.01	439.0	0.0615	0.0089	(.06)	0.0576	(.55)	0.0472	(.52)	56.8	56.8	58.8	0.49	1.00	0.99	3.35	0.25	0.19	0670401
	s22z	6.91	1.0	0.01	448.7	0.0734	0.0075	(.06)	0.0484	(.49)	0.0469	(.46)	48.1	48.0	45.7	0.47	1.12	1.00	-5.22	0.25	0.23	5357013
	s4z	5.73	0.4	0.00	329.7	0.0696	0.0081	(.10)	0.0537	(.89)	0.0479	(.85)	52.2	53.1	96.4	0.47	0.72	0.71	46.06	0.25	0.21	
	s9z	5.92	0.8	0.01	547.6	0.0820	0.0075	(.06)	0.0486	(.44)	0.0471	(.42)	48.1	48.2	54.9	0.41	0.73	0.73	12.51	0.25	0.26	
	s5z	4.67	1.1	0.01	654.8	0.0825	0.0075	(.07)	0.0488	(.75)	0.0473	(.71)	48.1	48.4	62.2	0.55	0.85	0.85	22.74	0.25	0.26	

‡ correction coefficient

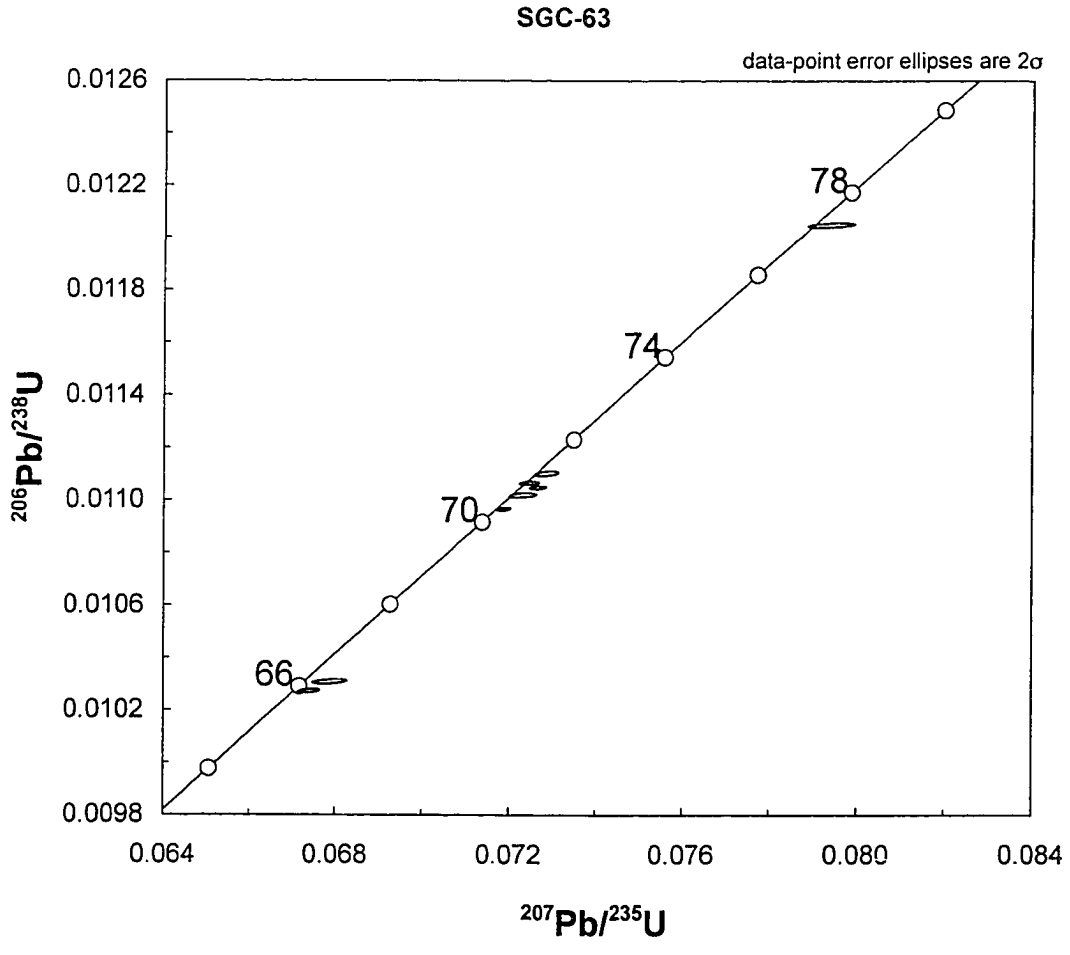

Figure 14. U-Pb concordia diagram for 8 zircon single grain fractions of Stehekin orthogneiss.

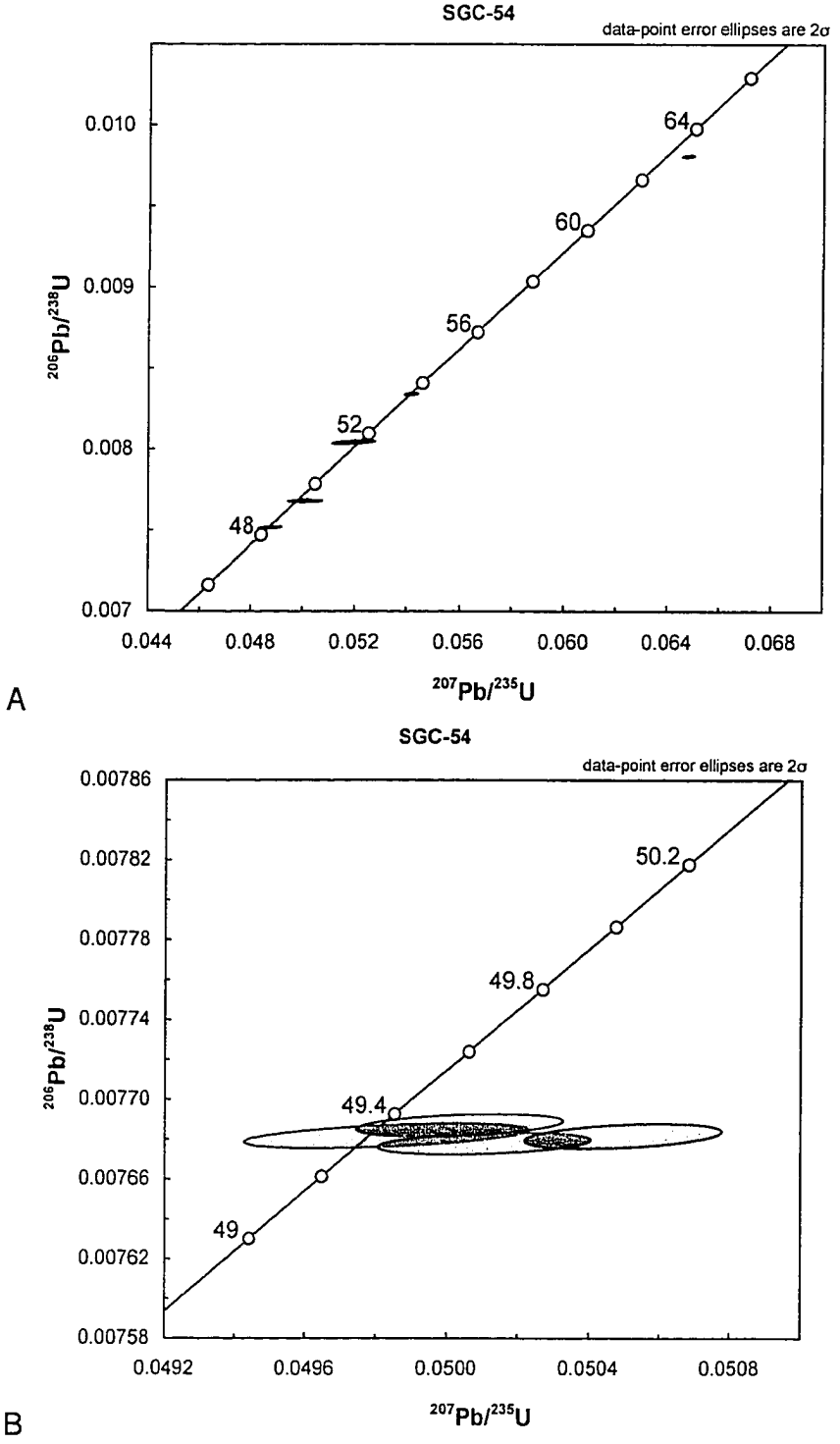

Figure 15. U-Pb concordia diagrams for sample of the Purple Creek orthogneiss. (A) All zircon fraction analyses. (B) Zoomed view showing a cluster of 4 zircon data interpreted to record a crystallization age of 49.3 Ma.

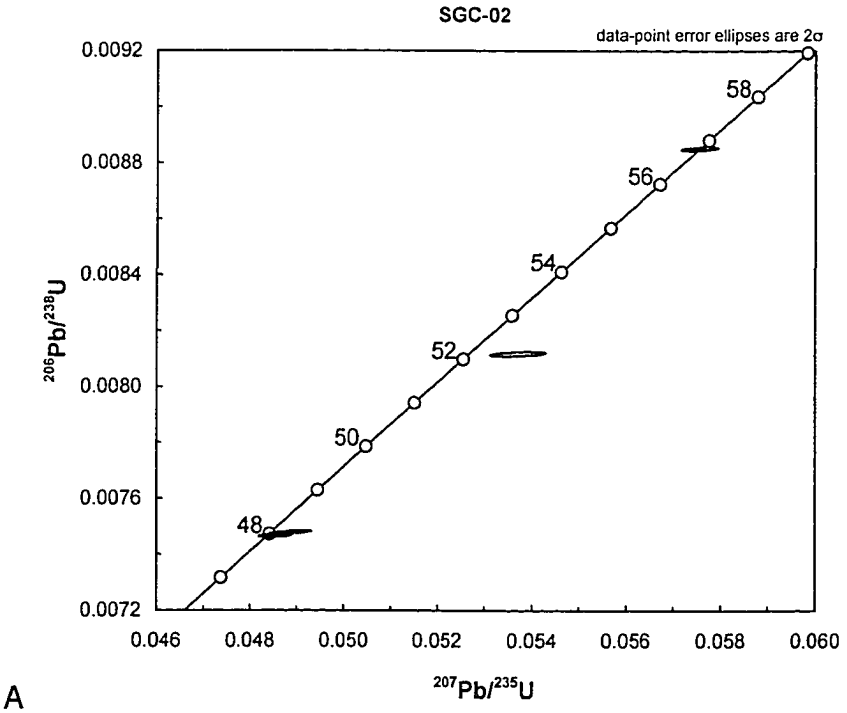

A

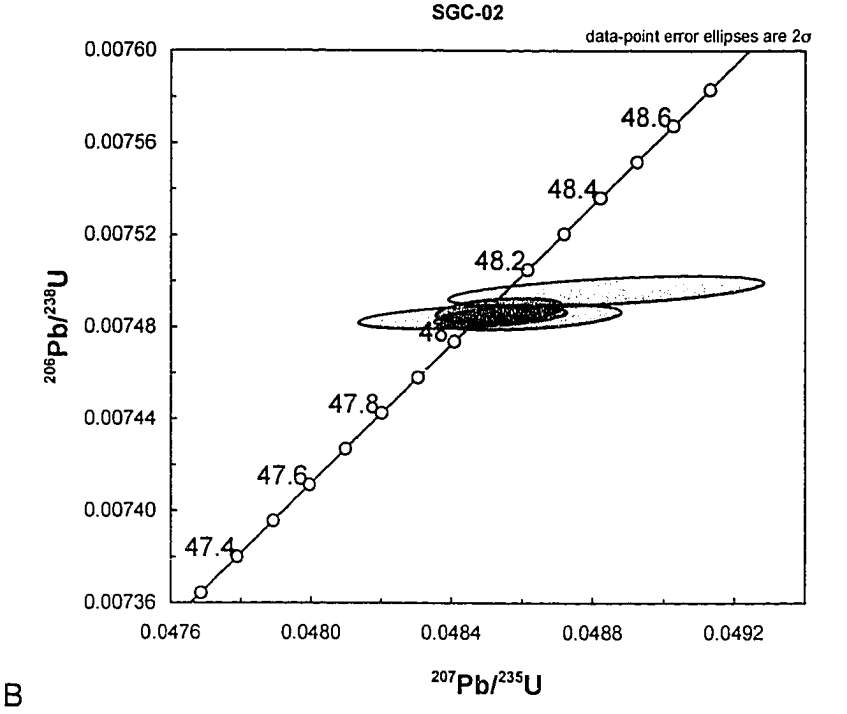

B

Figure 16. U-Pb concordia diagrams for zircon fractions of the Rainbow Falls orthogneiss. (A) All zircon fraction analyses. (B) Zoomed view showing a concordant cluster of 4 zircons interpreted to record a crystallization age of 48.1 Ma.

Planetary Sciences laboratories at the Massachusetts Institute of Technology (M.I.T.) during January of 2007. All processes of zircon separation and age determination (described by Schoene and Bowring, 2007) were overseen by Sam Bowring and Noah McLean.

The separation of heavy minerals was carried out at M.I.T. according to standard crushing, Wilfley table, heavy-liquid, and magnetic separation techniques. Zircon crystals were then hand-picked in ethanol under a binocular microscope and sorted by their morphology, color, clarity, and inclusion characteristics. Representative zircons were mounted in epoxy and polished to approximately half their original thickness for image analysis. Cathodoluminescence (CL) and backscattered electron (BSE) imaging were carried out using the M.I.T. JEOL 733 Superprobe electron microscope. CL images were obtained (Fig. 17) to reveal the internal structure of each zircon grain. Separates chosen for isotopic analysis were oscillatory zoned, had little or no rim, and were interpreted to be the most likely to represent single crystallization ages.

All sampled fractions, except for SGC-54z1 (see Table 1), were leached in HF and annealed at 900 °C for 60 hrs (Mattinson, 2005). Highly purified reagents, special handling, and extra cleaning steps were used during every stage of laboratory procedures to minimize common Pb lab blank. Individual zircon grains were dissolved in hydrofluoric acid after the addition of a mixed ^{205}Pb-^{233}U-^{235}U isotopic tracer. U and Pb were eluted in

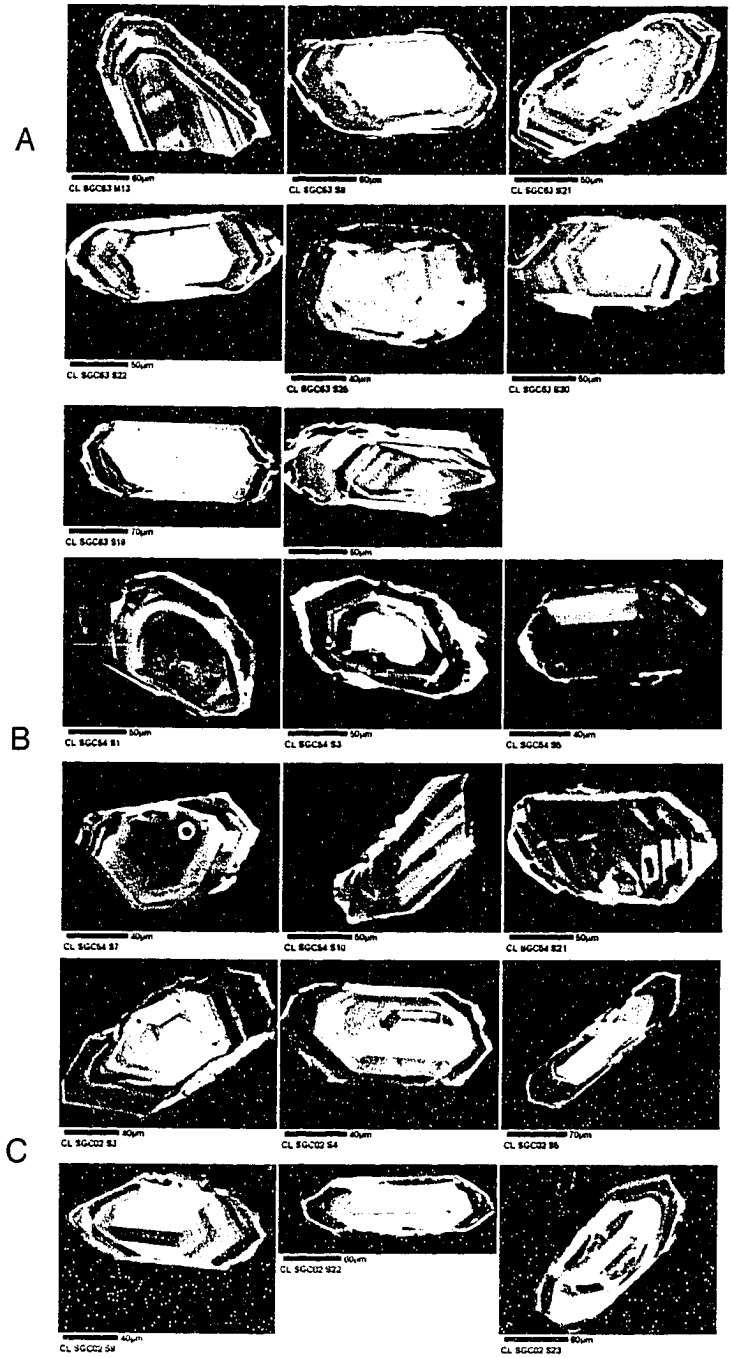

Figure 17. Cathodoluminescence images of the interior structure of zircon grains analyzed from samples (A) SGC-63, (B) SGC-54, and (C) SGC-02.

3N nitric acid through micro-columns using standard ion-exchange chemistry and anion exchange resin. The resultant material was mixed with a silica gel emitter and mounted onto a filament and analyzed using a VG Sector 54 mass spectrometer.

Stehekin Orthogneiss (SGC-63)

Sample SGC-63 is from a strongly deformed zone within the Stehekin orthogneiss near the base of McGregor Mountain (Fig. 3). Zircons from the Stehekin orthogneiss are clear, colorless, euhedral, magmatic crystals with aspect ratios of about 3:1. Eight fractions of zircon give U-Pb ages that range from 77 Ma to 66 Ma (Fig. 14). Most of the fractions yield concordant to slightly discordant ages within 2-sigma uncertainty of U decay constants. Two fractions give ages of ~66 Ma, and are interpreted to record the final crystallization age of the orthogneiss. Other fractions probably reflect inheritance of zircons.

Purple Creek Orthogneiss (SGC-54)

Sample SGC-54 is a medium-grained, hornblende-biotite tonalite orthogneiss collected from the middle of the well-lineated portion of the Purple

Creek unit (Plate 1). Zircons from this orthogneiss are mainly contained in biotite flakes and plagioclase phenocrysts. The zircons are clear, light pink to colorless and euhedral, with aspect ratios of about 5:1.

Eight fractions of zircon give U-Pb ages that range from 63 to 48 Ma (Fig. 15). Four of the fractions yield concordant to slightly normally discordant ages of ~49 Ma, and are inferred to date the final crystallization of the orthogneiss. One fraction dated at 52 Ma is mildly reversely discordant, with an error ellipse that overlaps concordia. One other fraction yields a highly normally discordant age of ca. 63 Ma, which is inferred to represent inherited Pb.

Rainbow Falls Orthogneiss (SGC-02)

Sample SGC-02 is a medium-grained, hornblende-biotite tonalite orthogneiss of the Rainbow Falls orthogneiss. It was collected near the base of Rainbow Falls in Stehekin Valley (Fig. 3 and Plate 1). Zircon grains are clear, euhedral crystals that have aspect ratios ranging up to 10:1. They contain oscillatory zoning consistent with igneous zircon growth.

Six zircon fractions yield U-Pb ages that range from 57 to 48 Ma (Fig 16). Two grains give ages that are interpreted to represent inherited Pb. The inferred crystallization age of the Rainbow Falls orthogneiss is 48.1 Ma.

STRUCTURAL ANALYSIS

Orthogneiss Microstructures

Mechanisms of crystal-plastic deformation are variable throughout the study area. The following section summarizes the most common deformation mechanisms observed in orthogneisses with different crystallization ages. The temperature dependencies of the mechanisms (Passchier and Trouw, 2005) are used to interpret the possible range of temperatures during deformation in each unit.

Stehekin Orthogneiss

Solid state deformation in the Stehekin orthogneiss is characterized by initially high-temperature (500–700 °C) dynamic recrystallization of quartz and plagioclase that is overprinted by subsequent lower-temperature ductile and brittle deformation. Large quartz grains with elongate subgrains pass laterally into domains of smaller, new grains and are interpreted to result from bulging and subgrain rotation recrystallization (>400 °C; Passchier and Trouw, 2005). Evidence of high-temperature (>500 °C) grain boundary migration recrystallization is inferred from local lobate quartz that contains subgrains that form a chessboard pattern (e.g., Passchier and Trouw, 2005).

Plagioclase deformation is highly variable in the orthogneiss. Lobate

grain boundaries and local growth of new grains by bulging recrystallization are evidence of medium to high temperatures (450–600 °C). Microfracturing, microfaulting, microkinking, and deformation twins overprint recrystallization structures, indicating that subsequent deformation occurred at a lower temperature (<450 °C) or a higher strain rate.

Purple Creek Orthogneiss

Quartz ribbons contain abundant elongate subgrains that pass laterally into recrystallized quartz. Some elongated subgrains are subparallel to the ribbons and some are discordant by up to 20°. New grains are predominantly the result of subgrain rotation recrystallization Locally, a few quartz grains display chessboard subgrains. Plagioclase deformation is dominated by microfracturing, twinning, and microkinking. Local evidence of recrystallization includes core-and-mantle structure and growth of new grains by bulging recrystallization along grain boundaries. Together, quartz and plagioclase microstructures in the orthogneiss suggest medium temperatures (450-550 °C) during deformation.

Rainbow Falls Orthogneiss

Recrystallization in the Rainbow Falls unit is less intense than in the older orthogneisses. Quartz grains are lobate with undulose extinction and contain elongate subgrains. Formation of new grains is achieved

predominantly by bulging recrystallization, and locally by progressive subgrain rotation recrystallization. Many plagioclases contain deformation twins, and locally core-and-mantle structures are present. The abundance of microfaults and microkinks indicates that much of the plagioclase deformation is brittle. Overall, microstructures in the orthogneiss suggest that ductile deformation occurred at 350–450 °C (e.g., Passchier and Trouw, 2005).

Significance of Orthogneiss Deformation Mechanisms

The Stehekin orthogneiss (ca. 66 Ma) is the oldest dated Skagit orthogneiss in the study area. Microstructures in the orthogneiss indicate temperatures of up to 700 °C during deformation. Eocene orthogneisses (Purple Creek and Rainbow Falls) are dominated by lower-temperature ductile (<500 °C) and brittle (<350 °C) structures. Thus, older orthogneisses were deformed at higher temperatures (Fig. 18) and/or lower strain rates than subsequent orthogneisses in the study area.

Deformation Patterns

The Rainbow Lake schist and mylonites of the Cretaceous Black Peak batholith are dominated by NE-dipping foliations and oblique lineations that rake 5–40° NE. In the Skagit orthogneisses, foliation and lineation patterns vary with proximity to the Gabriel Peak tectonic belt. From SW to NE

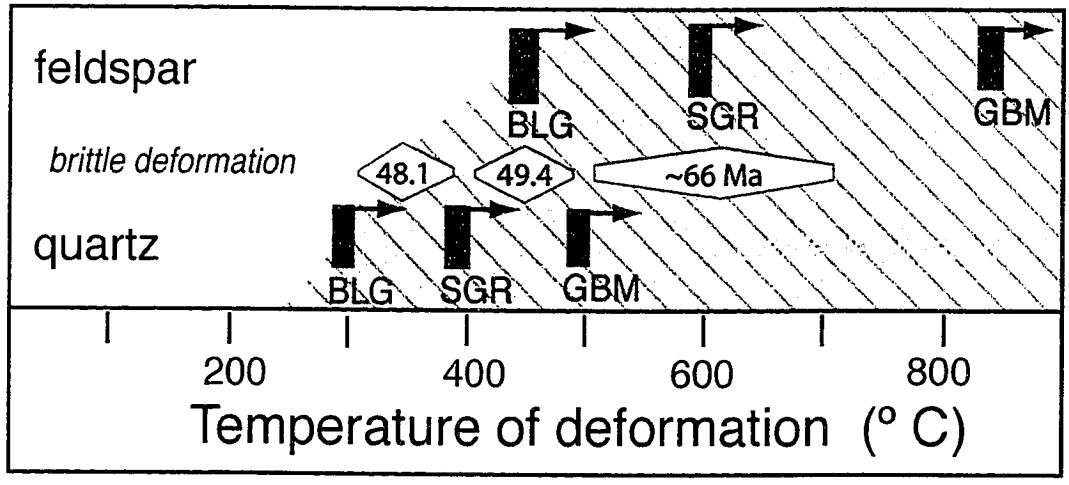

Figure 18. Temperature dependencies of microstructures (modified after Passchier and Trouw, 2005). Orange field indicates temperatures associated with ductile deformation. BLG, bulging recrystallization; GBM, grain boundary migration recrystallization; SGR, subgrain rotation recrystallization. Blue diamonds indicate the inferred range of temperatures during recrystallization in the dated orthogneisses from the study area. Ages shown in millions of years. The decreasing maximum temperatures of ductile structures indicate cooling of the complex and/or an increase in strain rate during progressive deformation.

across the study area, orthogneiss foliation and lineation swing from NW–SE to NE–SW orientations (Figs. 19 and 20). In the SW part of the study area, orthogneiss structures strike mostly NW–SE. To the NE, within 3 km of the Gabriel Peak tectonic belt, NE-striking Eocene orthogneisses dominantly record subhorizontal NE–SW stretching fabrics.

Rainbow Lake Schist

Compositional layers (S_1) in the Rainbow Lake schist probably formed by tight folding and transposition (D_1) of bedding (S_0). A continuous axial-planar foliation (S_2) is superposed on the layering. S_2 strikes subparallel to the NW strike of the Gabriel Peak tectonic belt (Fig. 19) and is chiefly defined by aligned biotite, muscovite and locally hornblende, and by elongate quartz and plagioclase aggregates. Medium- to high-temperature lineation (L_2) is marked by aligned quartz aggregates, muscovite, biotite, and locally hornblende. Mean foliation in the Rainbow Lake schist dips moderately NE (334°, 54° NE; Fig. 21). Mean mineral lineation is subhorizontal and plunges 10° to 355° (Fig. 21). Local open to tight folds (F_3) with 0.5 m to >15 m wavelengths modify foliation and lineation; these folds have rounded hinges that plunge moderately to steeply ENE (mean of 53° to 057°; Fig. 21).

Foliation (S_2) in the Rainbow Lake schist is deflected around garnet and staurolite porphyroblasts. The staurolites display sieve texture and do not contain recognizable patterns of inclusions. In contrast, garnets are

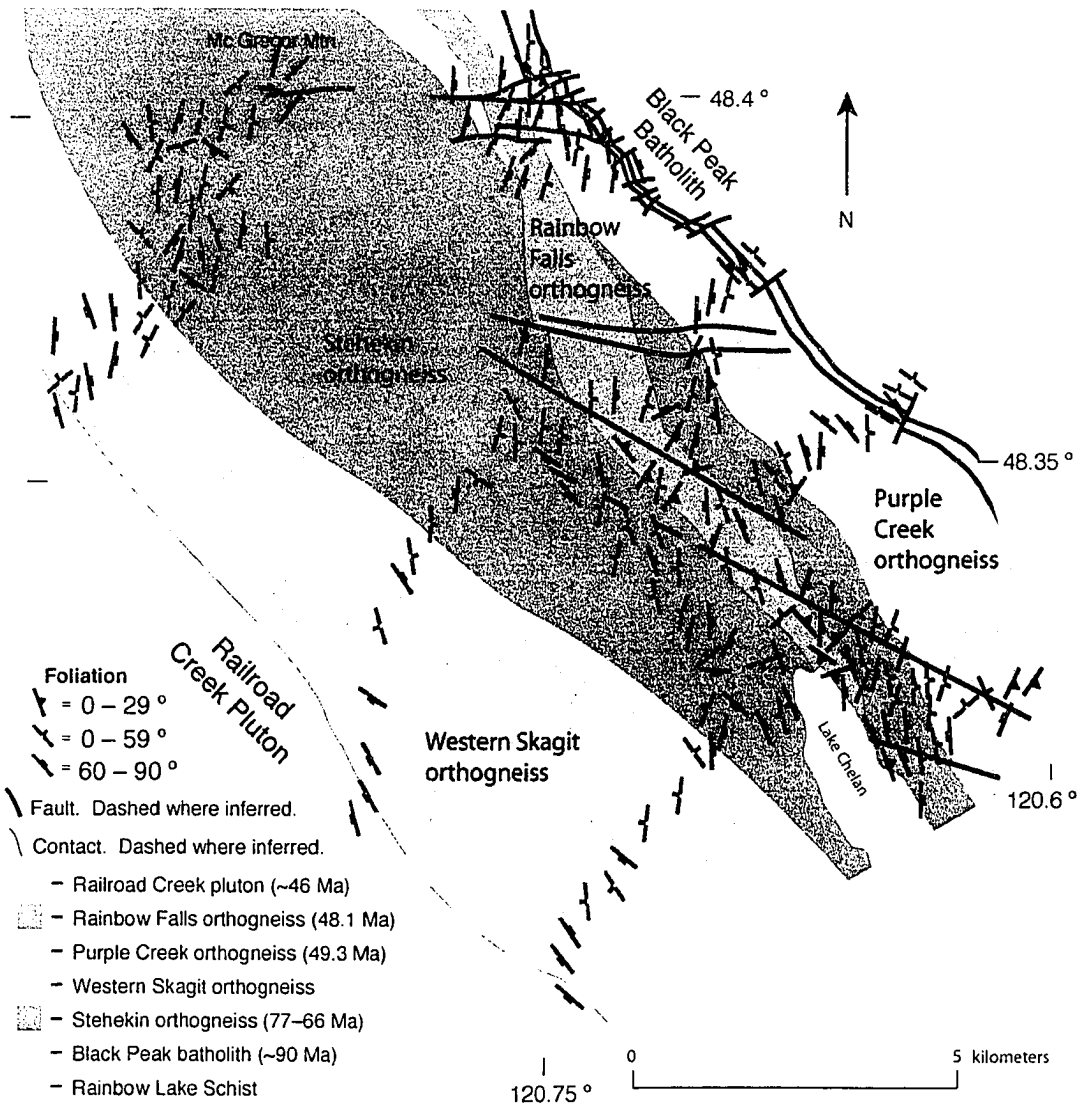

Figure 19. Simplified map of foliation orientations.

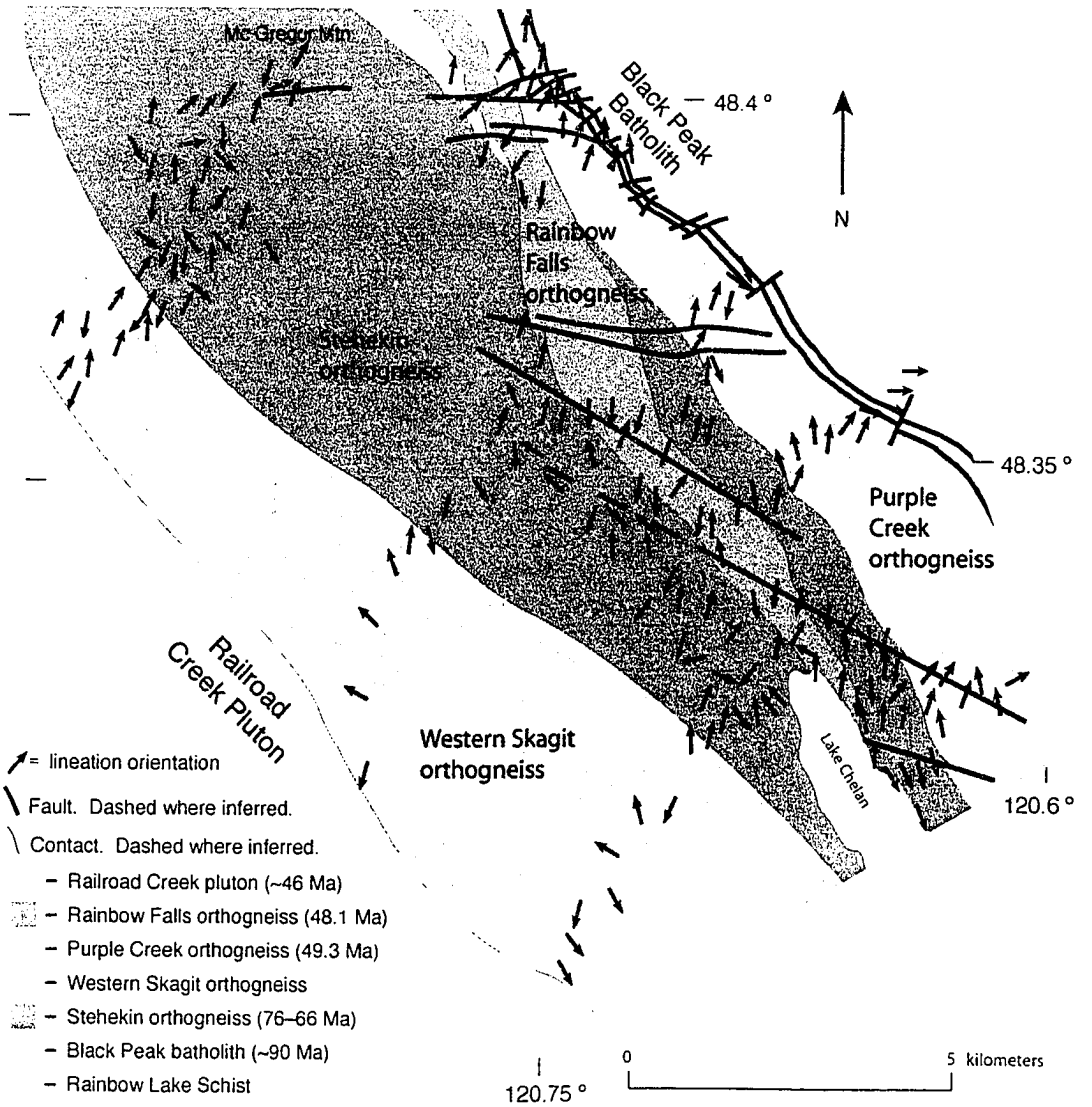

Figure 20. Simplified map of lineation orientations. Plunges shown in the orthogneisses are subhorizontal (0°–13°). Lineations typically rake <10° in the Rainbow Lake schist and 10°–40° in Black Peak rocks.

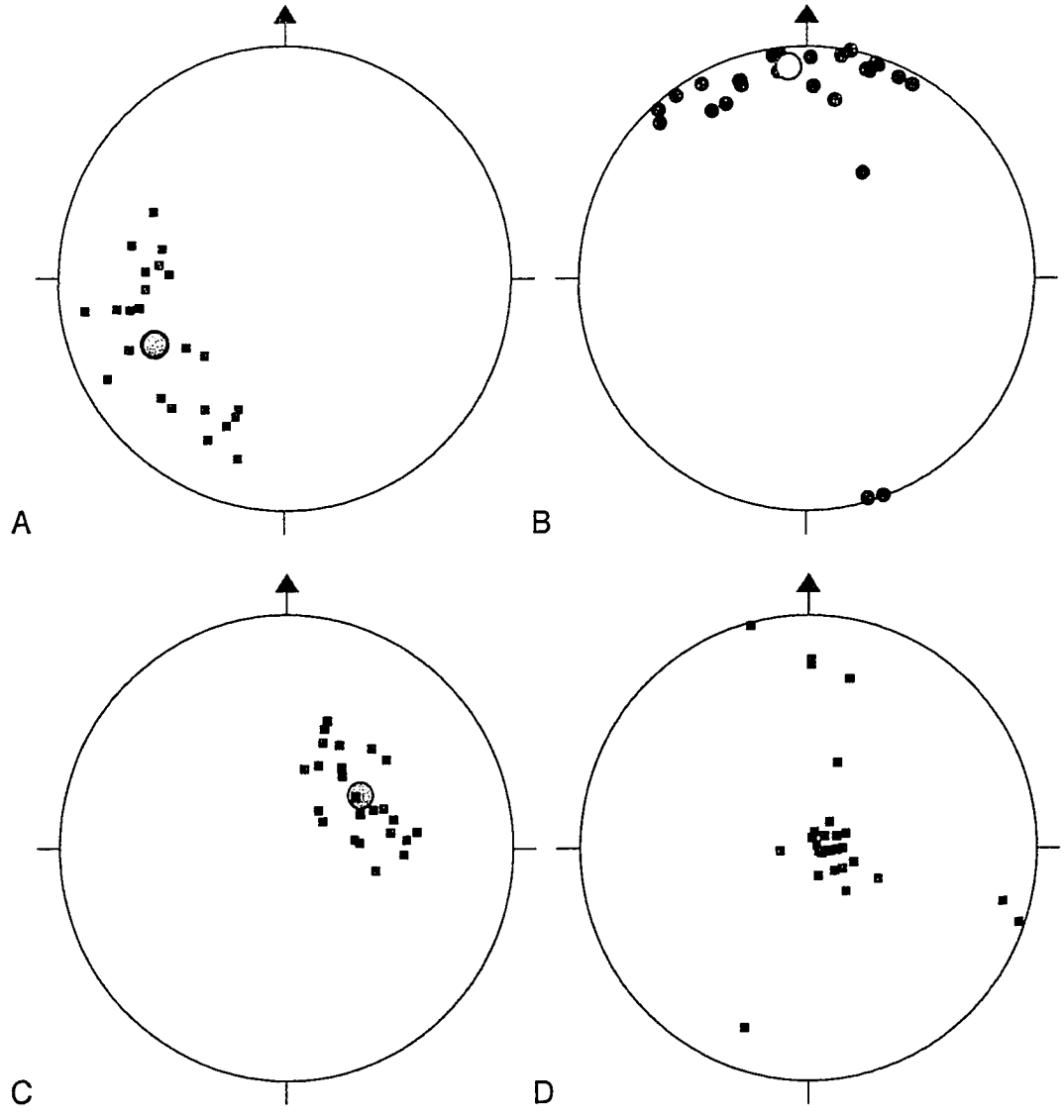

Figure 21. Structural data from the Rainbow Lake schist. (A) Poles to foliation (n = 26 data); and (B) mineral lineations (n = 26 data). Average orientation of foliation (334°, 54° NE) is shown by the red circle. Mean lineation direction is 10° to 355° (yellow circle). (C) Hinge lines to latest folds in the Rainbow Lake schist. Mean orientation is 53° to 057° (shown by blue circle). (D) Latest folds in schistose to gneissose supracrustal lenses within the orthogneisses (n = 29 data).

widely varied with respect to their inclusion patterns and are inferred to record growth during at least three different stages with respect to D_2. For example, some garnets that lack inclusion trails and deflect S_2 (Fig. 22) overgrew a fine-grained matrix prior to the development of any foliation and are interpreted as pre-tectonic with respect to D_1 and D_2. Other garnets associated with the two latest stages of garnet growth contain straight to tightly folded (Figs. 23 and 24) inclusion trails (S_i) of opaque minerals that partly preserve a pre-existing crenulated foliation (S_1). Most of the inclusion trails are discontinuous (Figs. 23 and 24) with respect to the external foliation (S_2) and are interpreted to have formed in garnets that overgrew S_1 foliation prior to or during D_2 deformation. Some garnet porphyroblasts have inclusion-free outer rims and contain inclusions in their centers (Fig. 22). Lineation-perpendicular surfaces also reveal tightly folded garnet inclusion trails that are discontinuous with the external foliation (Fig. 23).

Metasedimentary Lenses

Lenses of biotite schist, garnet-biotite schist, and amphibolite in the migmatitic portion of the Stehekin orthogneiss (Fig. 25) contain an S_2 axial-planar fabric and superposed F_3 hinge lines similar to those in rocks within the tectonic belt. The plunges of hinge lines in the lenses are variable (Fig. 21); many are steep, but about 15% are gentle, in contrast to the uniformly steeply plunging F_3 folds in the tectonic belt. The folding of these rocks is interpreted

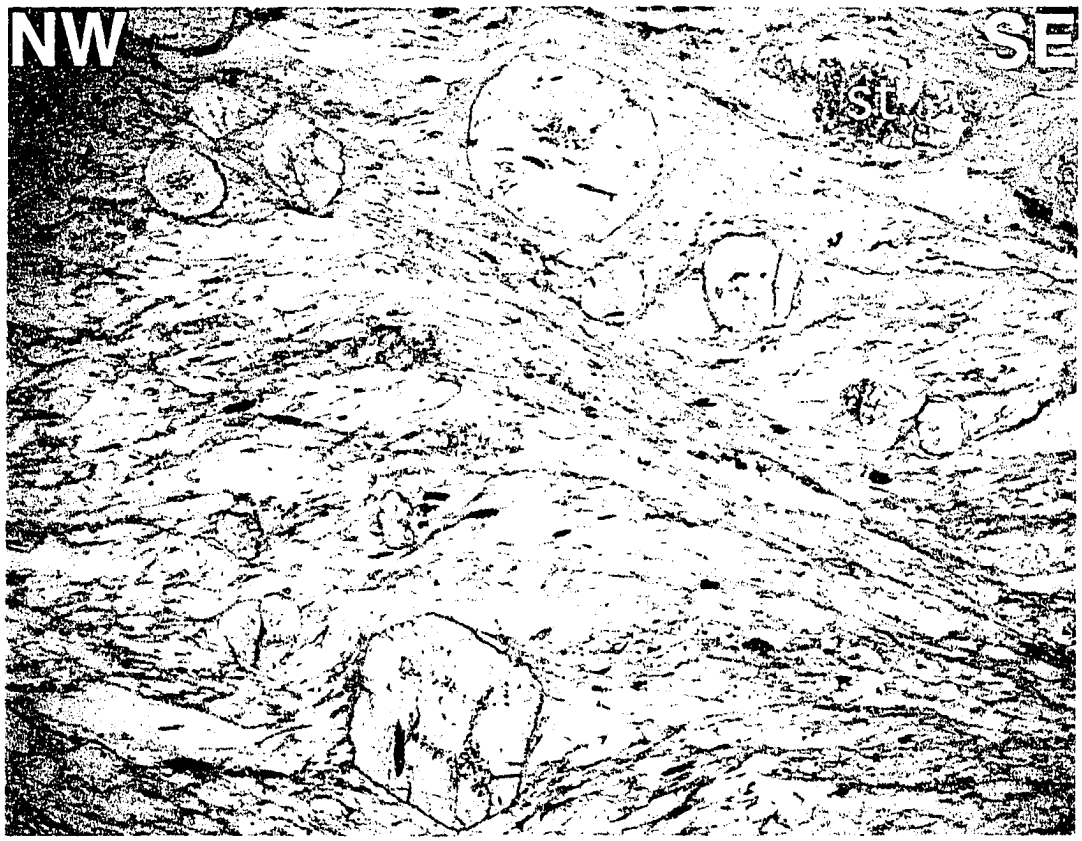

Figure 22. Garnet and staurolite (st) porphyroblasts in a biotite schist from the Rainbow Lake schist. The horizontal foliation is the continuous cleavage S_2, which is transected by C'-type shear bands filled by recrystallized biotite that cut from upper-left to lower-right. Note the dextral curvature of foliation into the shear bands. Garnet porphyroblasts lack inclusion trails and deflect foliation (S_1), and are interpreted as pre-tectonic with respect to D_1. St, staurolite (plane polarized light; base of photo = 8 mm).

Figure 23. Lineation-perpendicular section of a garnet porphyroblast (~2 mm diameter) with a folded inclusion pattern in a biotite-staurolite-garnet schist from the Rainbow Lake schist; the horizontal foliation is parallel to the continuous cleavage S_2 and roughly parallel to axial planes of folds defined by inclusion trails. Foliation deflects around the garnet, which is interpreted as syn-tectonic with respect to D_2 (plane polarized light; base of photo = 4 mm).

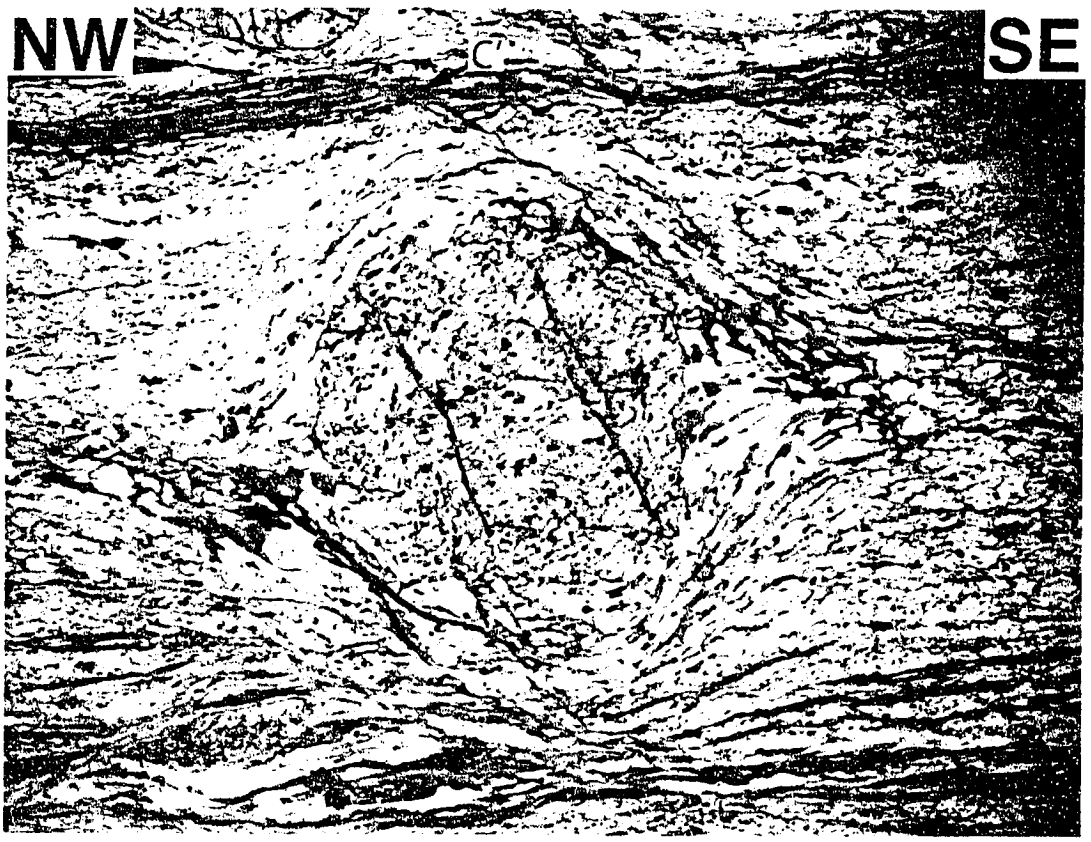

Figure 24. Garnet porphyroblast (~1.5 mm diameter) in garnet-biotite-sillimanite schist from the Rainbow Lake schist; the horizontal foliation is a continuous cleavage, S2. The garnet contains folded inclusion trails of opaque minerals that are discontinuous with the surrounding foliation (S2). The garnet is interpreted as pre-tectonic to early syn-tectonic with respect to D2. Note the deflection of S2 around the garnet and the relatively coarse-grained strain shadow. C'-type shear bands cut horizontal S2 foliation at the top (center) of the photomicrograph. The shear bands cut from upper-left to lower-right, consistent with dextral shear (plane polarized light; base of photo = 4 mm). This sample contains fibrolite along some of the shear bands.

Figure 25. (A) Tight folds of biotite schist and pegmatite veins in a supracrustal lens cut by E-W faults with cm-offsets in the Stehekin orthogneiss; view is looking west. (B) Same outcrop as shown in A, emphasizing east-plunging hinge lines (dashed arrows). East-west fractures cutting into the outcrop shown by thick black dashes. Base of picture is approximately 0.75 m across.

to predate deformation of the orthogneisses, as the orthogneisses are not folded. Conversely, as the supracrustal rocks are weaker than the surrounding orthogneisses, folds may have formed preferentially in the lenses.

Orthogneisses

Foliations in orthogneisses are best defined by aligned biotite, elongate quartz and plagioclase aggregates, and locally aligned hornblende and sphene. The dominant mineral lineation in the orthogneisses is defined by stretched quartz grains, elongate quartz and plagioclase aggregates, aligned biotite, and locally aligned hornblende. Lineation commonly dominates in strength over the foliation ($L > S$ or $L >> S$). Mean lineation is horizontal and trends NNE (00° to 013°; Figs. 26 and 27). Mean foliation strikes NNE and dips steeply ESE (009°, 63° E; Figs. 26 and 28). Foliation is commonly subparallel to the contacts of orthogneiss sheets and supracrustal lenses, but locally cuts contacts. Foliation is not folded at the outcrop scale.

Stereographic projections of lineation (Fig. 27) and foliation (Fig. 28) in different units show slightly different mean orientations (Table 2) and varying degrees of scatter. The Stehekin orthogneiss is the most structurally variable orthogneiss. It is also the oldest unit, very heterogeneous, and may include orthogneisses with a variety of ages. Thus, the variability of structures (e.g., Fig. 28) in the Stehekin orthogneiss may be due to a combination of rocks

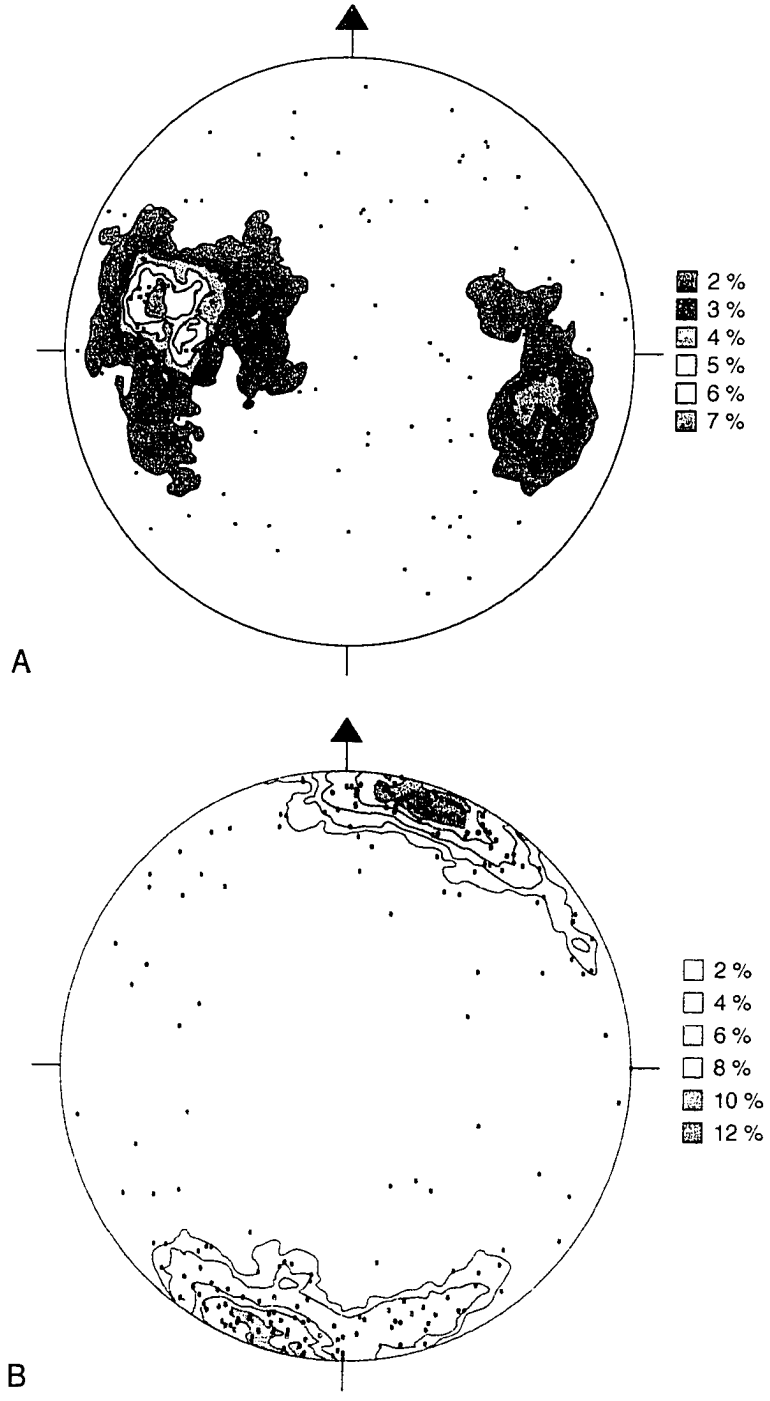

Figure 26. Contoured stereonet plots of orthogneiss ductile structures. (A) Poles to foliation (S_G); mean is 009°, 63° E (n = 367 data). (B) Orthogneiss lineation (L_g); mean is 00° to 013° (n = 281). Note the different contour intervals between A and B.

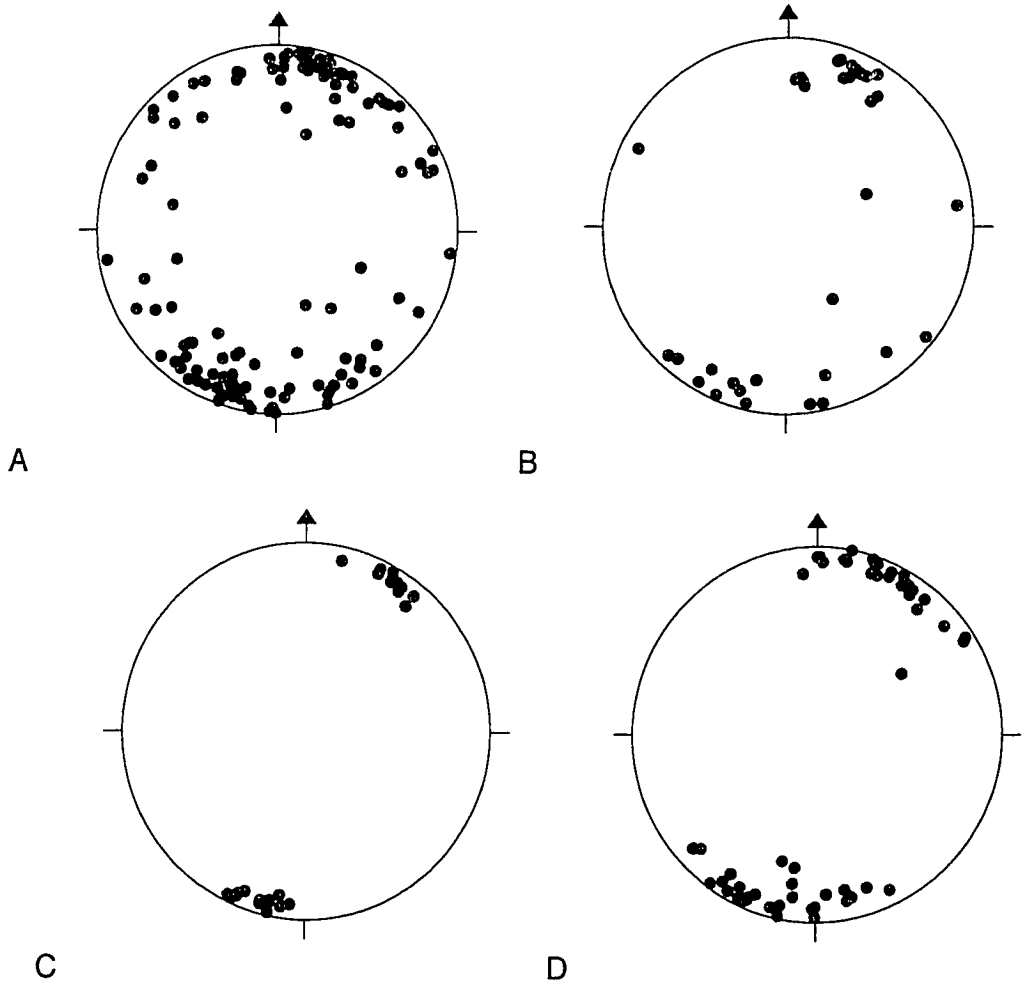

Figure 27. Stereonet plots of orthogneiss lineation (L_g). (A) Stehekin orthogneiss (n = 126). (B) Western Skagit orthogneiss (n = 37). (C) Purple Creek orthogneiss (n = 38). (D) Rainbow Falls orthogneiss (n= 76).

Table 2. Summary of orthogneiss structural data.

UNIT	Mean foliation	Mean lneation
All orthogneisses	009 °, 63 ° SE	00 ° to 013 °
Stehekin orthogneiss	015 °, 57 ° SE	01 ° to 193 °
Western Skagit orthogneiss	177 °, 80 ° SW	05 ° to 018 °
Purple Creek orthogneiss	017 °, 59 ° SE	00 ° to 022 °
Rainbow Falls orthogneiss	020 °, 76 ° SE	02 ° to 199 °

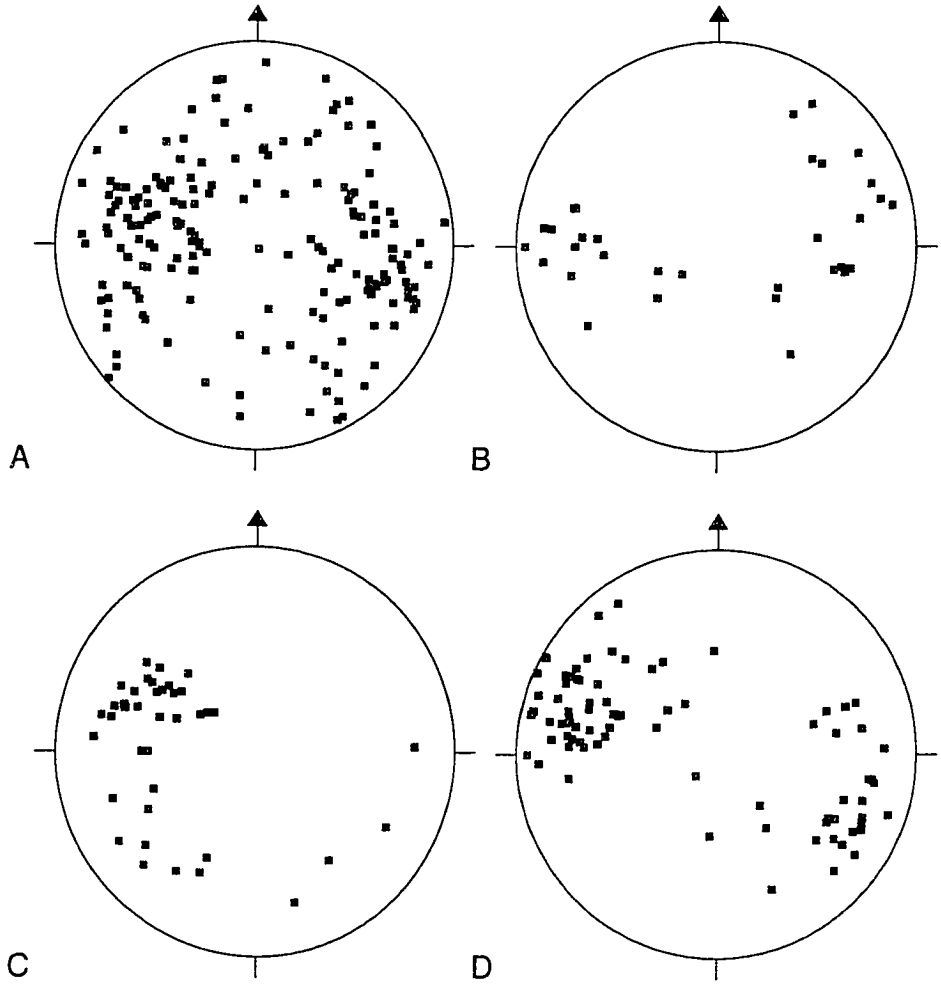

Figure 28. Poles to foliation (S_G) in orthogneisses. (A) Stehekin orthogneiss; ~66 Ma (n=179). (B) Western Skagit orthogneiss; ~65–50 Ma (n = 38). (C) Purple Creek orthogneiss; 49.3 Ma (n = 46). (D) Rainbow Falls orthogneiss; 48.1 Ma (n = 80).

of different ages recording different strain fields and the mechanical heterogeneity of more- or less-competent orthogneisses. Alternatively, the NE swing of foliation and lineation approaching the Gabriel Peak tectonic belt (e.g., Figs. 19 and 20; Plate 1) suggests that the variability in structural orientations may be more spatial than temporal, and related to proximity to the tectonic belt.

Farthest from the tectonic belt, foliation in the undated Western Skagit orthogneiss averages 177°, 80° SW (Figs. 19 and 28; Table 2). Lineation typically rakes <20°, and averages 05° to 018°. Mean foliation in the Purple Creek and Rainbow Falls orthogneisses is steep (>65°) and strikes N–NNE (e.g., Figs. 19 and 20; Plate 1). Foliation is best developed in rocks that are <2 km from the contact with the Rainbow Lake schist and Gabriel Peak tectonic belt. Lineation in this part of the study area is typically subhorizontal and trends NNE to NE (Fig. 20; Plate 1).

Orthogneiss Fabric Shape and Intensity

The following analysis classifies structural data measured from all of the orthogneisses to interpret the significance of the fabric shape and intensity. Measurements are classified by the strength of lineation relative to foliation at individual outcrops ($L = S$, $L > S$, $L >> S$, etc.; Fig. 29). Data are also classified by the intensity of solid-state deformation (Fig. 30). Intensity is

qualitatively indexed from 0 to 5 (Table 3) based on interpretation of outcrop-scale deformation of rocks.

Figure 29 shows that both L > S and L = S fabrics record dominantly NNE stretching in the Central Skagit orthogneisses. Figure 30 shows that the highest strain fabrics in the orthogneisses are dominantly oriented NNE–SSW and that the oldest orthogneisses are the most deformed. The strongest fabrics (4 and 5; Fig. 30) are recorded throughout the ~66 Ma Stehekin orthogneiss, and locally within the Western Skagit unit (age uncertain). The Purple Creek (~49.3 Ma) and Rainbow Falls (~48.1 Ma) units mainly contain weaker (1, 2, and 3; Fig. 30) solid-state fabrics. The orientations of the most intense fabrics closely approximate the NNE mean orientation of structures in the younger orthogneiss units and the Central Skagit Gneiss Complex as a whole. Measurements are classified by the strength of lineation relative to foliation at individual outcrops ($L_g = S_G$, $L_g > S_G$, $L_g >> S_G$, etc.; Fig. 29). This relationship demonstrates that orientations of structures associated with the highest degrees of strain in the orthogneisses are similar to the orientation of the most recent ductile fabrics in weakly deformed rocks in the complex.

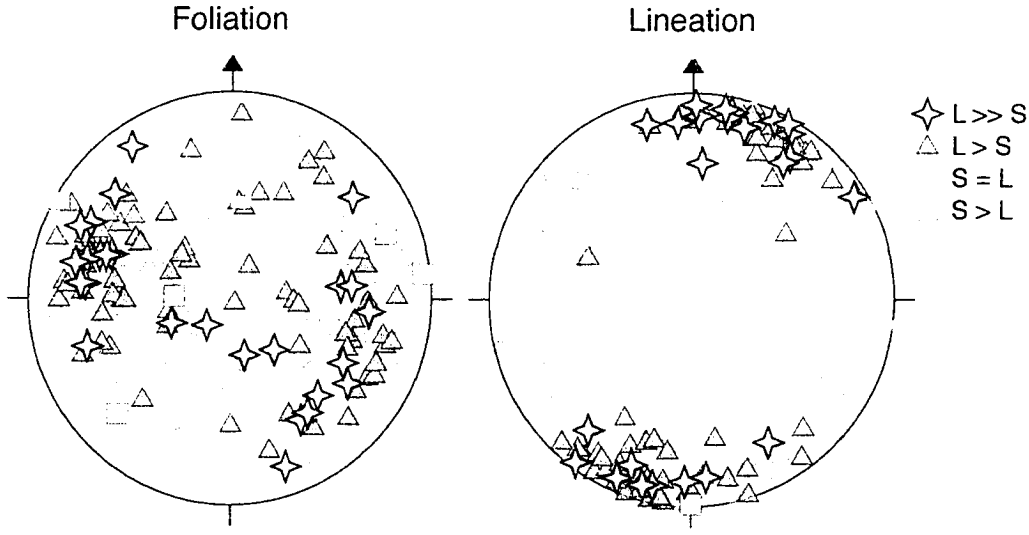

Figure 29. Stereographic plots of all orthogneiss structural data (poles to foliation, n = 297; lineation, n = 267) showing fabric shape (L = lineation; S = foliation).

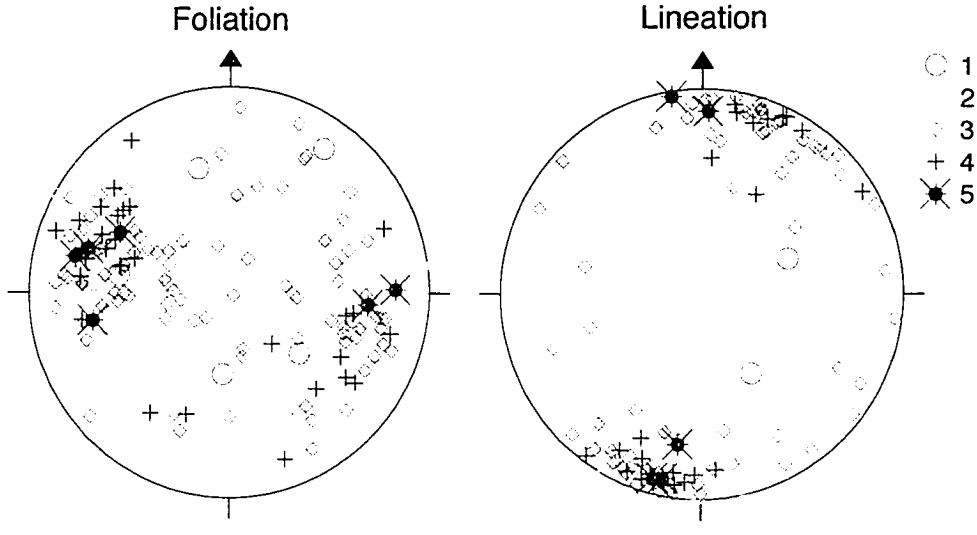

Figure 30. Stereographic plots of all orthogneiss structural data (poles to foliation, n = 297; lineation, n = 267) showing fabric intensities (see Table 3).

Table 3. Solid-state fabric intensity index.

Intensity	Fabric Description
0	Minerals are randomly oriented and do not define a foliation or lineation.
1	Quartz is slightly elongated and locally defines a preferred orientation subparallel to a weak alignment of other mineral grains.
2	Elongate quartz grains are well-aligned and define a continuous foliation and/or lineation subparallel to aligned minerals such as biotite and/or hornblende.
3	Compositional bands of quartz and plagioclase are locally present and are parallel to the preferred orientation of other mineral grains.
4	Rocks are well-banded with discrete layers of quartz and plagioclase aggregates defining foliation, and grain size may be reduced.
5	Grain size is significantly reduced and mylonitic structures develop.

Dikes

Late dikes in the study area are undeformed and cut orthogneiss fabrics at high angles (Fig. 31). The dikes are subvertical and strike E–W on average (mean orientation is 275°, 86°; Fig. 32). The mean subhorizontal extension direction, calculated normal to the average orientation of dikes, is 005°–185° (Fig. 32), indicating N–S extension. The dikes are cut by E–W faults with sinistral-normal separation. Extension during dike emplacement thus postdates the youngest orthogneiss fabrics, and predates brittle deformation in the Skagit Gneiss Complex.

Kinematics

Kinematics of non-coaxial general shear strain in the study area are interpreted from mesoscopic and microscopic structural indicators. The following section summarizes observations of asymmetric structures used to determine the shear-sense in the study area. The results are organized relative to proximity to the Gabriel Peak tectonic belt.

Gabriel Peak Tectonic Belt

The kinematics of ductile deformation in the Gabriel Peak tectonic belt were determined in mylonitic schists of the Rainbow Lake schist and

Figure 31. Late dike cross-cutting foliation in Stehekin orthogneiss (pencil is ~15 cm long).

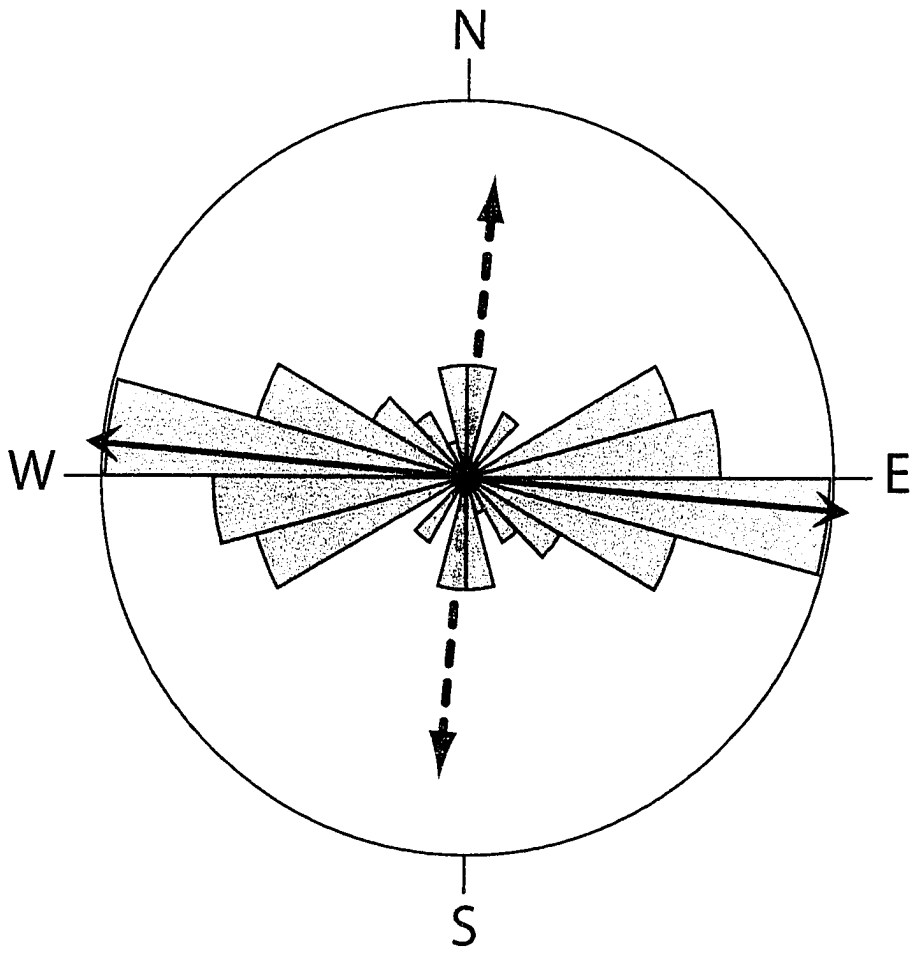

Figure 32. Rose diagram of strikes from undeformed subvertical dikes intruding Skagit orthogneisses. Mean strike direction (shown by black double-headed arrow) is 095°–275°. The inferred subhorizontal extension direction, shown as dashed red arrows, is 005°–185° (n = 49 data). Counting interval = 15°; radius = 10 count.

protomylonites and mylonites of the marginal Black Peak batholith. Kinematic indicators in these rocks include foliation curvature, C'-type shear bands, asymmetric porphyroclast mantles, mica "fish", syntectonic garnet inclusion trails, and sigmoidal polycrystalline aggregates of quartz and plagioclase.

Foliation in the Rainbow Lake schist is deflected by N-striking, steeply E-dipping, C'-type extensional shear bands (Figs. 22 and 24). The shear surfaces contain recrystallized aggregates of mainly quartz and biotite, but also sillimanite (Fig. 24) and/or hornblende (Fig. 33), indicating medium to high temperatures during deformation. In lineation-parallel surfaces, bands are interpreted to record dextral shear that characterizes D_3 deformation.

Sheets of the marginal Black Peak batholith (ca. 90 Ma) concordantly intrude the NE boundary of the Rainbow Lake schist and contain mylonites and protomylonites with asymmetrical microstructures. S-shaped, asymmetric biotite "fish" with tails of recrystallized hornblende (Fig. 34) are interpreted to record post-90-Ma dextral shear. The mylonites contain E-dipping, C'-type extensional shear bands that cut the dominant S_2 foliation (Fig. 35). These shear bands and asymmetric mica "fish" are interpreted as indicators of dextral motion that was coeval with formation of dextral C'-type shear bands in the Rainbow Lake rocks.

On the SW side of the tectonic belt, sparse ductile shear zones deflect subvertical orthogneiss sheets (Fig. 36) included in the Eocene Purple Creek

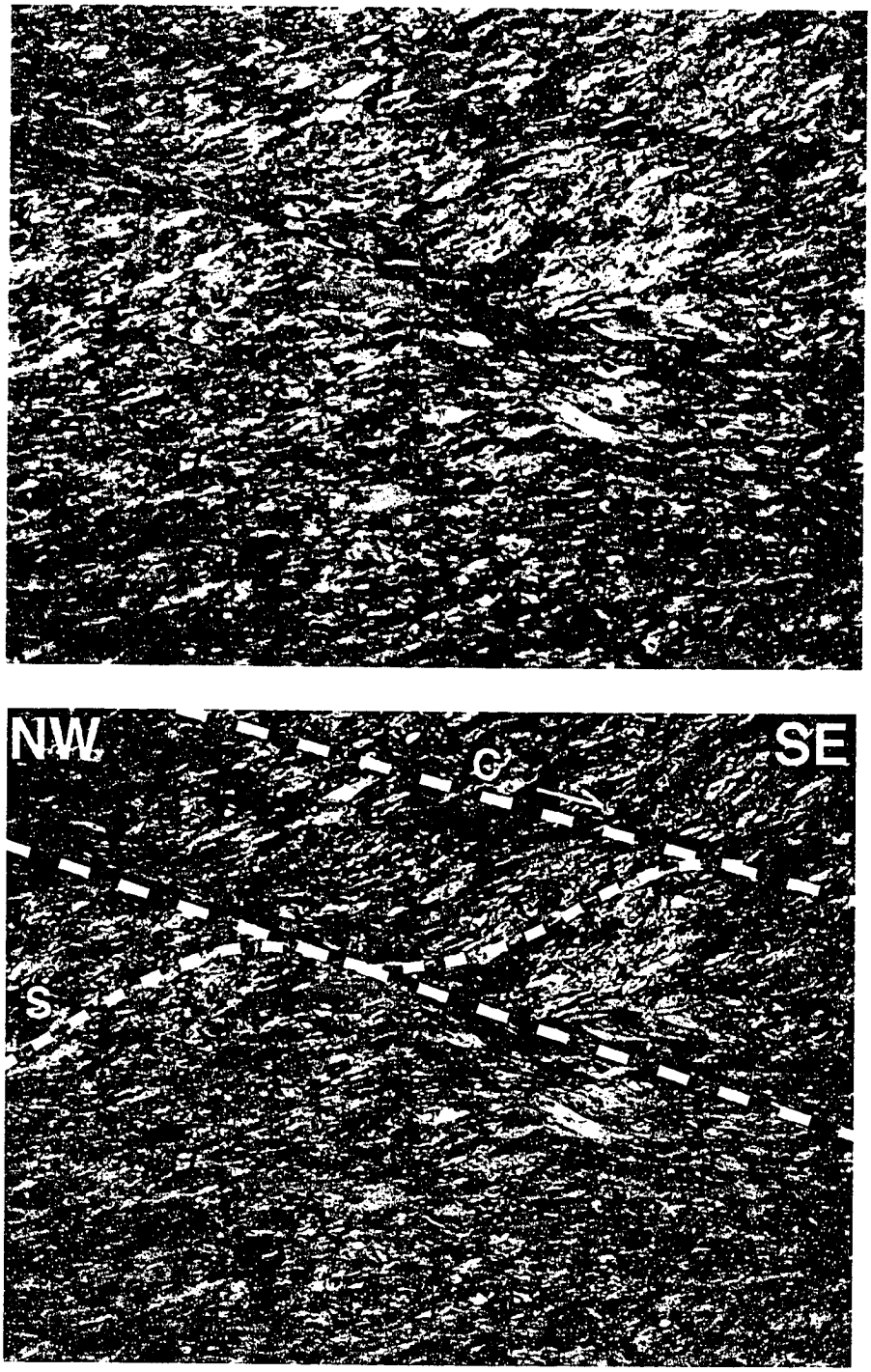

Figure 33. (A) Fine-grained amphibolite from the Rainbow Lake schist; subhorizontal foliation (S_2) is transected from upper-left to lower-right by dextral shear bands containing recrystallized hornblende, quartz and biotite. (B) Dashed lines show interpreted S-C' relationship (crossed-polars; base of photo = 4 mm).

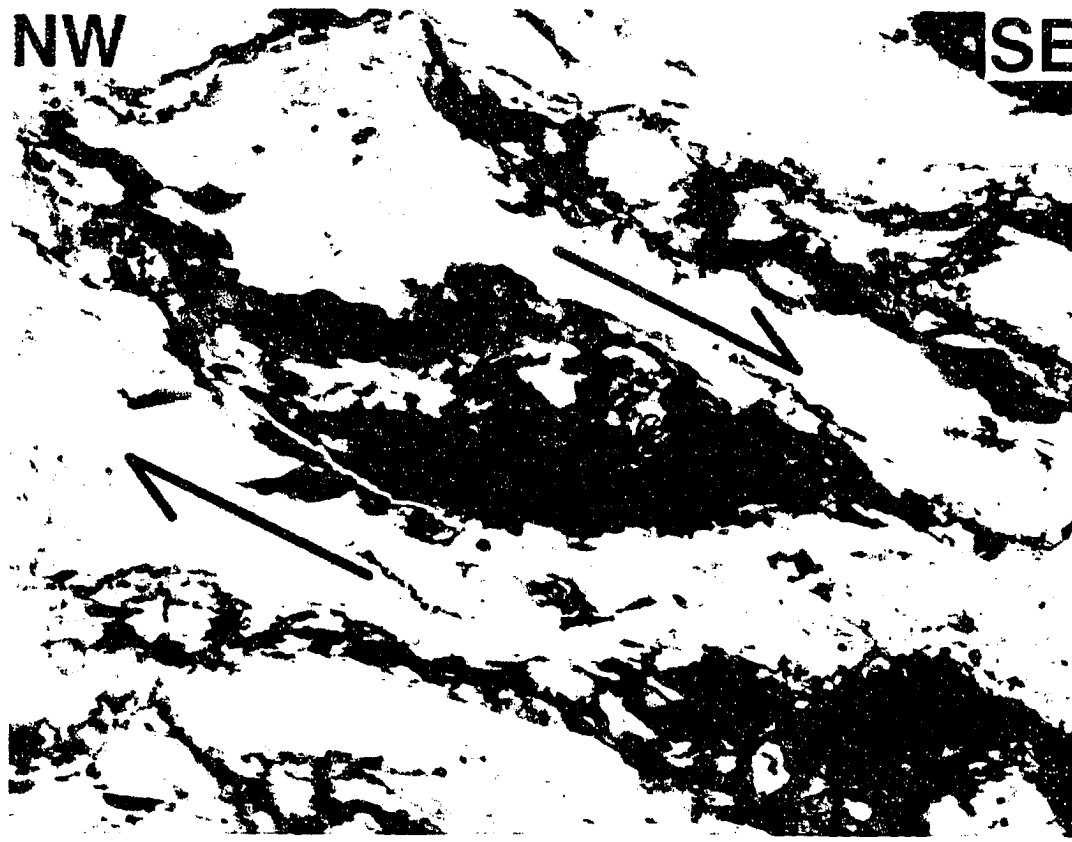

Figure 34. Biotite fish with asymmetric tails of partly recrystallized hornblende in a coarse-grained tonalitic augen gneiss from the Black Peak batholith in the Gabriel Peak tectonic belt. The asymmetry and curvature of the mineral fish is compatible with dextral shear (plane polarized light; base of photo = 8 mm).

Figure 35. Tonalitic mylonite from the marginal Black Peak batholith in the Gabriel Peak tectonic belt emphasizing recrystallized hornblende and biotite and tails on sigmoidal plagioclase aggregates curving into shear planes that cut from upper left to lower right, compatible with dextral (top-to-SE) shear (crossed-polars; base of photo = 8 mm).

Figure 36. Subvertical tonalite orthogneiss sheets in the Gabriel Peak tectonic belt, which are separated by ~20 cm in a dextral ductile shear zone (pencil for scale is ~15 cm long).

unit. The sheets curve into steep N-striking shear zones that are oblique to the NW strike of the tectonic belt. Asymmetric stacks of hornblende and biotite in tonalite gneiss of the Purple Creek unit yield dextral kinematics.

In summary, kinematic indicators observed in 22 samples from 17 stations in the Gabriel Peak tectonic belt yield dextral shear associated with D_3 deformation. Only samples from one location yield sinistral kinematics.

Skagit Gneiss Complex

The kinematics of non-coaxial shear in Skagit orthogneisses are determined from rare ductile shear zones that deflect foliation and lineation, asymmetric boudins of xenoliths, and asymmetric augen and plagioclase aggregates. Ductile shear zones in the Stehekin orthogneiss strike NNE–NE and dip moderately to steeply (up to 65°) SE. These structures consistently record sinistral (top-to-N) separation. Two thin sections out of 16 analyzed for kinematics from the Stehekin orthogneiss contain C'-type shear bands that also yield sinistral (top-to-N) shear sense (Fig. 37). Asymmetric structures are uncommon in most of the Central Skagit Gneiss Complex and typically record opposing senses of shear within the same sample, compatible with a history of dominantly coaxial strain.

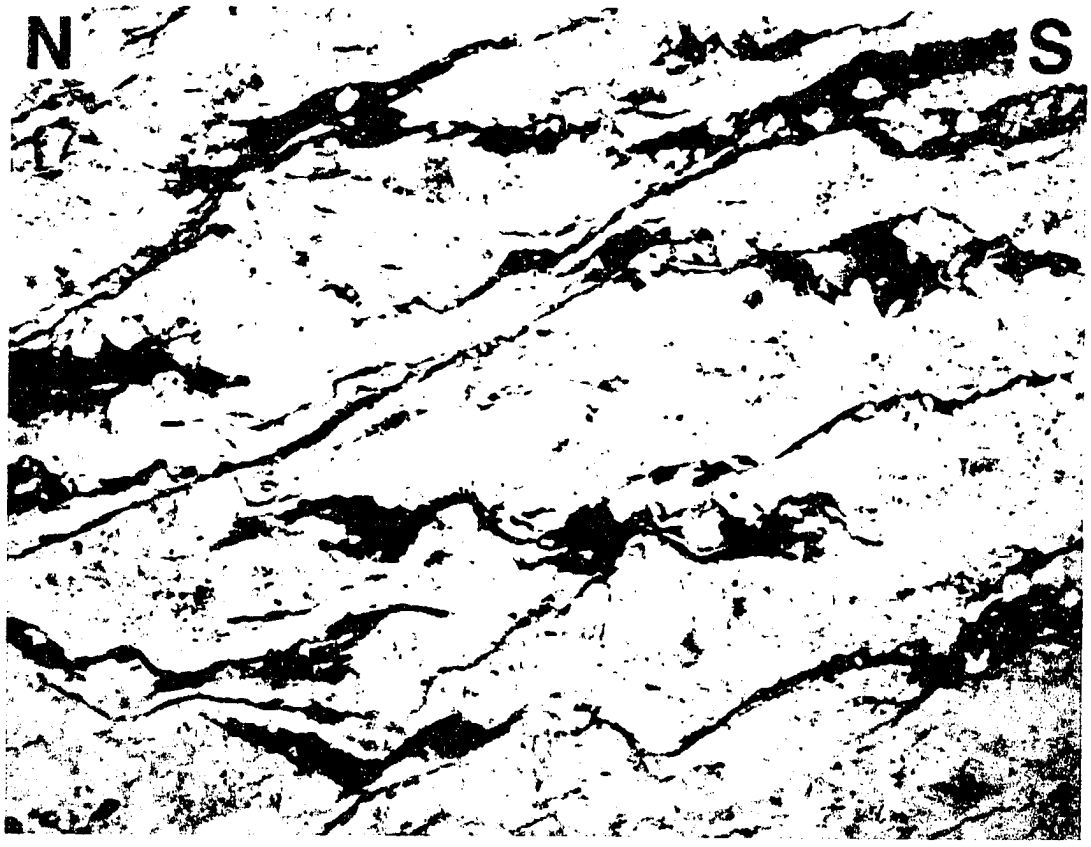

Figure 37. Photomicrograph of Stehekin orthogneiss; continuous horizontal foliation (S_G) is best defined by biotite and is cut by shear bands extending from upper-right to lower-left, consistent with top-to-the NNW sinistral transport (plane polarized light; base of photo = 8 mm).

Brittle Deformation

Faults cut ductile structures and dikes in Skagit orthogneisses and the Rainbow Lake schist. Most faults strike roughly E–W and dip greater than 60° to the north (average 271°, 81°; Fig. 38). These faults display cm- to m-scale sinistral-normal separation (Figs. 39 and 40). The amount and direction of slip on these faults is poorly constrained due to a lack of piercing points and slickensides. Faults with m- to km-scale sinistral separation cut the Rainbow Lake schist and Gabriel Peak tectonic belt in the northeastern part of the field area. Adams (1961) mapped up to ~1.5 km of sinistral strike-slip separation of the Rainbow Lake schist across individual E–W oriented faults north of the study area.

In the study area, faults dominantly display sinistral separation in plan view. Faults with m-scale slip also display a normal component of separation (Fig. 40). The components of normal and sinistral offset are not quantified, and it is possible that sinistral separations observed might be produced by dominantly normal displacements, rather than dominantly transcurrent motion (e.g., Fig. 41). If the motion is purely normal, the inferred N–S extension direction would suggest that crustal thinning continued after ductile deformation in a strain field consistent with orientations of stretching lineations and dikes.

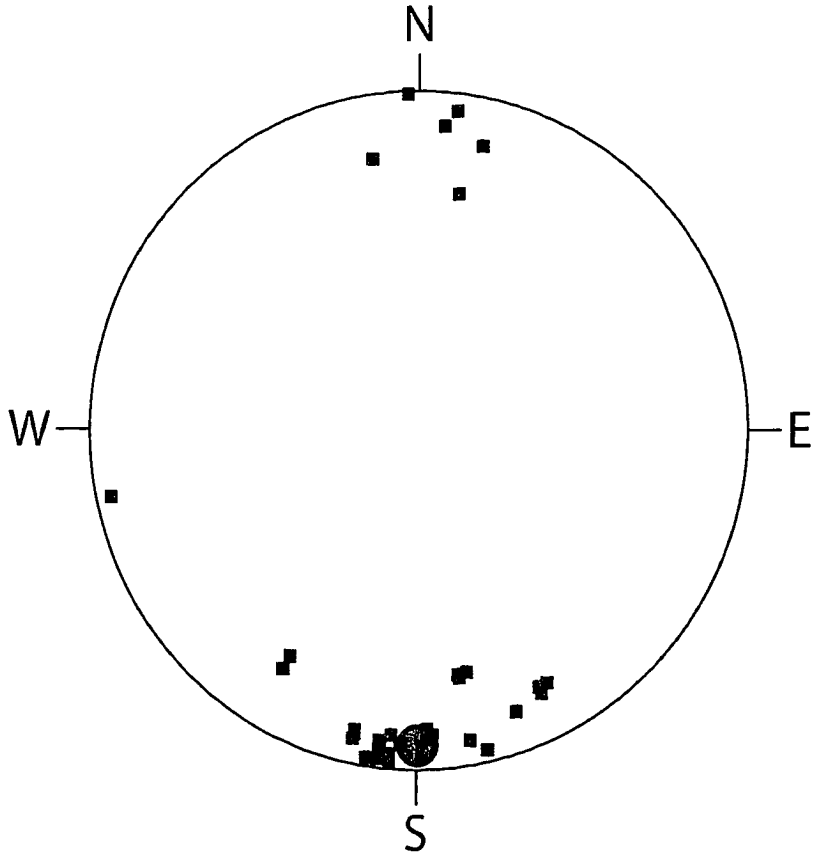

Figure 38. Stereographic plot of poles to outcrop-scale faults; average orientation shown by red circle is 271°, 81°N (n = 41 data).

Figure 39. Faults with cm-scale sinistral separation cutting Rainbow Lake schist. View is looking down at a subhorizontal surface; top of picture is east.

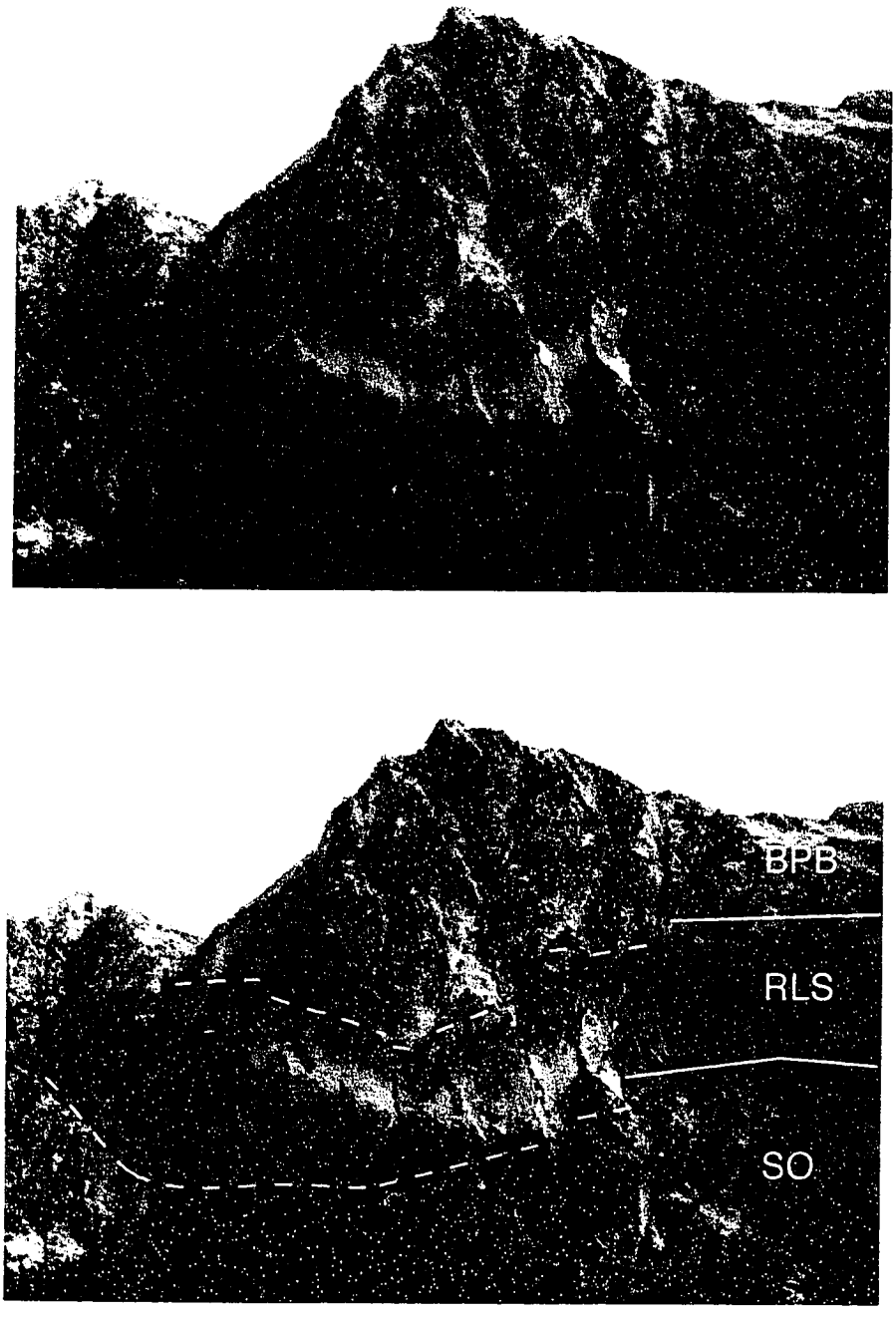

Figure 40. Faults displacing contacts of the Rainbow Lake schist (RLS). (A) View is looking east from the northeast corner of Rainbow Mountain ridge. (B) Steep faults cut the brown-weathering Rainbow Lake schist with apparent oblique sinistral-normal separation. View emphasizes normal separation. BPB, Black Peak batholith; SO, Skagit orthogneiss.

Plan-view configuration of NE-dipping rocks prior to normal faulting.

Faulted configuration following purely normal displacement. Note the sinistral separation shown by the arrows in plan view.

Figure 41. Schematic diagrams of contacts between units the study area, depicting how normal displacement may produce sinistral separation in plan view.

DISCUSSION

This study recognizes four rock units in the Central Skagit Gneiss Complex. The following section addresses the significance of structures and crystallization ages recorded by these rocks with respect to the structural and magmatic evolution of the North Cascades core. A particular focus is the relationship between structures in the Central Skagit Gneiss Complex and the Gabriel Peak tectonic belt.

Evidence of Eocene Deformation in the Central Skagit Orthogneisses

Previous studies of deformed dikes and plutons in the North Cascades (e.g., Richards and McTaggart, 1976; Hoppe, 1984; Miller et al., 1989; Haugerud et al., 1991) raise suspicion that middle Eocene ductile deformation was concentrated in warm rocks in the Skagit Gneiss Complex (e.g., Haugerud et al., 1991). Investigations of orthogneisses from elsewhere in the Skagit Gneiss Complex reveal Late Cretaceous crystallization between ~90 Ma and 65 Ma (e.g., Haugerud et al., 1991) and local Eocene ages (Hoppe, 1984; Miller et al., 1989). Zircon fractions from deformed orthogneisses in the Central Skagit Gneiss Complex dated for this study yield Eocene crystallization ages as young as 48.1 Ma. This work demonstrates that orthogneisses in the central part of the complex are younger than previously

known and extends the region of Eocene ductile deformation.

Orthogneiss crystallization ages indicate that weakly deformed rocks emplaced at ~48 Ma underwent the waning stage of solid-state deformation in the Central Skagit Gneiss Complex (Fig. 42). The adjacent ca. 46 Ma Railroad Creek pluton helps to bracket the end of solid-state deformation between ~48 Ma and ~46 Ma. Field observations, microstructures and inferred deformation mechanisms in the Skagit orthogneisses indicate that the intensity and temperature of deformation decrease with age of the units, and the latest stage of ductile deformation occurred at relatively low temperatures (ca. 300-400 °C) and gave way to subsequent brittle deformation. These changes in deformation are interpreted to reflect Eocene cooling of the gneiss complex near the end of progressive deformation.

Significance of the Gabriel Peak Tectonic Belt

The Gabriel Peak tectonic belt is a continuous, ~100-km long, NE-dipping mylonite zone that forms the SW extent of the Ross Lake fault system (Misch, 1977; Miller, 1994), a 500-km-long zone of high angle faults. Slip on the fault zone is considered by most workers to be dominantly dextral, with components of ca. 65 Ma reverse and post-50 Ma, NE-down normal displacement (Misch, 1966; Haugerud, 1985; Miller and Bowring, 1990; Miller, 1994). The Gabriel Peak tectonic belt merges to the SE with the Foggy Dew

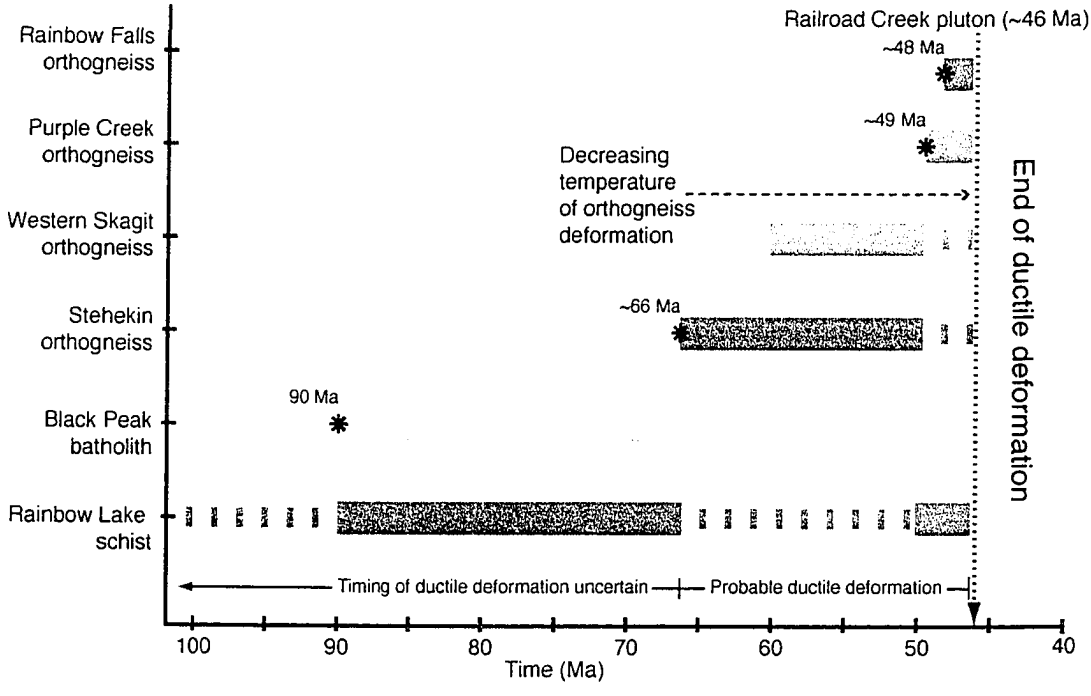

Figure 42. Timeline of ductile deformation in the study area. Bands dashed where timing of deformation is inferred, but uncertain. Asterisks indicate orthogneiss zircon crystallization ages.

fault zone of the Ross Lake fault system (Fig. 2). Mylonites in the Foggy Dew fault zone record a transition from transpression to transtension at ~57 Ma (Miller and Bowring, 1990), marked by down-to-E dextral-normal slip.

In the study area, kinematic indicators in the Rainbow Lake schist and the SW margin of the Black Peak batholith record dextral to dextral-reverse slip that in part post-dates crystallization of the Purple Creek orthogneiss at 49.3 Ma. There is considerable uncertainty about how much, if any, ductile deformation in the Rainbow Lake schist predates intrusion of the Black Peak batholith. Some deformation in the Rainbow Lake schist predates crystallization of Eocene orthogneisses and likely predates deformation of the Central Skagit Gneiss Complex as a whole. The Twisp Valley schist, inferred to be correlative with the Rainbow Lake schist, contains structures that can be demonstrated to predate intrusion of the Black Peak batholith (Miller et al., 1993b). However, in the study area, strong ductile deformation in the Rainbow Lake schist and the batholith probably overprinted earlier structures and obscured any definitive evidence of the timing of the onset of ductile deformation (Fig. 42).

Eocene orthogneisses adjacent to the tectonic belt contain subhorizontal NNE-trending lineations. Previous workers have puzzled over the enigmatic discordance of these orthogneiss lineations relative to the NW strike of the dominantly dextral tectonic belt (e.g., Adams, 1961; Libby, 1964; Miller, 1994; Dragovich and Norman, 1995). This study extends the

recognized areal extent of discordance to >75 km^2. Moreover, the obliquity is most pronounced in the younger Skagit orthogneisses and in rocks nearest the Gabriel Peak tectonic belt (Figs. 19 and 20; Plate 1).

The following section discusses possible deformation scenarios for rocks in the Gabriel Peak tectonic belt and adjacent Central Skagit Gneiss Complex. A major focus of the discussion is the discordance between NW-striking foliation in the tectonic belt and NE-striking Eocene fabrics in the Skagit orthogneisses.

One scenario for the deformation history of the tectonic belt involves motion on an unrecognized belt-parallel brittle fault that truncates NNE-striking structures in the gneiss complex. This model allows for two separate interpretations. In one, NE-striking structures in the Skagit orthogneisses are not rotated, and brittle slip juxtaposes them against the NW-striking Rainbow Lake schist. The second interpretation is that dextral motion along the tectonic belt causes clockwise block rotation of structures in the Skagit Gneiss Complex (Fig. 43). Sinistral slip on faults at high angles to the dextral tectonic belt leads to clockwise rotation of blocks of Skagit orthogneiss.

Fault-block rotation explains the discordance between structures in the gneiss complex and the tectonic belt. The number and size of E–W faults mapped in the study area appears insufficient to cause the necessary rotation, but faults may be much more abundant than recognized. Also, a scenario involving fault block rotation requires the presence of an

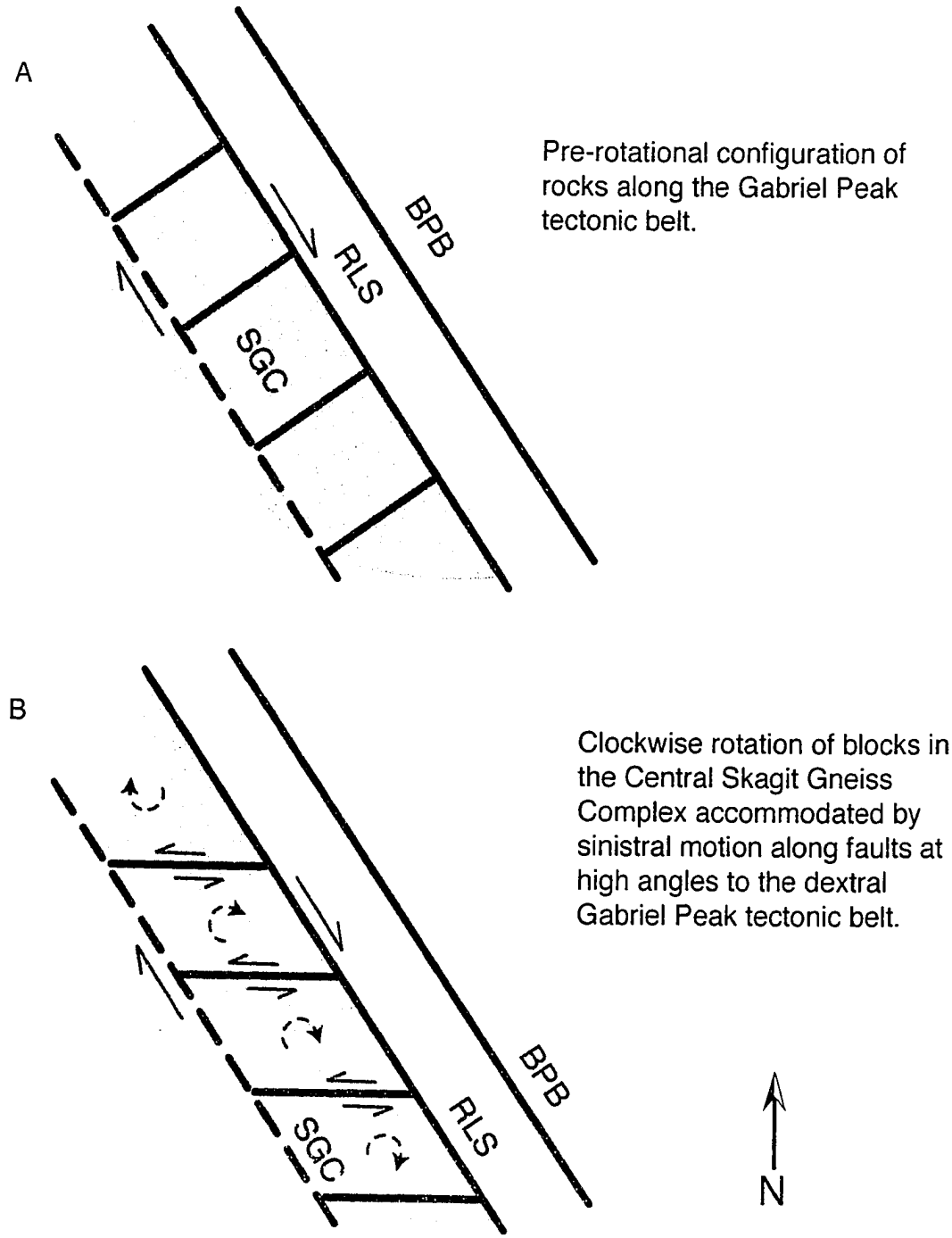

Figure 43. Schematic diagram showing clockwise rotation of blocks of the Central Skagit Gneiss Complex.

unrecognized NW-striking dextral fault or fault zone in the Skagit Gneiss Complex (Fig. 43). However, there is no evidence of post-48 Ma brittle motion where the contact is well-exposed. Additionally, many E–W faults cut across the tectonic belt, making it difficult to support models involving clockwise rotation of structures in the Skagit orthogneisses independent of structures in the Rainbow Lake schist and Black Peak batholith.

A second scenario to explain the discordance of Skagit lineations considers a likely significant rheological contrast between rocks along the SW margin of the tectonic belt during Eocene times. The Rainbow Lake schist and Black Peak batholith predate crystallization of ca. 48 Ma Skagit tonalites by >40 Ma, and thus were probably colder and stronger than the adjacent, newly crystallized Skagit rocks. Thus, Eocene NNE stretching in the Cascades core (e.g., Paterson et al., 2004) that followed the onset of transtension at ca. ~57 Ma (e.g., Miller and Bowring, 1990) may have been more easily accommodated in the younger, warmer Skagit orthogneisses. This scenario also posits that the rheological contrast between rocks in the tectonic belt acted as a NE barrier to Eocene ductile stretching, which is compatible with the lack of NNE-trending lineations in the Black Peak batholith and Rainbow Lake schist.

CONCLUSIONS

1. The Central Skagit Gneiss Complex in the study area is composed of greater than 90% tonalitic orthogneiss.
2. The Gabriel Peak tectonic belt is a major dextral structure, which has modified the intrusive contact between the Rainbow Lake schist and the Black Peak batholith, and the intrusive contact with adjacent rocks of the Central Skagit Gneiss Complex.
3. Orthogneisses yield zircon crystallization ages ranging from ca. 66 to 48.1 Ma.
4. Rocks in the Central Skagit Gneiss Complex record post-48.1-Ma deformation.
5. The southwest boundary of the Central Skagit Gneiss Complex is concordantly intruded by the undeformed Railroad Creek pluton (ca. 46 Ma), bracketing the latest ductile deformation to between 48.1 and 46 Ma.
6. Solid-state deformation in the Skagit Gneiss Complex is characterized by progressively decreasing temperature conditions, such that the oldest rocks are the most strained and contain the highest-temperature microstructures.
7. Regionally discordant, subhorizontal, NNE-trending lineations are more extensive than previously mapped, and dominate >75 km^2 of the study area.

REFERENCES CITED

Adams, J.B., 1961, Petrology and structure of the Stehekin-Twisp Pass area, Northern Cascades, Washington [Ph.D. thesis]: Seattle, University of Washington, 172 p.

Adams, J.B., 1964, Origin of the Black Peak Quartz Diorite, Northern Cascades, Washington: American Journal of Science, v. 262, p. 290–306.

Alsleben, H., 2000, Structural analysis of the Swakane terrane, North Cascades core, Washington [M.S. thesis]: , San Jose, San Jose State University, 168 p.

Brandon, M.T., Cowan, D.S., and Vance, J.A., 1988, The Late Cretaceous San Juan thrust system, San Juan Islands, Washington: a case history of terrane accretion in the western Cordillera: Geological Society of America Special Paper 221, 88 p.

Brown, E.H., and Walker, N.W., 1993, A magma-loading model for Barrovian metamorphism in the southeast Coast Plutonic Complex, British Columbia and Washington: Geological Society of America Bulletin, v.105, p. 479-500.

Cater, F.W., 1982, Intrusive rocks of the Holden and Lucerne quadrangles, Washington – The relation of depth zones, composition, textures, and emplacement of plutons: U.S. Geological Survey Professional Paper 1220, 108 p.

Cater, F.W., and Wright, T.L., 1967, Geologic map of the Lucerne quadrangle, Chelan County, Washington: U.S. Geological Survey Geologic Quadrangle Map GQ-647, 1 sheet, scale 1:62,500.

Dragovich, J.D., and Norman, D.K., 1995, Geologic map of the west half of the Twisp 1:100,000 quadrangle, Washington: Washington State Geological Survey Open-File Report 95-3, 63 p., 1 plate.

Engels, J.C., Tabor, R.W., Miller, F.K., and Obradovitch, J.D., 1976, Summary of K–Ar, Rb–Sr, U–Pb, and fission track ages of rocks from Washington State prior to 1975 (exclusive of Columbia Plateau Basalts): United States Geological Survey, Miscellaneous Field Studies Map, MF-710.

Evans, B.W., and Davidson, G.F., 1999, Kinetic control of metamorphic imprint during synplutonic loading of batholiths: an example from Mount Stuart, Washington: Geology, v. 27, p. 415–418.

Gordon, S.M., Bowring, S., Whitney, D.L.,Miller, R.B., and McLean, N., 2007, High-precision dating of migmatites in an exhumed continental arc: American Geophysical Union, Fall Meeting 2007, abstract #V34C-02.

Gordon, S.M., Whitney, D.L.,Miller, R.B., McLean, N, and Bowring, S., 2008, The Skagit Gneiss (North Cascades, Washington) revisited: New P-T results from recently discovered Al2SiO5-bearing gneiss: Geological Society of America Abstracts with Programs, v. 40, no. 1, p. 75.

Haugerud, R.A., 1985, Geology of the Hozameen Group and the Ross Lake shear zone, Maselpanik area, North Cascades, southwest British Columbia [Ph.D. thesis]: Seattle, University of Washington, 263 p.

Haugerud, R.A., van Der Heyden, P., Tabor, R.W., Stacey, J.S., and Zartman, R.E., 1991, Late Cretaceous and early Tertiary plutonism and deformation in the Skagit Gneiss, North Cascade Range, Washington and British Columbia: Geological Society of America Bulletin, v. 103, p. 1297-1307.

Hoppe, W.J., 1984, Origin and age of the Gabriel Peak Orthogneiss, North Cascades, Washington [M.S. thesis]: Lawrence, University of Kansas, 79 p.

Hurlow, H.A.,and Nelson B.K., 1991, Late Cretaceous–Eocene dextral transpression in the North Cascades metamorphic core, Washington: Structural styles, U-Pb chronologic constraints, and relation to plate motions: Geological Society of America Abstracts with Programs, v. 23, p. 433.

Libby, W.G., 1964, Petrography and structure of the crystalline rocks between Agnes Creek and the Methow Valley, Washington [Ph.D. thesis]: University of Washington, 133 p., 2 plates.

Mattinson, J.M., 1972, Ages of zircons from the Northern Cascade Mountains, Washington: Geological Society of America Bulletin, v. 83, p. 3769–3783.

Mattinson, J.M., 2005, Zircon U-Pb chemical abrasion ("CA-TIMS") method: Combined annealing and multi-step partial dissolution analysis for improved precision and accuracy of zircon ages: Chemical Geology, v. 220, p. 47-66.

Matzel, J.P., Bowring, S.A., and Miller R.B., 2004, Protolith age of the Swakane Gneiss, North Cascades, Washington: Evidence of rapid underthrusting of sediments beneath an arc: Tectonics, v. 23, no. 6, TC6009, doi:10.1029/2003TC001577.

Matzel J.E.P., Bowring S.A., Miller R.B. 2006, Time scales of pluton construction at differing crustal levels; Examples from the Mount Stuart and Tenpeak Intrusions, North Cascades, Washington: Geological Society of America Bulletin, v. 118. p 1412–1430.

McGroder, M.F., 1991, Reconciliation of two-sided thrusting, burial metamorphism, and diachronous uplift in the Cascades of Washington and British Columbia: Geological Society of America Bulletin, v. 103, p. 189-209.

McLean, N., Bowring, S.A., Miller, R.B., Whitney, D.L., and Gordon, S.M., 2006, North Cascades, WA: The collapse of a continental magmatic arc: American Geophysical Union, Fall Meeting 2006, abstract #T31C-0469.

Miller, R.B., 1985, The ophiolitic Ingalls Complex, North-Central Cascade Mountains, Washington: Geological Society of America Bulletin, v. 96, p. 27-42.

Miller, R.B., 1994, A mid-crustal contractional stepover zone in a major strike-slip system, North Cascades, Washington: Journal of Structural Geology, v. 16, p. 47-60.

Miller, R.B., and Bowring, S., 1990, Structure and chronology of the Oval Peak batholith and adjacent rocks: Implications for the Ross Lake fault zone, North Cascades, Washington: Geological Society of America Bulletin, v.102, p. 1361-1377.

Miller, R.B., and Paterson, S.R., 2001a, Influence of lithological heterogeneity, mechanical anisotropy, and magmatism on the rheology of an arc, North Cascades, Washington: Tectonophysics, v. 342, p. 351–370.

Miller, R.B., and Paterson, S.R., 2001b, Construction of mid-crustal sheeted plutons: Examples from the North Cascades, Washington: Geological Society of America Bulletin, v. 113, p. 1423–1442.

Miller, R.B., Bowring, S.A., and Hoppe, W.J., 1989, Paleocene plutonism and its tectonic implications, North Cascades, Washington: Geology, v. 17, p. 846-849.

Miller, R.B., Brown, E.H., McShane, D.P., and Whitney, D.L., 1993a, Intra-arc crustal loading and its tectonic implications, North Cascades crystalline core, Washington and British Columbia: Geology, v. 21, p. 255-258.

Miller, R.B., Whitney, D.L., and Geary, E.E., 1993b, Tectono-stratigraphic terranes and the metamorphic history of the northeastern part of the crystalline core of the North Cascades: evidence from the Twisp Valley Schist: Canadian Journal of Earth Sciences, v. 30, p. 1306-1323.

Miller, R.B., Haugerud, R.A., Murphy, F., and Nicholson, L.S., 1994, Tectonostratigraphic framework of the Northeastern Cascades: Washington Division of Geology and Earth Resources Bulletin, v. 80, p. 73-92.

Miller, R.B., Paterson, S.R., Lebit, H., Alsleben, H., and Luneburg, C., 2006, Significance of composite lineations in the mid- to deep crust: a case study from the North Cascades, Washington: Journal of Structural Geology, v. 28 p. 302-322.

Misch, P., 1952, Geology of the North Cascades of Washington: The Mountaineer, v. 45, no. 13, p. 4-22.

Misch, P.,1966,Tectonic evolution of the Northern Cascades of Washington State, *in* Gunning, H.C., ed., Tectonic history and mineral deposits of the western Cordillera: Canadian Institute of Mining and Metallurgy Special Volume 8, p. 101-148.

Misch, P., 1968, Plagioclase compositions and non-anatectic origin of migmatitic gneisses in the Northern Cascade Mountains of Washington State: Contributions to Mineralogy and Petrology, v. 17, p. 1-70.

Misch, P., 1977, Dextral displacement at some major strike faults in the North Cascades: Geological Association of Canada, Program with Abstracts, v. 2, p. 37.

Monger, J.W.H., Price, R.A., and Templeman-Kluit, D.J., 1982, Tectonic accretion and the origin of the two major metamorphic and plutonic welts in the Canadian Cordillera: Geology, v. 10, p. 70-75.

Passchier, C.W., and Trouw, R.A.J., 2005, Microtectonics; 2nd, Revised and enlarged edition: Berlin, Springer-Verlag, 325 p.

Paterson, S.R., Miller, R.B., Alsleben, H., Whitney, D.L., Valley, P.M., and Hurlow, H., 2004, Driving mechanisms for >40 km of exhumation during contraction and extension in a continental arc, Cascades core, Washington: Tectonics, v. 23, p. 1-30.

Richards, T.A., and McTaggart, K.C., 1976, Granitic rocks of the southern Coast Plutonic Complex and northern Cascades of British Columbia: *Geological Society of America Bulletin*, v. 87, p. 935–953.

Schoene B., and Bowring, S.A., 2007, Determining accurate temperature–time paths from U–Pb thermochronology: An example from the Kaapvaal craton, southern Africa: Geochimica et Cosmochimica Acta, v. 71 p. 165-185.

Tabor, R.W., Frizzell,V.A., Jr.,Vance, J.A., and Naeser, C.W., 1984, Ages and stratigraphy of lower and middle Tertiary sedimentary and volcanic rocks of the central Cascades, Washington: Application to the tectonic history of the Straight Creek fault: Geological Society of America Bulletin,v. 95, p. 26–44.

Tabor, R.W., Zartman, R.E., and Frizzell, V.A., Jr., 1987, Possible tectonostratigraphic terranes in the North Cascades crystalline core, Washington, *in* Schuster, J.E., ed., Selected papers on the geology of Washington: Washington Division of Geology and Earth Resources Bulletin, v. 77, p. 107-127.

Tabor, R.W., Haugerud, R.A., and Miller, R.B., 1989, Overview of the geology of the North Cascades, *in* International Geologic Congress, 28th, Field Trip Guidebook T307, Washington, D.C.: American Geophysical Union, 62 p.

Valley, P.M., Whitney, D.L., Paterson, S.R., Miller, R.B., and Alsleben, H., 2003, Metamorphism of deepest exposed arc rocks in the Cretaceous to Paleogene Cascades belt, Washington: evidence for large-scale vertical motion in a continental arc: Journal of Metamorphic Geology, v. 21, p. 203-220.

Wernicke, B., and Getty, S.R., 1997, Intracrustal subduction and gravity currents in the deep crust: Sm-Nd, Ar-Ar, and thermobarometric constraints from the Skagit Gneiss Complex, Washington: Geological Society of America Bulletin, v. 109, p. 1149–1166.

Whitney, D.L., 1992, High-pressure metamorphism in the Western Cordillera of North America: an example from the Skagit Gneiss, North Cascades: Journal of Metamorphic Geology, v. 10, p. 71–75.

Winter, J.D., 2001, An introduction to igneous and metamorphic petrology: Upper Saddle River, New Jersey, Prentice-Hall Inc., 697 p.

Yardley, B.W.D., 1978, Genesis of the Skagit Gneiss migmatites, Washington, and the distinction between possible mechanisms of migmatization: Geological Society of America Bulletin, v. 89, p. 941–951.

Plate 1

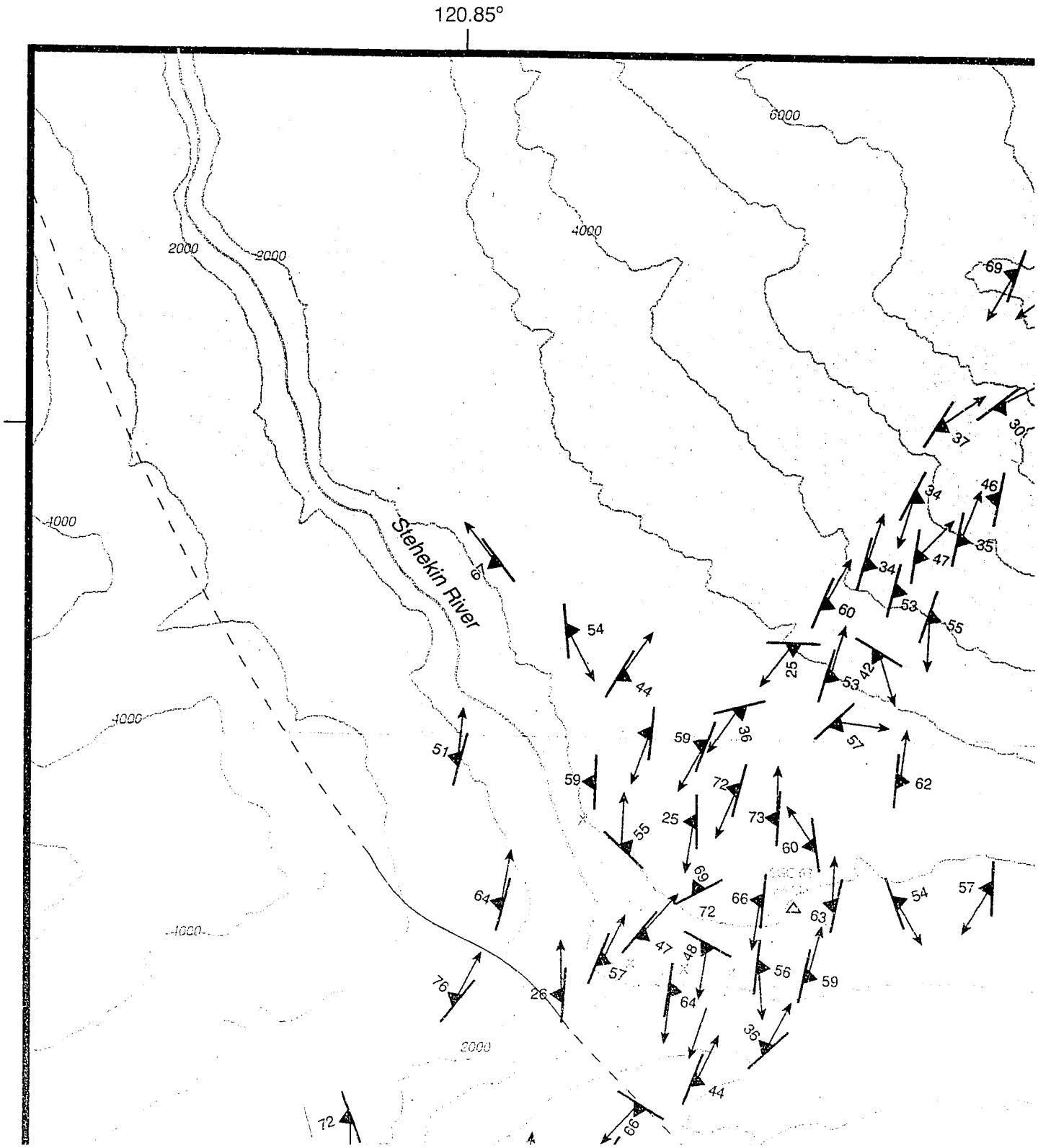
120.85°
6000
4000
2000
2000
1000
1000
4000
4000
2000
Stehekin River

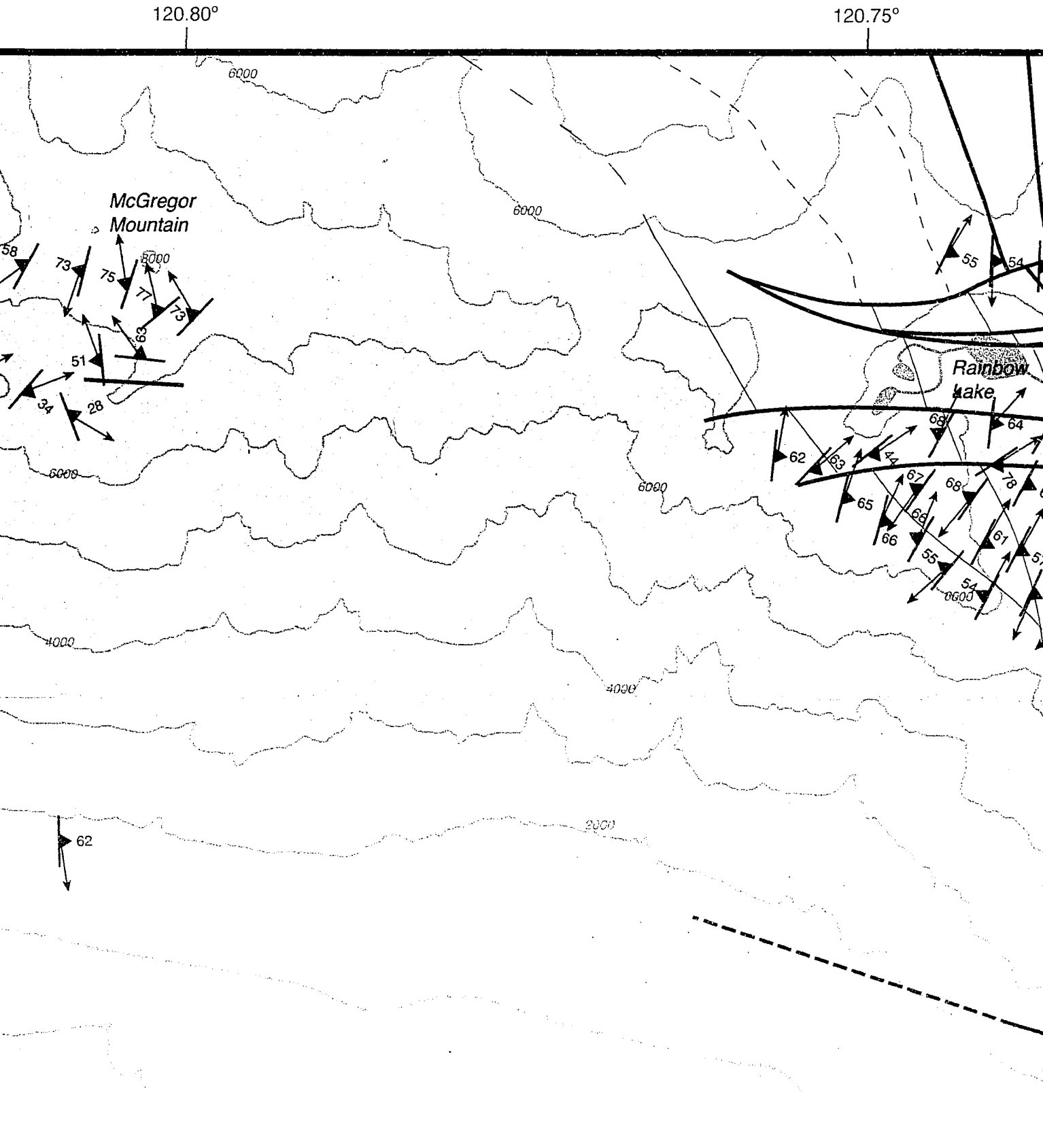
120.80°
120.75°
McGregor
Mountain
Rainbow
Lake
6000
4000
2000
58
73
75
77
73
63
51
34
28
62
63
44
64
65
66
67
68
78
61
55
54
62

CEN
STEHEKIN A

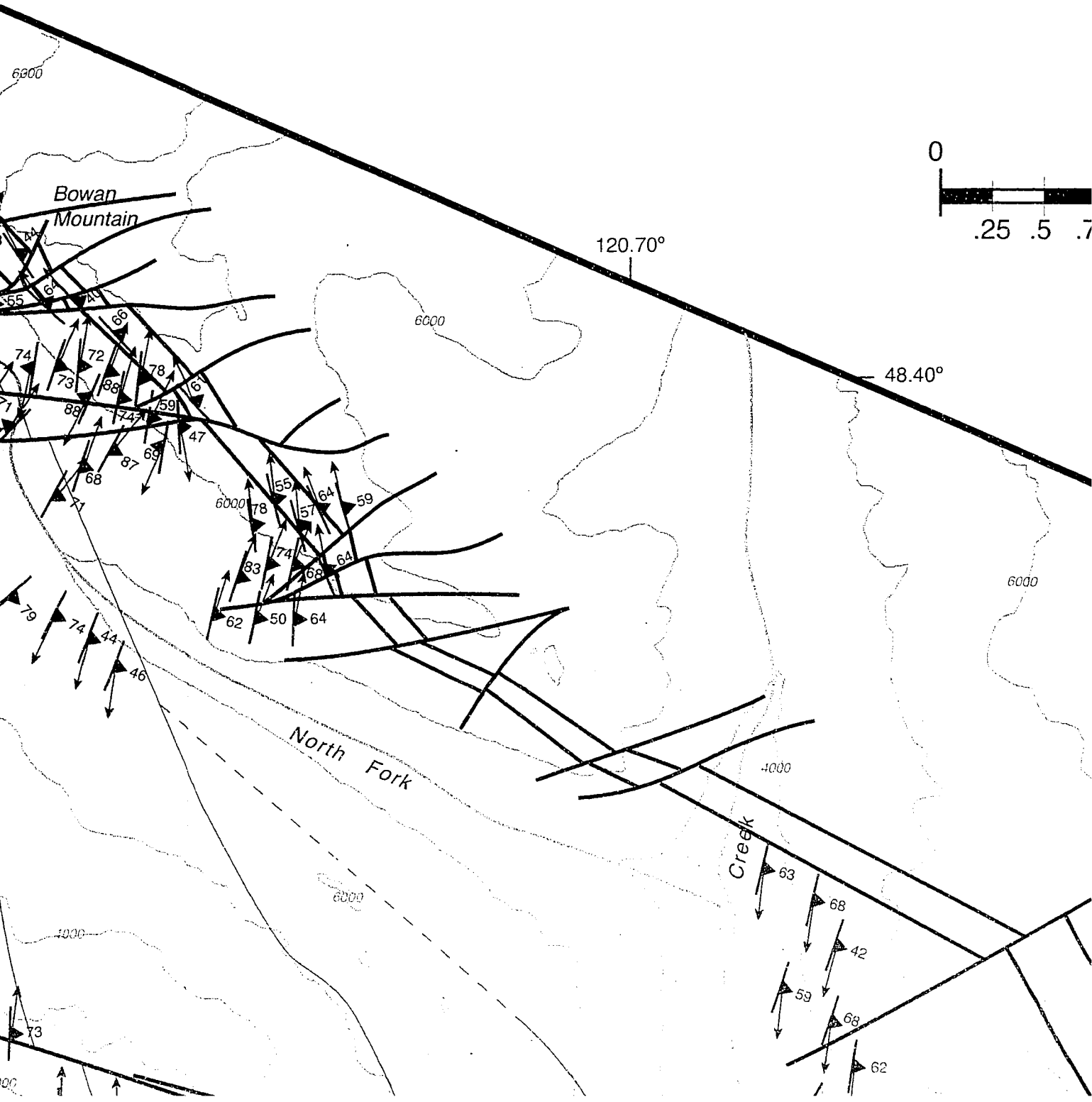

GEOLOGIC MAP
of
ENTRAL SKAGIT GNEISS COMPLEX
N AREA, NORTH CASCADES, WASHINGTO

Mapped by Zachary D. Michels (2006)

SCALE 1 : 24,000

1 2 3 4 5 km

.5 .75

CONTOUR INTERVAL = 100 ft

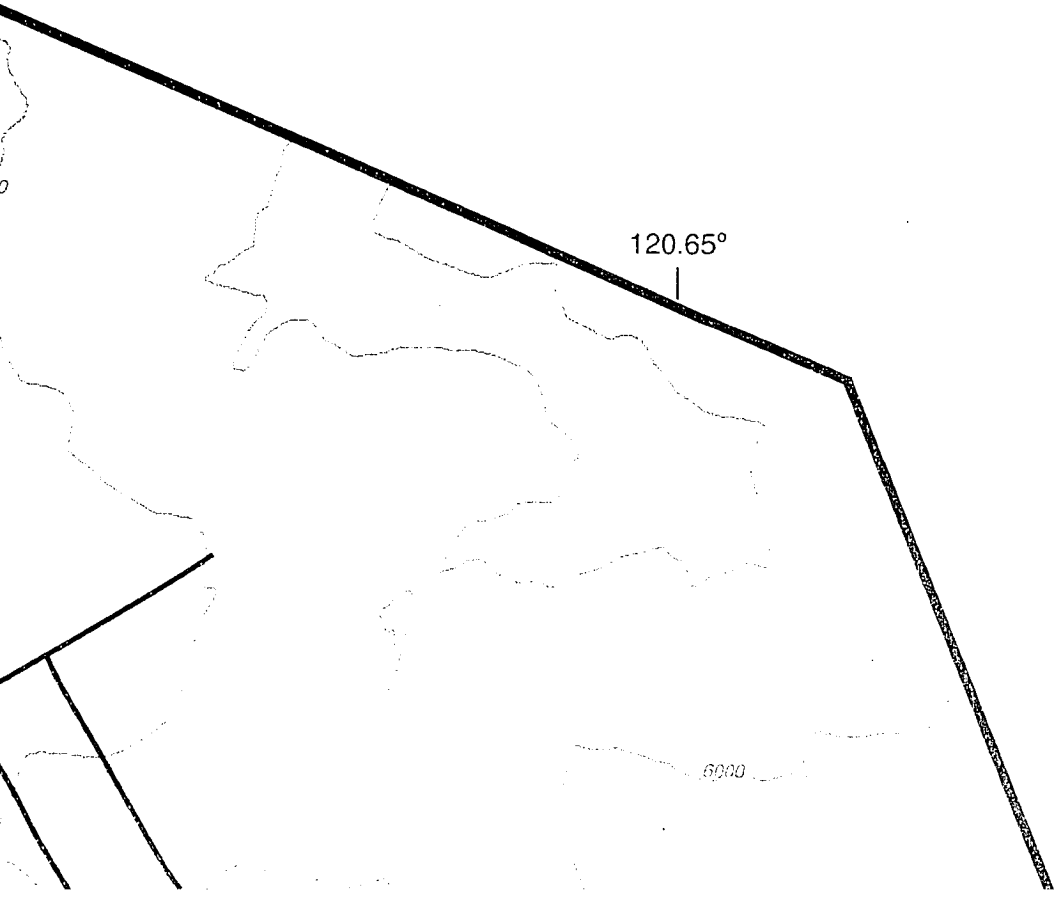

GEOLOGIC MAP
of
SKAGIT GNEISS COMPLEX
NORTH CASCADES, WASHINGTON

pped by Zachary D. Michels (2006)

SCALE 1 : 24,000

2 3 4 5 km

CONTOUR INTERVAL = 100 ft

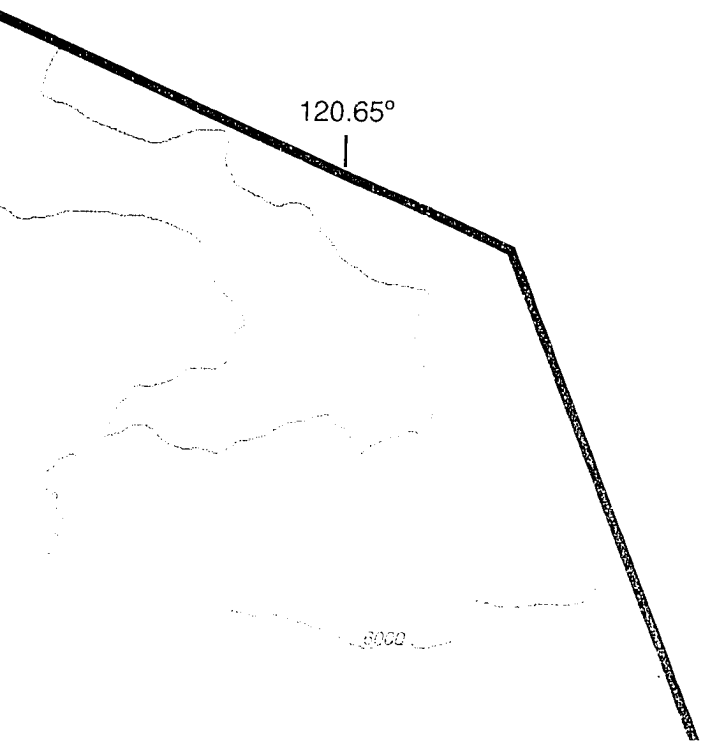

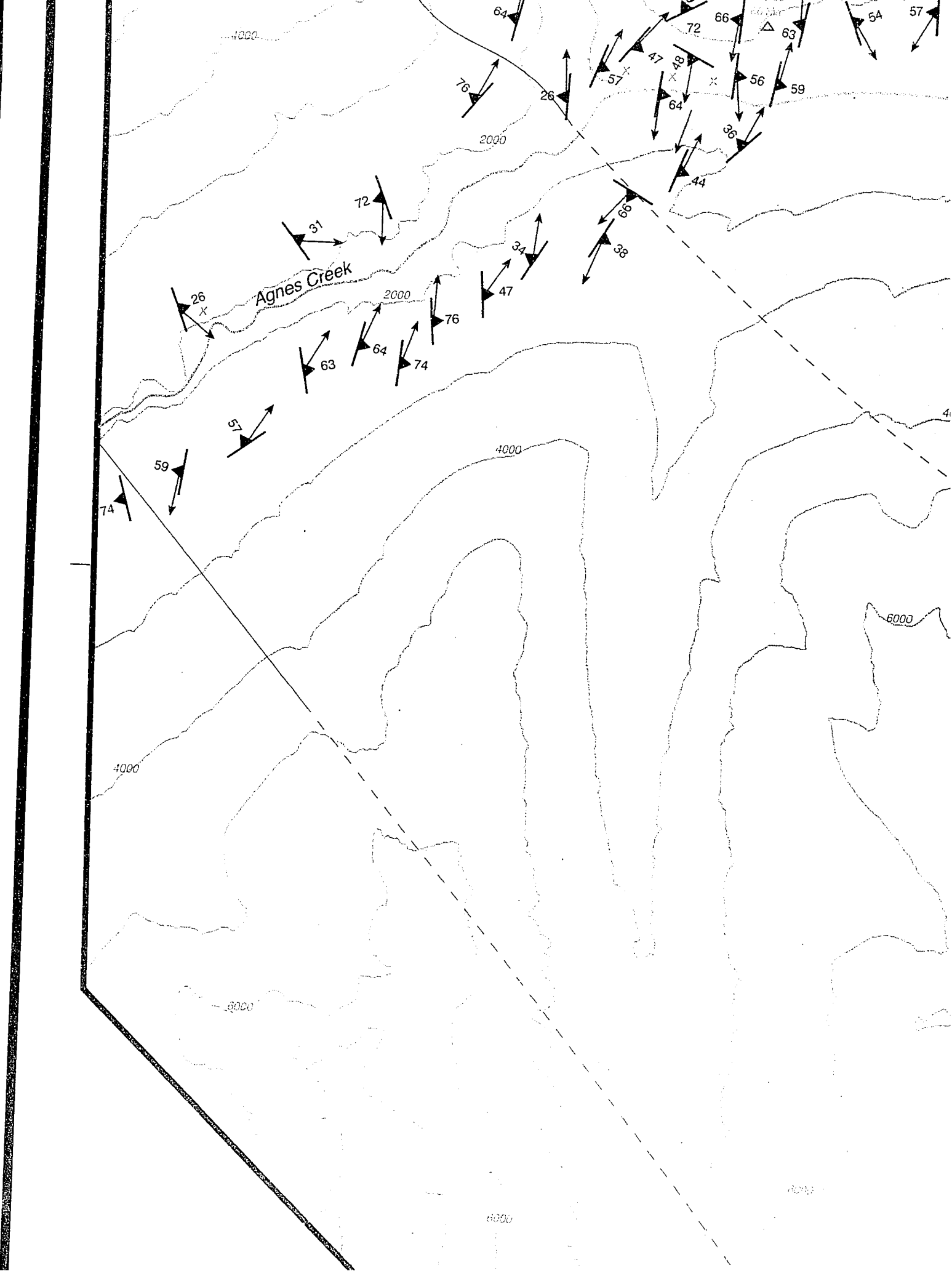
Agnes Creek
2000
4000
6000
64
72
66
63
54
57
76
26
47
48
57
56
59
64
36
44
72
31
66
38
34
47
26
76
64
63
74
57
59
74

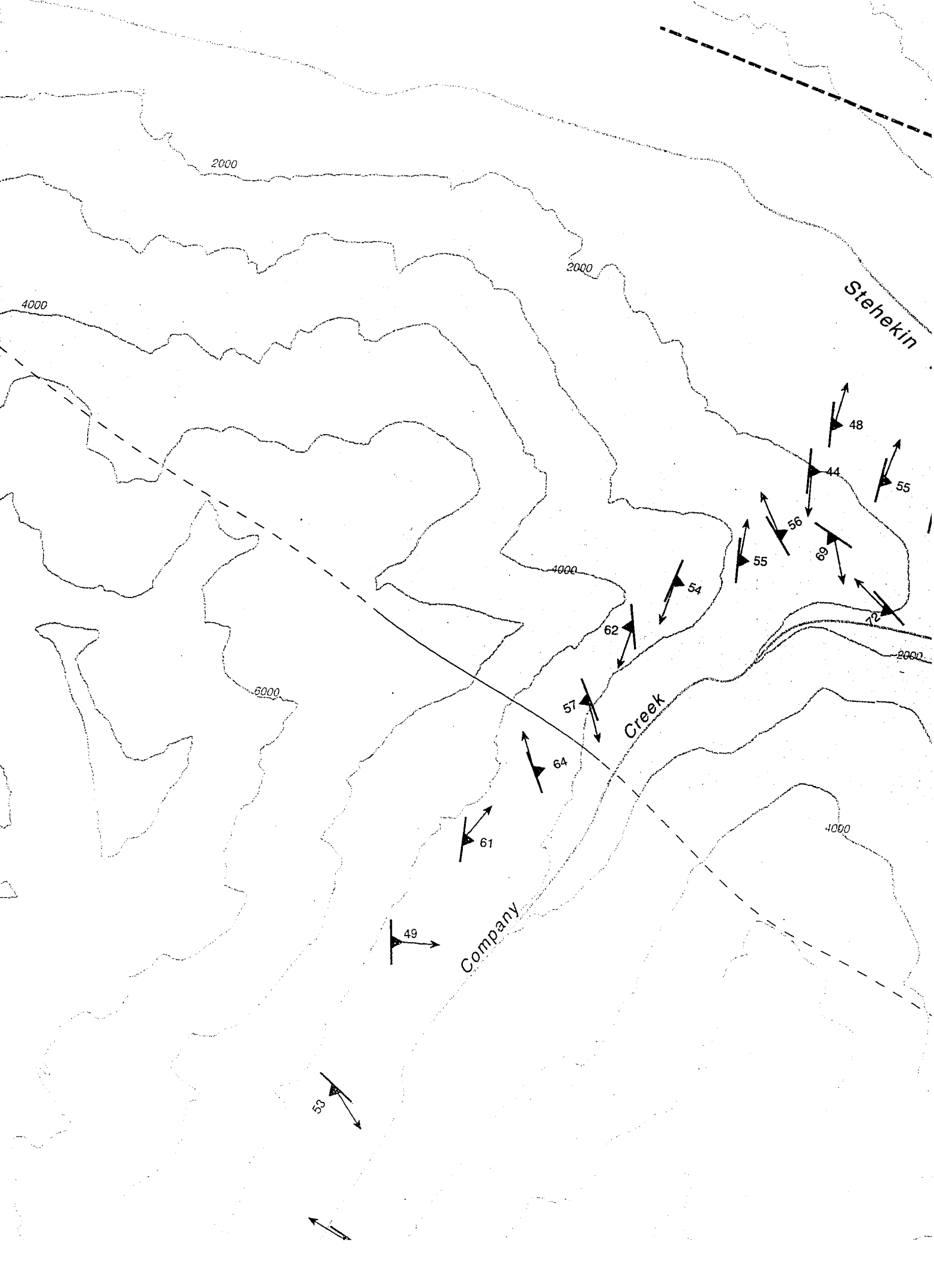
2000
2000
4000
Stehekin
48
44
55
56
55
68
4000
54
62
57
Creek
64
61
4000
49
Company
53

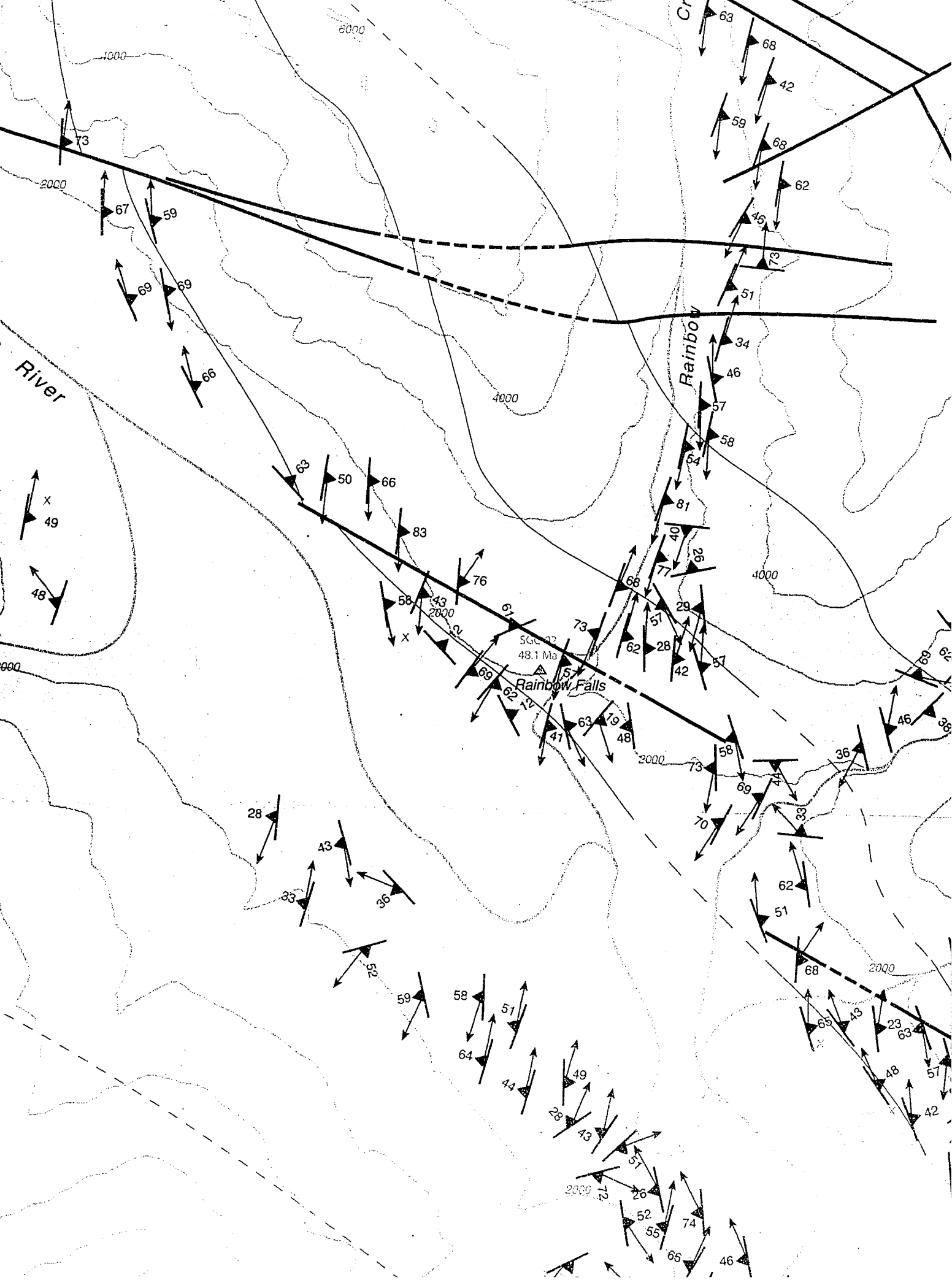
River
Rainbow
Rainbow Falls
48.1 Ma
6000
4000
2000

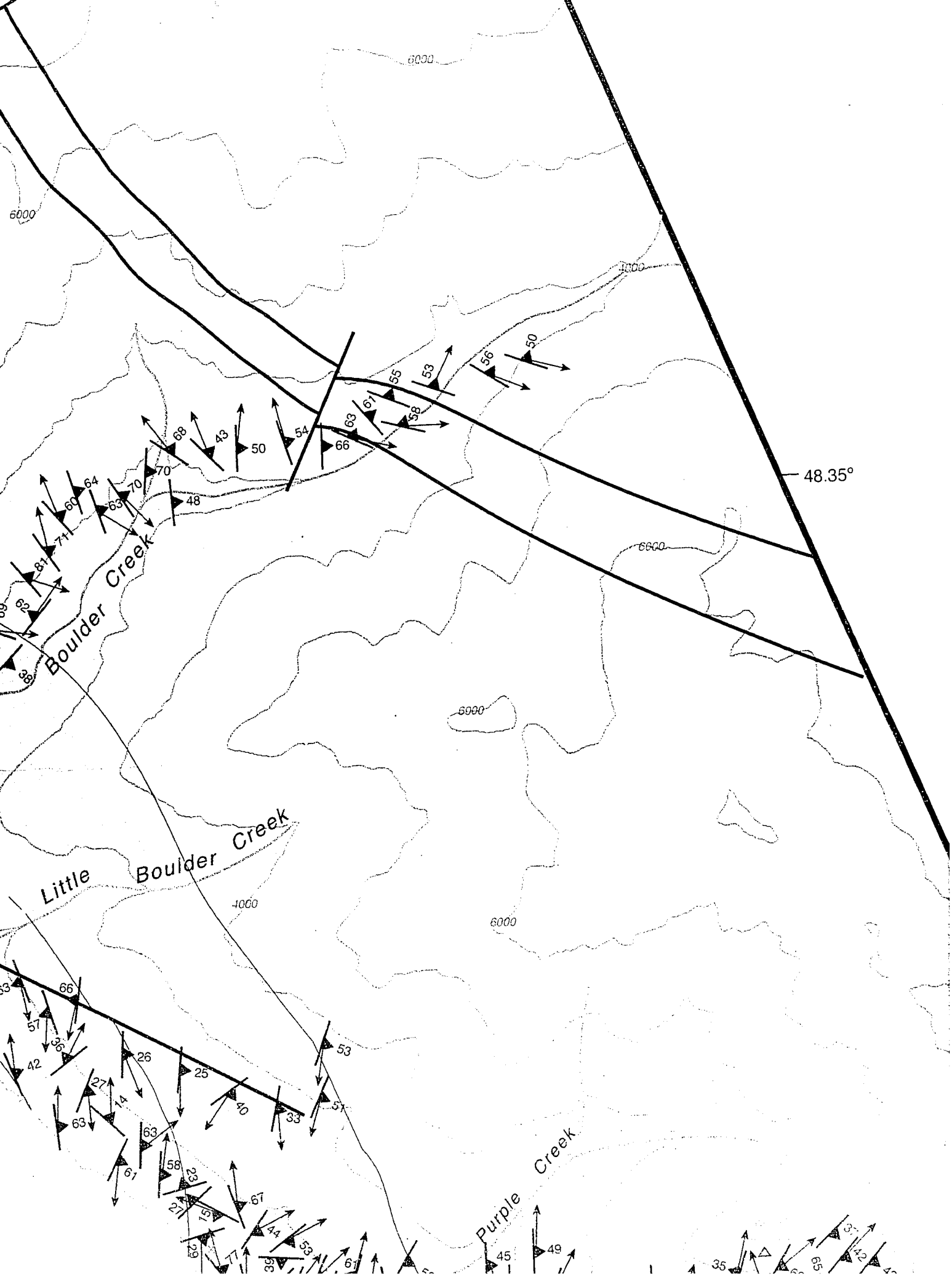
6000
6000
6000
6000
6000
4000
4000
48.35°
Boulder Creek
Little Boulder Creek
Purple Creek

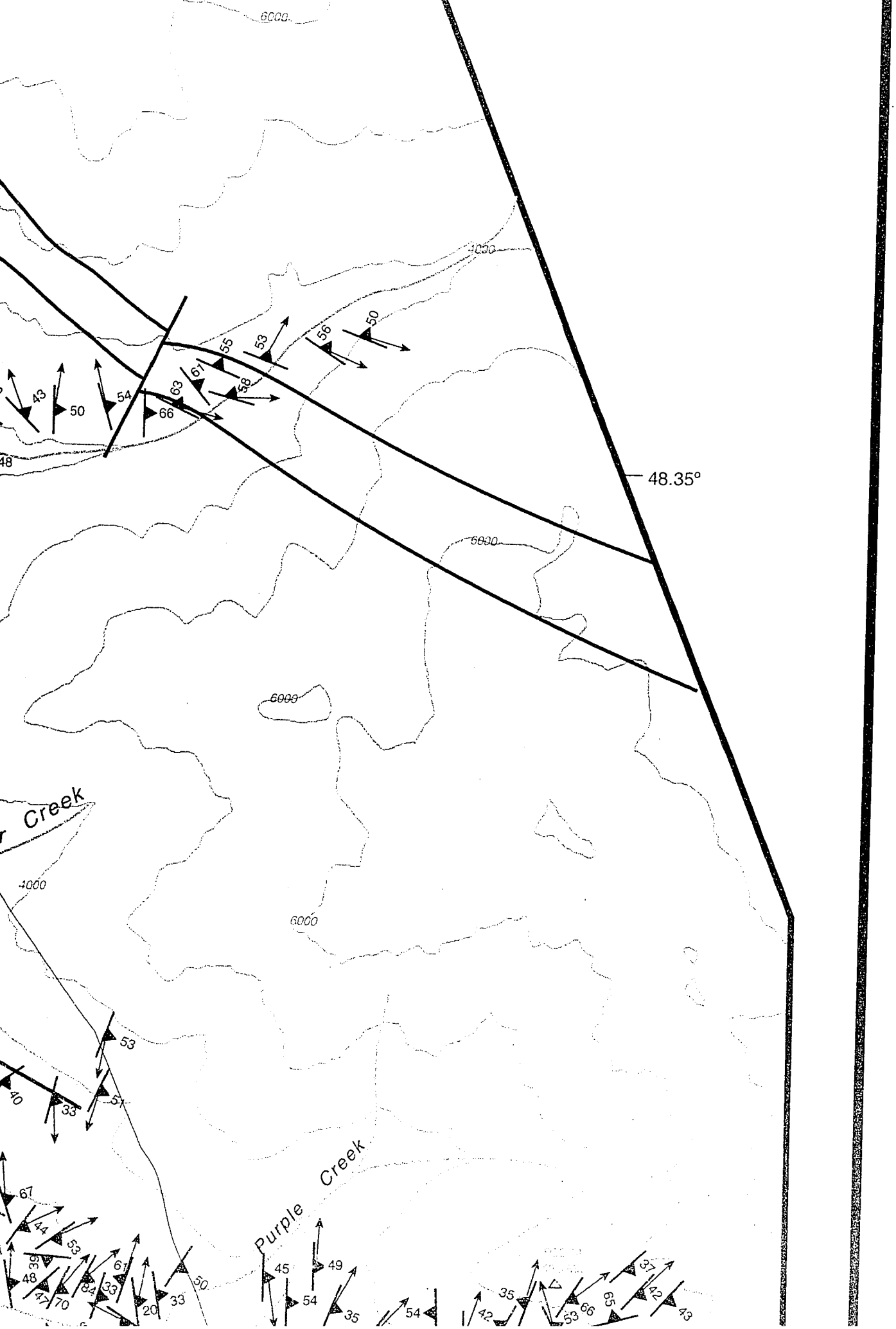
6000
1000
48.35°
6000
6000
6000
r Creek
4000
Purple Creek

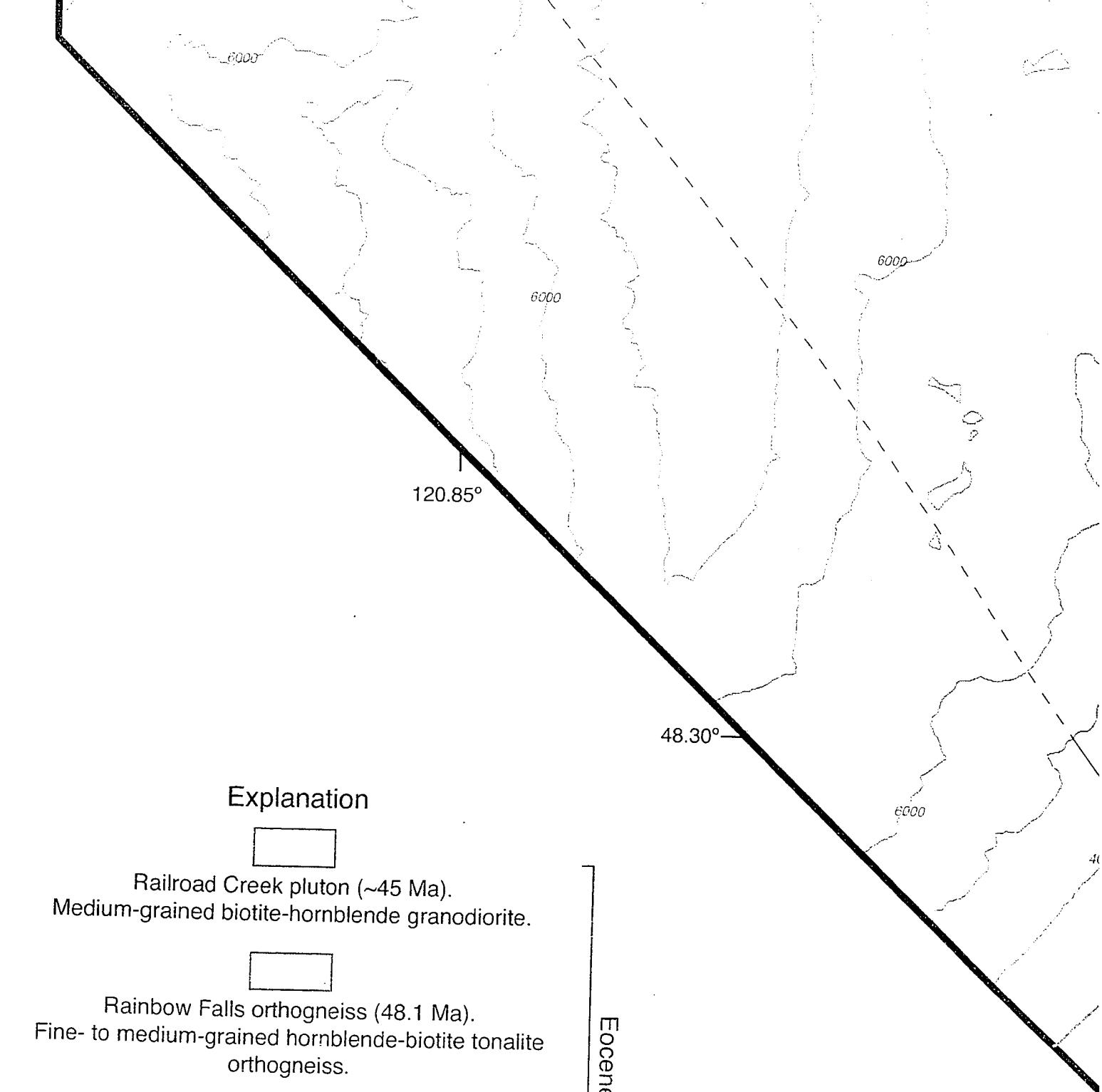

Explanation

Railroad Creek pluton (~45 Ma).
Medium-grained biotite-hornblende granodiorite.

Rainbow Falls orthogneiss (48.1 Ma).
Fine- to medium-grained hornblende-biotite tonalite orthogneiss.

Purple Creek orthogneiss (49.3 Ma).
Medium- to coarse-grained sheeted horblende-biotite tonailite orthogneiss. Eastern half of unit is well-foliated to mylonitic.

Western Skagit orthogneiss.
Heterogeneous medium-to fine-grained biotite tonalite orthogneiss with abundant pegmatite and local hornblende.

Eocene

Fault. Dashed where inferred.

Contact. Dashed where inferred

Symbol showing solid-state foliat

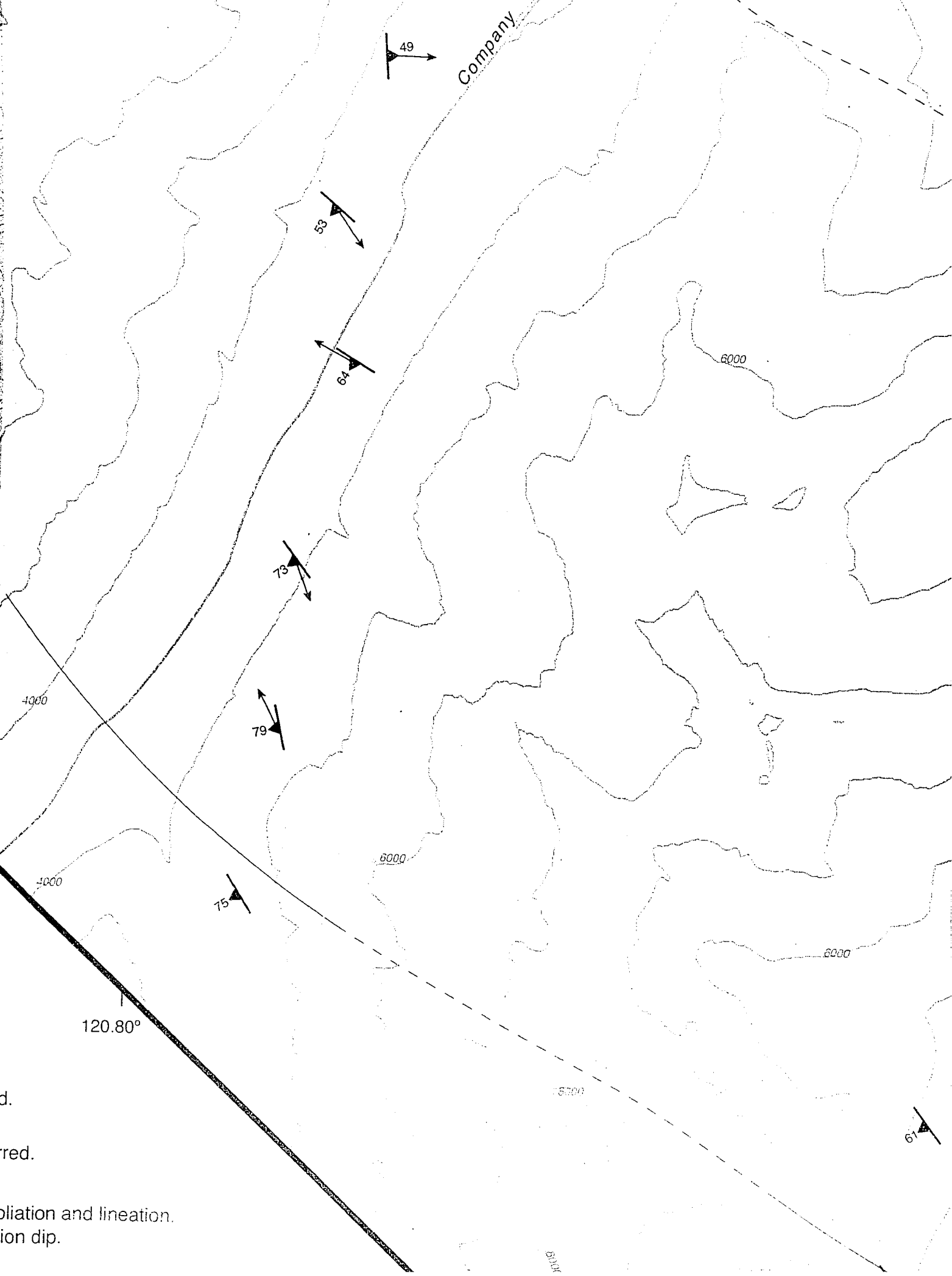

d.

rred.

bliation and lineation.
ion dip.

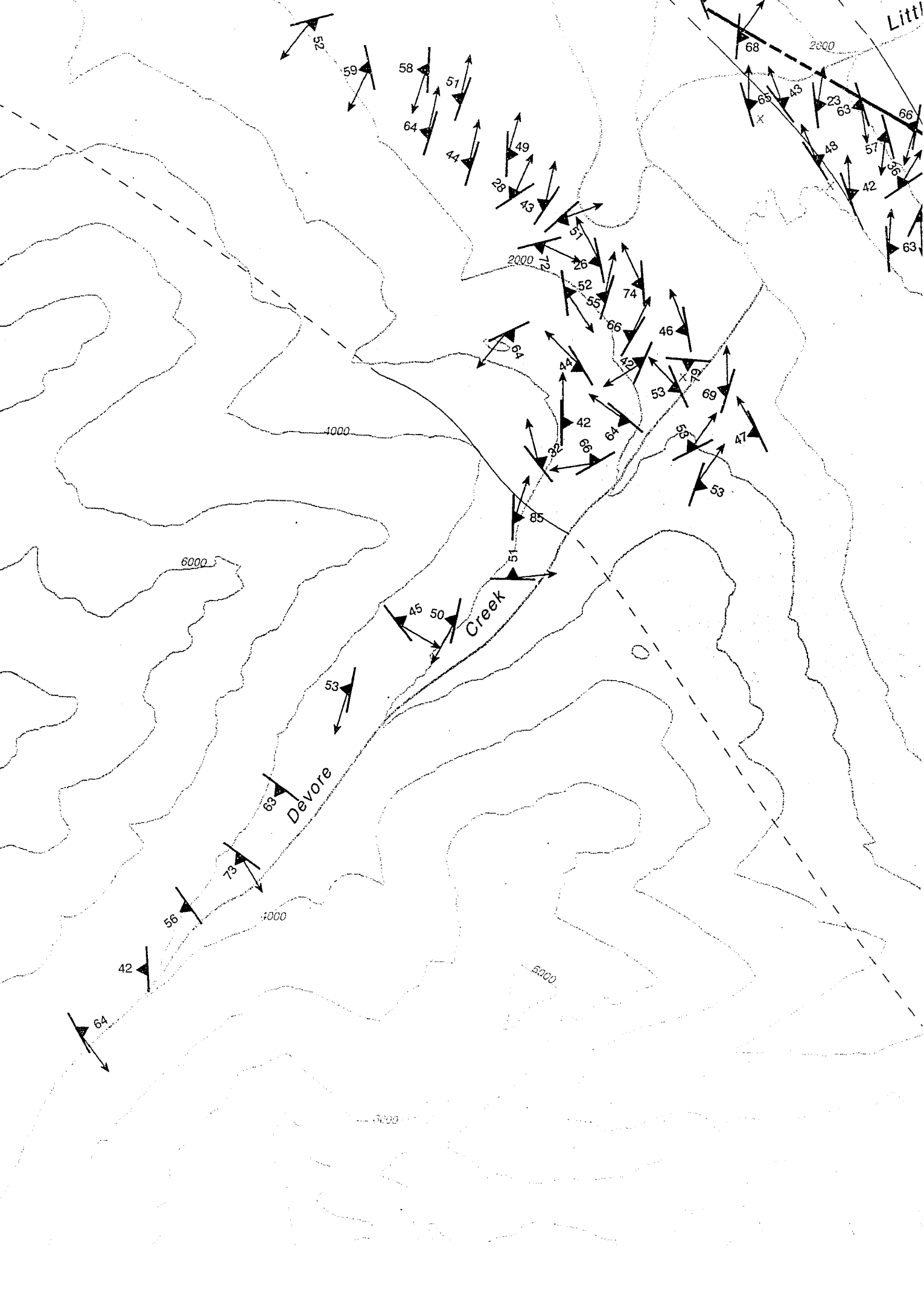
Devore
Creek
2000
4000
6000

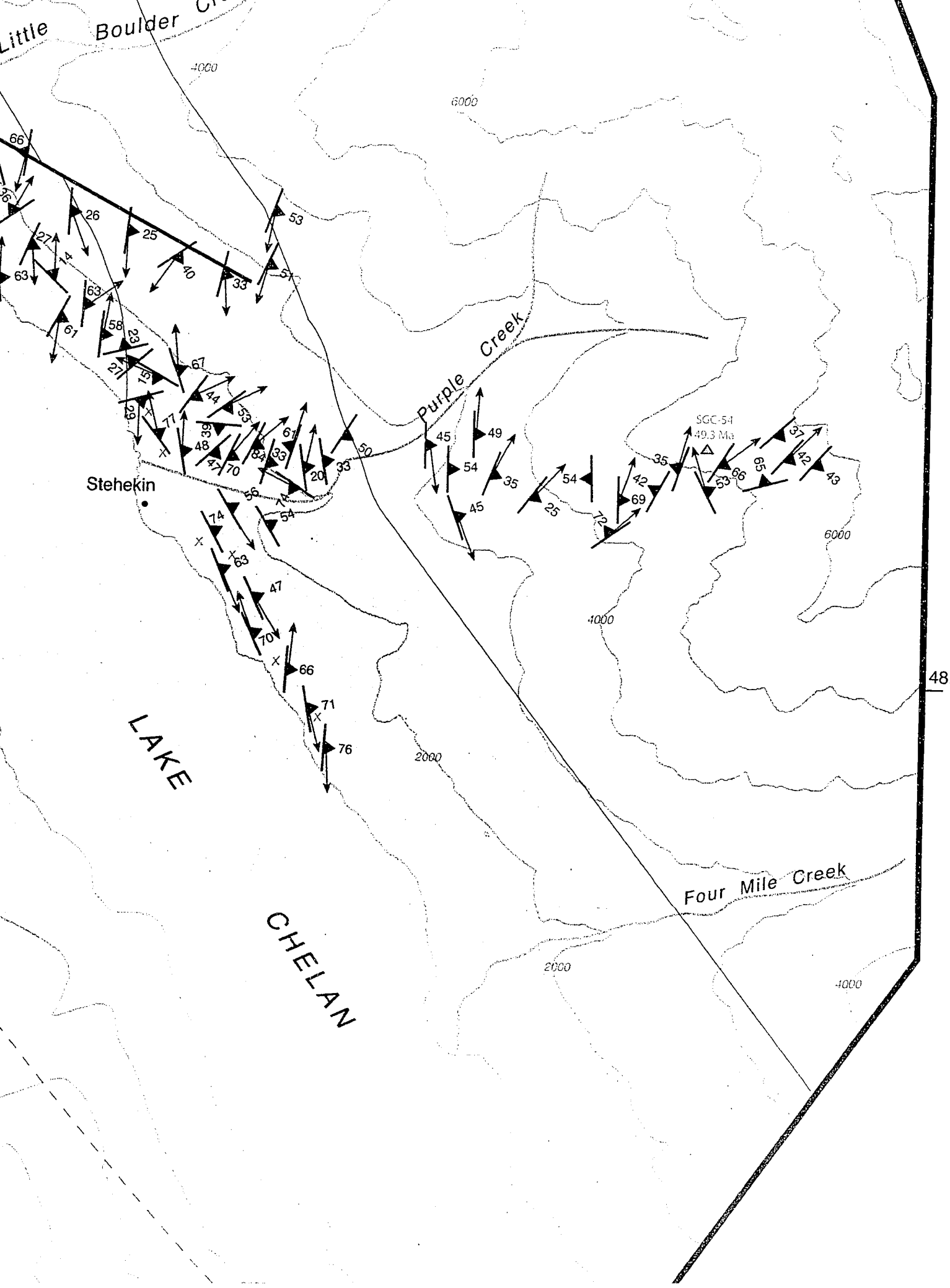
Little Boulder Cr
4000
6000
Purple Creek
SGC-54
49.3 Ma
Stehekin
LAKE CHELAN
Four Mile Creek
2000
4000
6000
48.30

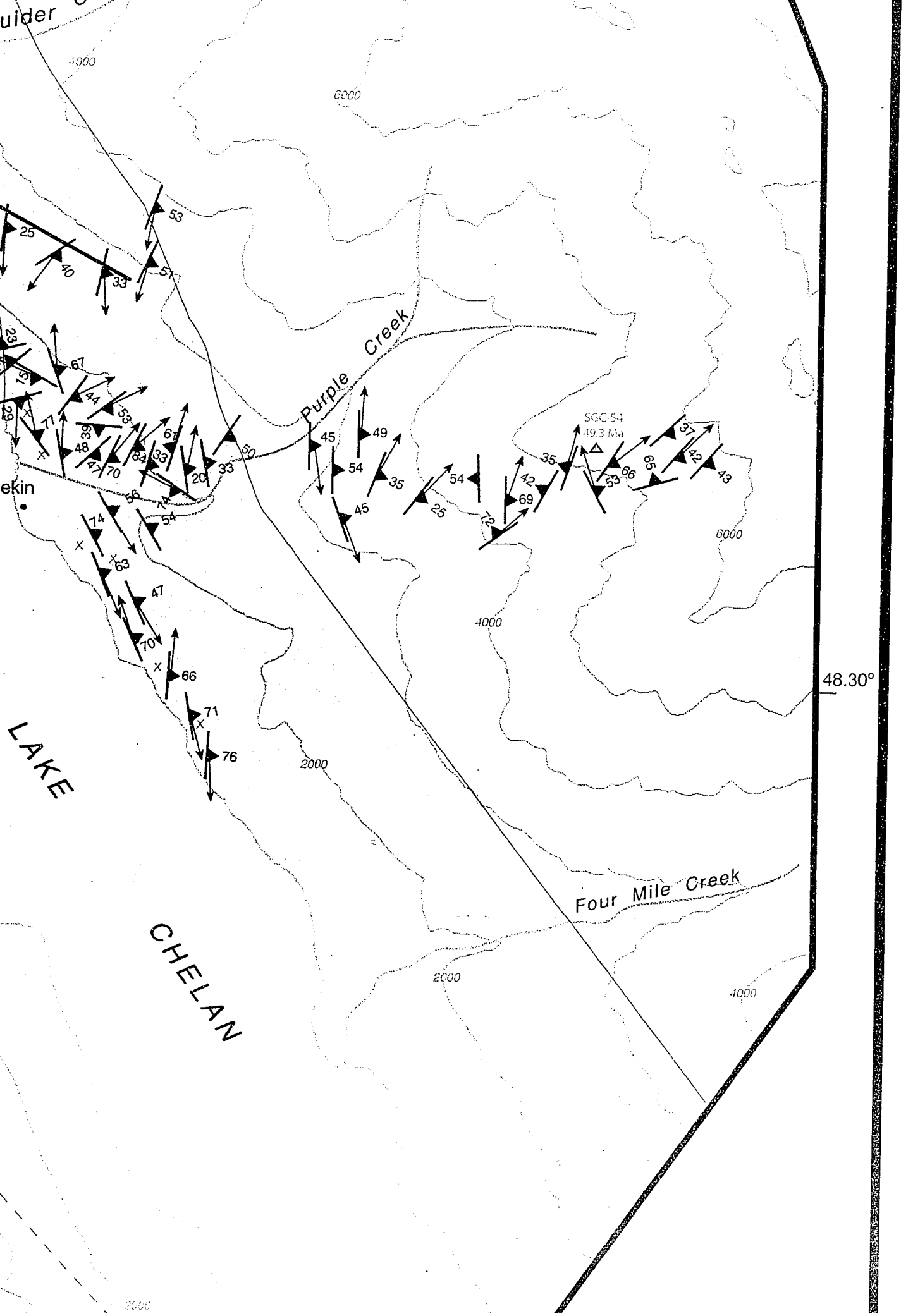
Purple Creek
SGC-5-1
49.3 Ma
48.30°
LAKE
CHELAN
Four Mile Creek
6000
4000
2000

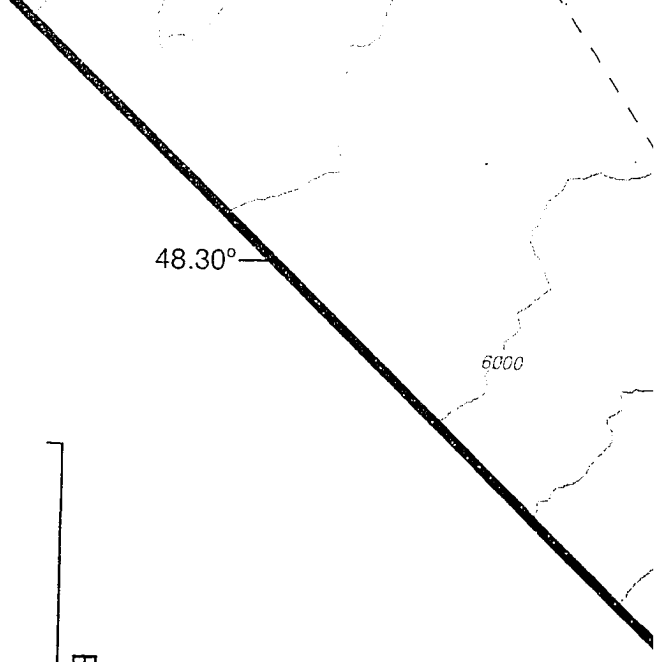

Explanation

Railroad Creek pluton (~45 Ma).
Medium-grained biotite-hornblende granodiorite.

Rainbow Falls orthogneiss (48.1 Ma).
Fine- to medium-grained hornblende-biotite tonalite orthogneiss.

Purple Creek orthogneiss (49.3 Ma).
Medium- to coarse-grained sheeted horblende-biotite tonailite orthogneiss. Eastern half of unit is well-foliated to mylonitic.

Eocene

Western Skagit orthogneiss.
Heterogeneous medium-to fine-grained biotite tonalite orthogneiss with abundant pegmatite and local hornblende.

Stehekin orthogneiss (~ 66 Ma).
Heterogeneous coarse-grained biotite tonalite orthogneiss with abundant pegmatite and local hornblende. Locally contains lenses of supracrustal rocks.

Black Peak batholith (Cretaceous).

Cretaceous

Rainbow Lake Schist.
Biotite ± garnet schist, amphibolite, siliceous schist, marble. Inferred to be correlative with rocks of the Napeequa complex.

Fault. Dashed where in

Contact. Dashed where

Symbol showing solid-st
Text indicates degree of

Geochronology sample (
Age shown in millions of

Location of migmatitic ou

WASHING

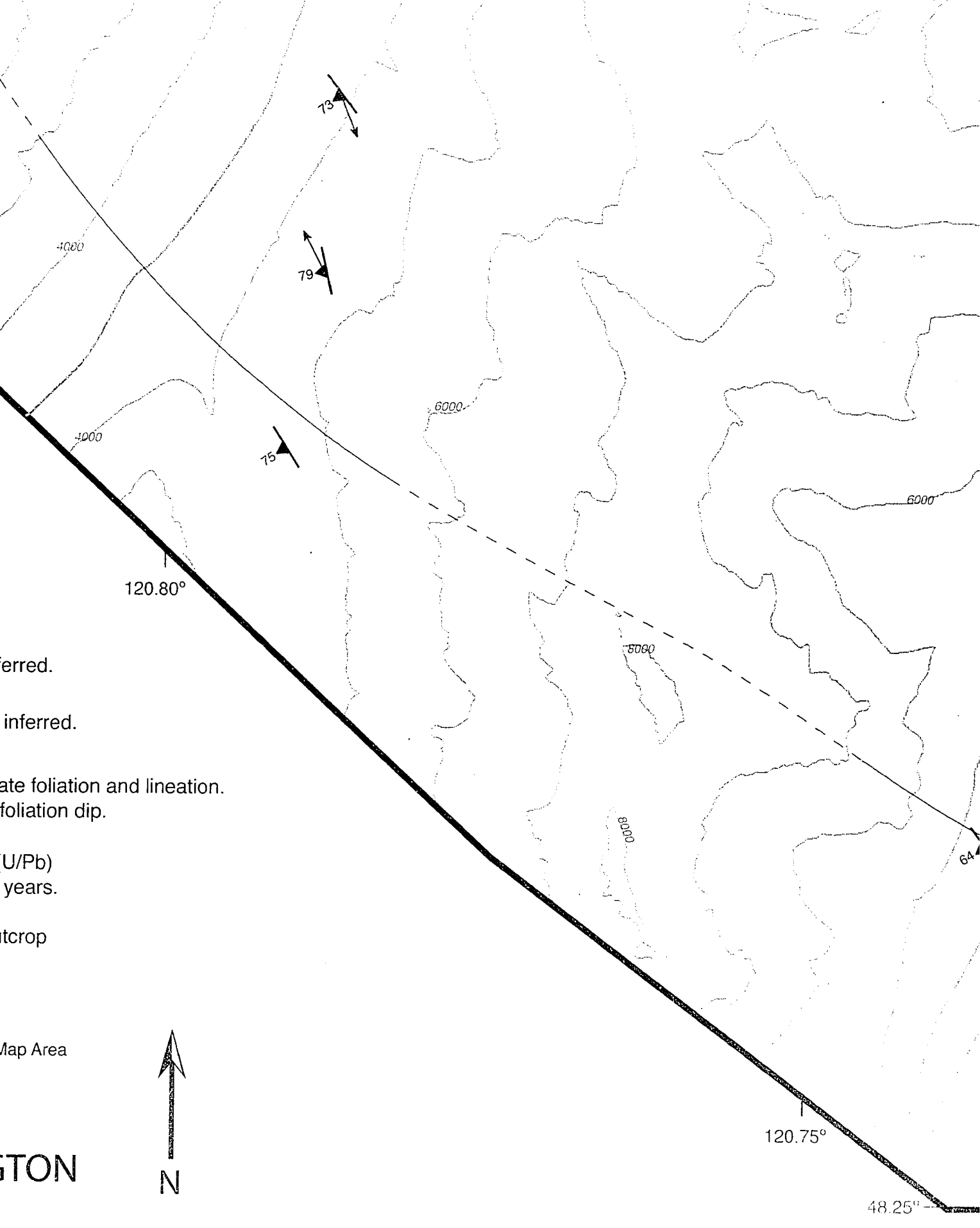

ferred.

inferred.

ate foliation and lineation.
foliation dip.

U/Pb)
years.

tcrop

Map Area

GTON

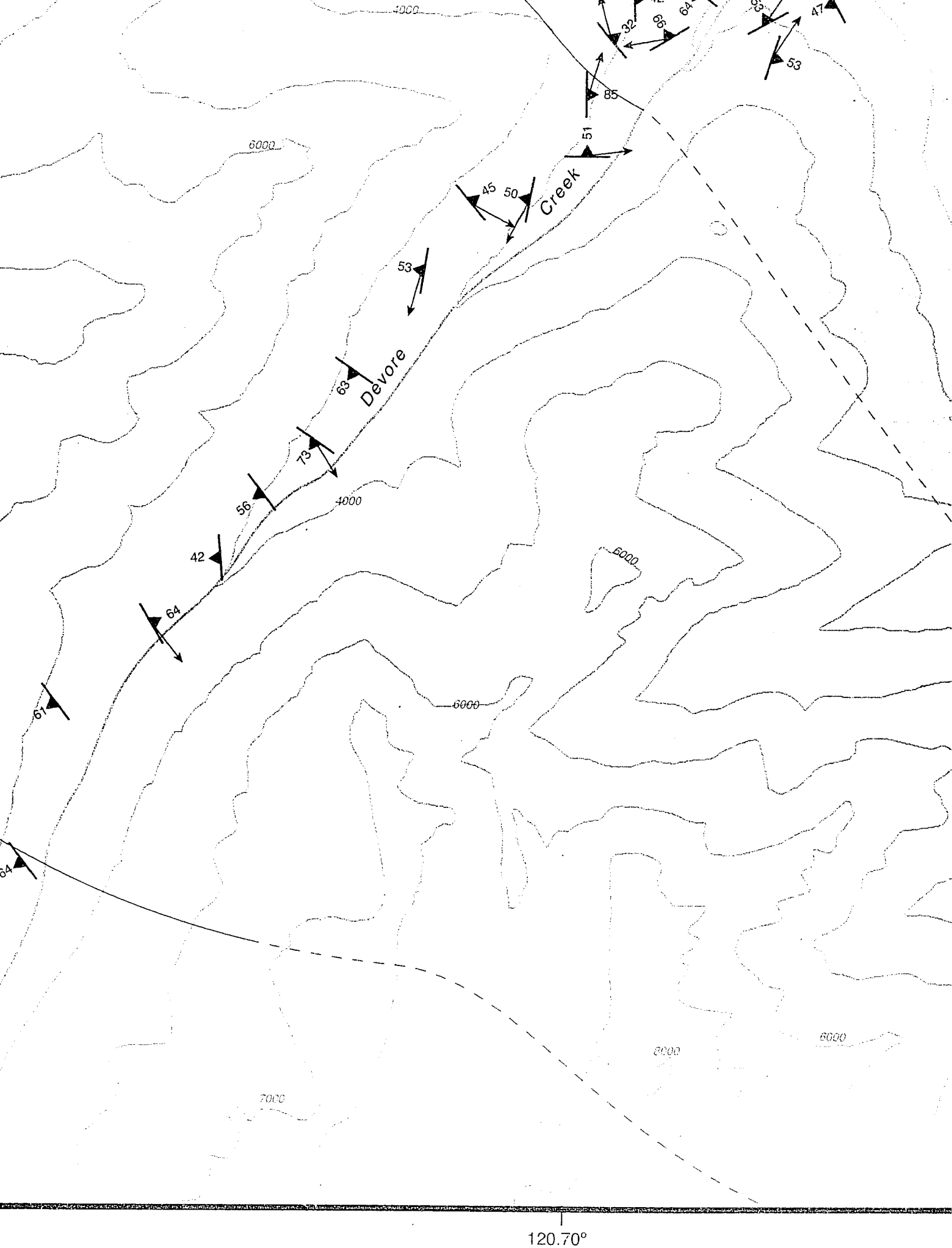
4000
6000
Devore
Creek
53
63
73
56
42
64
61
64
45
50
51
85
32
66
64
53
47
6000
6000
6000
7000
120.70°

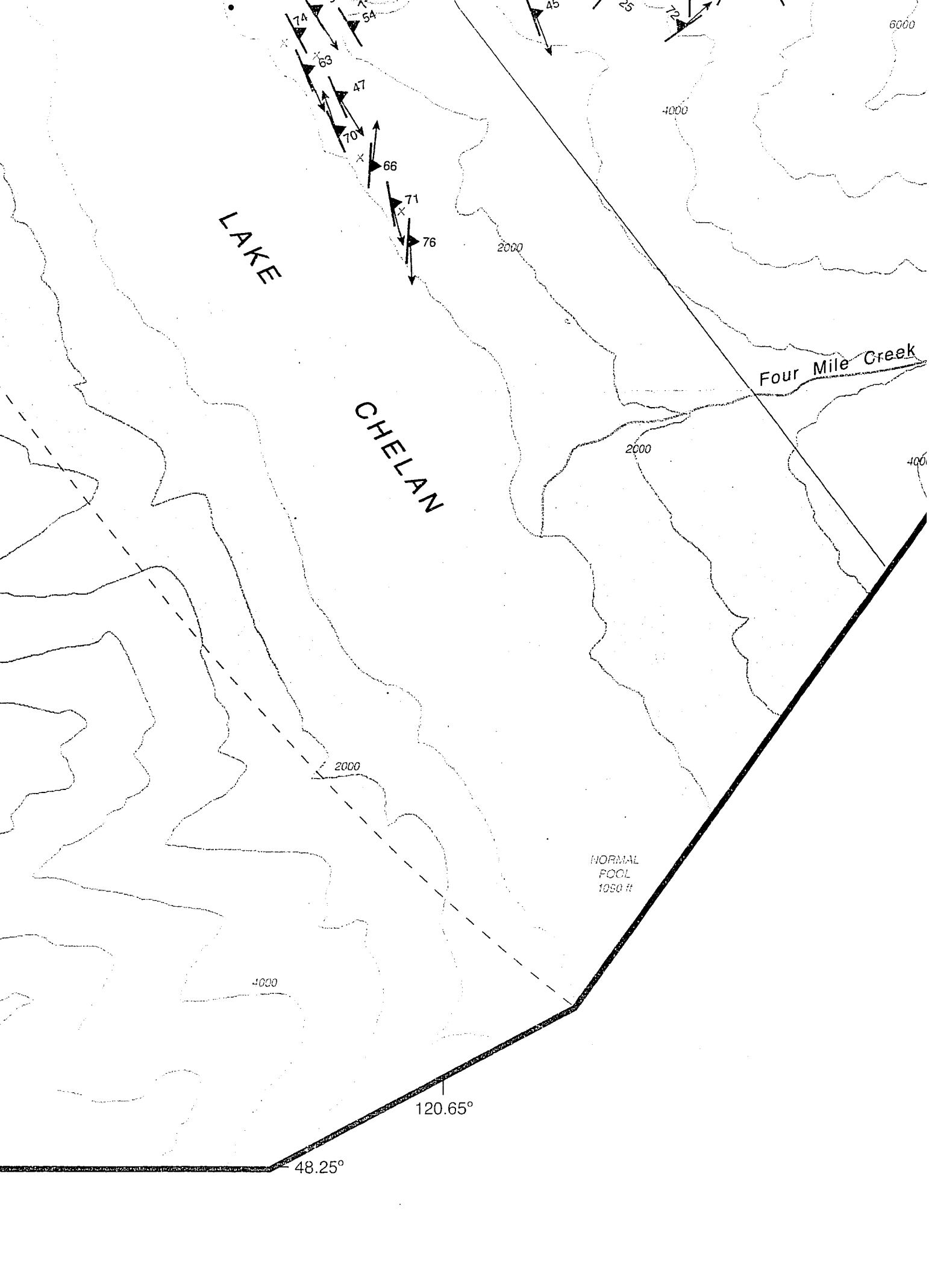
74
54
63
47
70
66
71
76
45
72
LAKE
CHELAN
Four Mile Creek
6000
4000
2000
2000
2000
4000
NORMAL
POOL
1050 ft
120.65°
48.25°

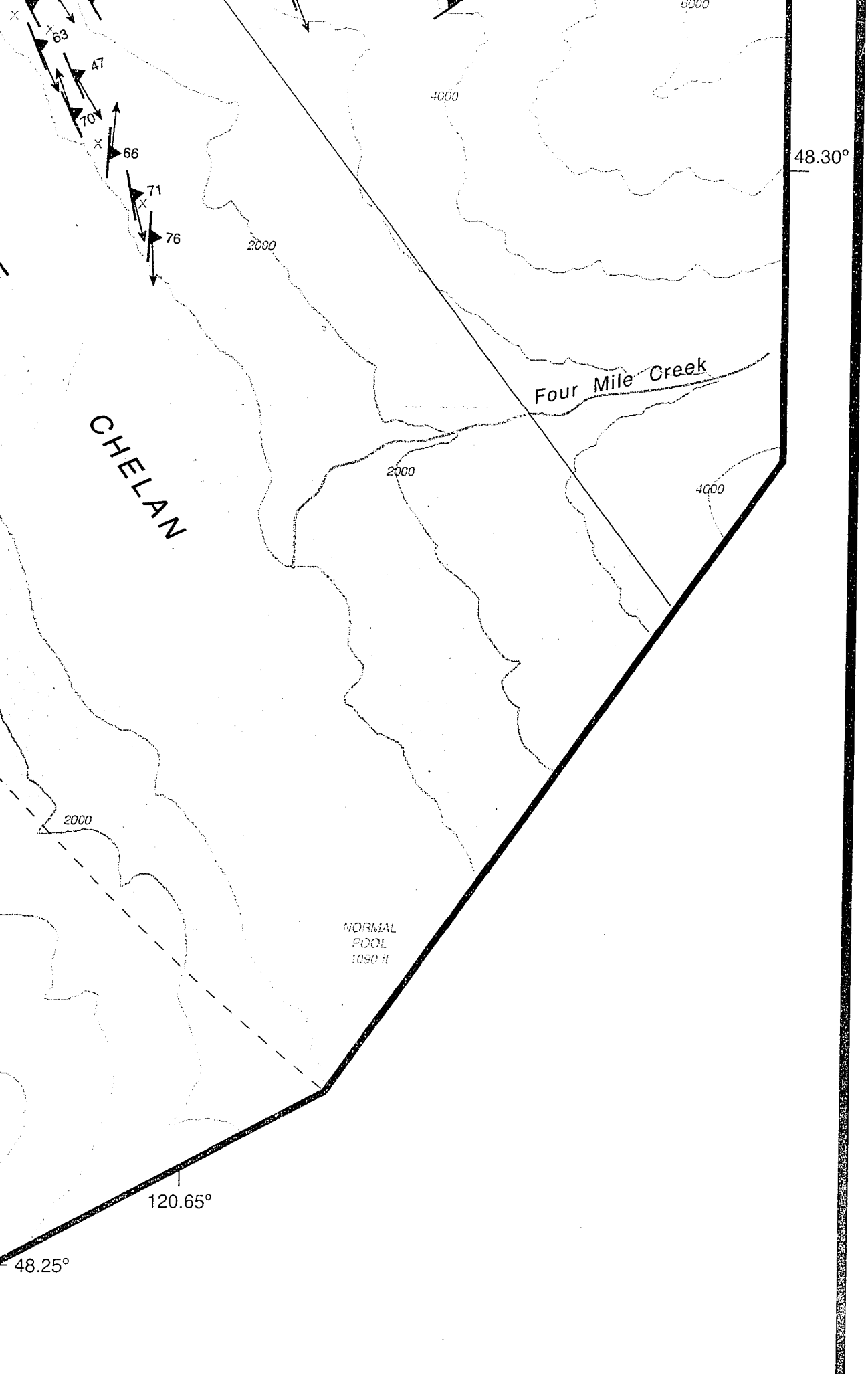
63
47
70
66
71
76
6000
4000
2000
48.30°
Four Mile Creek
CHELAN
2000
4000
2000
NORMAL
POOL
1090 ft
120.65°
48.25°